

AN ABSTRACT OF THE THESIS OF

James Hurley VanSant, Jr. for the Ph.D. in Mechanical Engineering
(Name) (Degree) (Major)

Date thesis is presented June 12, 1964

Title CONVECTION HEAT TRANSFER IN SEPARATED REGIONS -
SUBSONIC DIFFUSERS

Abstract approved 
(Major professor)

Heat transfer rates from a heated, plane-wall, symmetrical, two-dimensional, subsonic diffuser to a flowing gas (air) were measured at total divergence angles ranging from 0 to 45 degrees, at diffuser wall length to throat width ratios ranging from 6 to 18 and at Reynolds numbers based on throat velocity and throat width ranging from approximately 10,000 to 300,000. Diffuser flow conditions developed were: No "appreciable" separation, large transitory stall (separation) and fully-developed two-dimensional stall. Fluid boundary layers on the diffuser walls were always turbulent.

Flow studies were made in conjunction with the heat transfer measurements. These studies consisted of observing smoke filaments and tuft movements during all flow conditions developed and velocity measurements in fully-developed two-dimensional stall.

The flow patterns as affected by diffuser geometry were found to be the same as those observed by S. J. Kline, et al. in two-dimensional diffusers.

All heat transfer data were obtained from only one of the diverging walls of the diffuser which was heated to an isothermal condition. The other walls and the diffuser entrance sections were adiabatic.

Steady-state measurements were obtained with 28 electrically heated spot heaters that were mounted in the isothermal wall. Special transient heat meters, placed at five locations, were also used to conduct an exploratory study of heat transfer during transitory stall.

Predictions of heat transfer were made for the condition of no "appreciable" separation and for both walls during fully-developed two-dimensional stall by the application of an equation describing heat transfer from a flat plate with a turbulent boundary layer. For most cases, the difference between measured and predicted heat transfer rates was within the range of the experimental uncertainty.

For the flow condition of large transitory stall, no prediction could be made and the experimental data from measurements with the spot heaters were found to correlate best by plotting Nusselt number against Reynolds number based on throat velocity and distance from

the diffuser inlet. A line faired through the data plotted in this manner lies within ± 30 percent of the data.

Results of measurements with the transient heat meters are presented as the largest value of $(h_{\max} - h_{\min})/h_{\text{av}}$ obtained from all the transient meters over a long period of time. This parameter was found to be as large as 0.50.

CONVECTION HEAT TRANSFER IN SEPARATED REGIONS
- SUBSONIC DIFFUSERS

by

JAMES HURLEY VANSANT, JR.

A THESIS

submitted to


OREGON STATE UNIVERSITY

in partial fulfillment of
the requirements for the
degree of

DOCTOR OF PHILOSOPHY

August, 1964

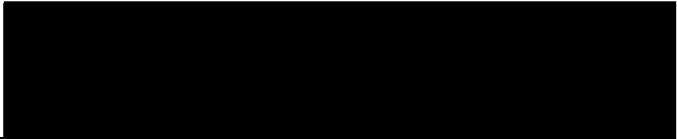
APPROVED:



Associate Professor of Mechanical Engineering
In Charge of Major



Head of Department of Mechanical Engineering



Dean of Graduate School

Date thesis is presented June 12, 1964

Typed by Illa W. Atwood

ACKNOWLEDGMENTS

The author gratefully acknowledges the following assistance:

The National Science Foundation supported the research through Grant GP293.

The Shell Oil Company awarded a fellowship to the author for the first year of his graduate program.

The Engineering Experiment Station of Oregon State University provided a research assistantship for the remainder of the author's graduate program.

Professor M. B. Larson gave helpful suggestions and criticisms for many problems concerned with the research program.

Members of the staff of the Mechanical Engineering Department gave assistance and suggestions for solving several problems concerned with the research.

The author's wife, Jo Ann, typed the preliminary drafts of the present thesis and contributed many helpful criticisms.

TABLE OF CONTENTS

	<u>Page</u>
I. INTRODUCTION	1
A. The Problem	1
B. The Selected Flow Geometry	1
C. The Nature of Separated Flow	2
II. LITERATURE REVIEW	
A. Discussions of Generalized Separated Flows	6
B. Laminar and Turbulent Separations	7
C. Jets, Wakes and Mixing Regions	10
D. Boundary Layer Transition and Separation	11
E. Heat Transfer Effects on Separation	12
F. Subsonic Diffusers	13
G. Heat Transfer in Separated Regions	14
H. Heat Transfer in Nozzles and Jets	16
I. Heat Transfer Correlations for Flat Plates	17
III. FLOW IN SUBSONIC DIFFUSERS	19
IV. PREDICTIONS OF HEAT TRANSFER IN TWO-DIMENSIONAL DIFFUSERS	24
A. Non-Separated Flow (No "Appreciable" Separation)	24
B. Fully-Developed Two-Dimensional Stall	26
C. Large Transitory Stall	34
V. EXPERIMENTAL PROGRAM	36
A. Scope	36
B. Experimental Apparatus	36
Over-all Description	36
Diffuser Assembly	37
Flow Control Equipment	39
Heat Transfer Equipment	41
Flow Visualization Equipment	45
C. Experimental Procedures	46
Flow Studies	46
Heat Transfer Measurements	47

	<u>Page</u>
VI. RESULTS	50
A. Flow Studies	50
B. Heat Transfer	55
No "Appreciable" Separation	56
Fully-Developed Two-Dimensional Stall	57
Large Transitory Stall	60
Additional Observations	64
VII. CONCLUSIONS	66
VIII. RECOMMENDATIONS	70
IX. BIBLIOGRAPHY	73
APPENDIX A Determination of Conduction Heat Losses From the Spot Heaters	79
APPENDIX B Evaluation of the Unheated Entrance	85
APPENDIX C Evaluation of Experimental Accuracies	88
APPENDIX D Consideration of Mixed Free and Forced Convection	89
APPENDIX E Computing Technique	91
APPENDIX F Figures	94
APPENDIX G Tables	123

INDEX TO FIGURES

Figure	Title	Page
1a	Flow Regimes in Two-Dimensional Straight-Walled Diffusers.	94
1b	Illustrations of No "Appreciable" Separation.	95
1c	Illustrations of Large Transitory Stall.	95
1d	Illustrations of Fully-Developed Two-Dimensional Stall.	96
2a	An Illustration of Streamlines in a Subsonic Diffuser during Fully-Developed Two-Dimensional Stall.	97
2b	An Illustration of Velocity Profiles in a Subsonic Diffuser during Fully-Developed Two-Dimensional Stall.	97
2c	An Illustration of Parameters used in Equation (14).	97
3a	Schematic Side View of the Test Apparatus.	98
3b	Schematic End View of the Test Apparatus.	99
3c	Photographs of Experimental Equipment.	100
4	Schematic Drawing of the Heated Plate Assembly.	101
5	Schematic Drawings of Heat Transfer Measuring Devices.	102
6	Schematic Drawing of the Smoke Generator.	103
7	Variation of Surface Temperature on the Heated Plate as Found by Electrical Analog.	104
8	Velocity Variation over the Diffuser Surface from a Flux Plot ($2\theta = 0^\circ$).	105

Figure	Title	Page
9	Correlation of δ_{2r} from Velocity Data.	106
10	Velocity Distribution in the Mixing Region during Fully-Developed Two-Dimensional Stall.	107
11	Correlation of the Maximum Velocity along the "Wall of Jet Flow" during Fully-Developed Two-Dimensional Stall.	108
12	Correlation of δ_{2w} along the "Wall of Jet Flow" during Fully Developed Two-Dimensional Stall.	108
13a	Comparison of Measured and Predicted Reversed Flow Velocities in Fully-Developed Two-Dimensional Stall.	109
13b	A Graphical Presentation of the Prediction of U_r/U_t [see Equation (17)].	110
14	Correlation of Measured Reversed Flow Velocities in Fully-Developed Two-Dimensional Stall.	111
15	A Typical Calibration Curve for Spot Heater Conduction Losses (position No. 1).	112
16	Results of Heat Transfer Measurements during No "Appreciable" Separation.	113
17a	Results of Heat Transfer Measurements on the "Wall of Jet Flow" during Fully-Developed Two-Dimensional Stall. (U_m determined from the correlation for a plane turbulent wall jet given by Myers, et al. (33).	114
17b	Results of Heat Transfer Measurements on the "Wall of Jet Flow" during Fully-Developed Two-Dimensional Stall. [U'_m determined from a correlation of experimental measurements, Equation (20)].	115

Figure	Title	Page
18a	Results of Heat Transfer Measurements on the "Wall of Reversed Flow" during Fully-Developed Two-Dimensional Stall.	116
18b	Correlation of Heat Transfer Measurements on the "Wall of Reversed Flow" during Fully-Developed Two-Dimensional Stall.	117
19a	Results of Heat Transfer Measurements during Large Transitory Stall. (Nu_{x_c} vs Re_x).	118
19b	Results of Heat Transfer Measurements during Large Transitory Stall. (Nu_{x_c} vs $Re_{x_t u_t}$).	119
20a	Results of Measurements taken with the Transient Heat Meters during Large Transitory Stall. (Re_w vs $(h_{max} - h_{min})/h_{av}$).	120
20b	Results of Measurements taken with the Transient Heat Meters during Large Transitory Stall. ($Re_{x_t u_t}$ vs $Nu_{x_t cav}$).	121
21	A Comparison of Heat Transfer Results from Three Regimes of Diffuser Flow.	122

INDEX TO TABLES

Table	Title	Page
I	Spot Heater Parameters	84
II	Experimental Uncertainties	88
III	Results of Transient Heat Transfer Measurements	123
IV	Heat Transfer Data From the No "Appreciable" Separation Regime	124
V	Heat Transfer Data From the Fully-Developed Two-Dimensional Stall Regime--On the "Wall of Jet Flow. "	128
VI	Heat Transfer Data From the Fully-Developed Two-Dimensional Stall Regime--On the "Wall of Reversed Flow. "	133
VII	Heat Transfer Data From the Large Transitory Stall Regime	139

LIST OF SYMBOLS

A, B, C	= Constants used in equation 6A.
A_f	= Flow area.
A_h	= Convection heat transfer area of spot heaters, .00136 feet ² .
c_p	= Constant pressure specific heat.
C_p	= Pressure coefficient.
D	= Diameter of the semi-cylindrical sections forming the diffuser entrance, 9.5 inches.
$f(W/L, D/L, \theta)$	= A functional relation for predicting U_t/U_r (see Equation 17).
Gr	= Grashof number.
h	= Heat transfer film coefficient.
k	= Thermal conductivity.
l	= Distance from the upstream edge of the plane section forming one of the two diverging walls in a direction parallel to the wall.
l_b	= Distance from the downstream edge of the plane section forming one of the two diverging walls in a direction parallel to the wall.
L	= Length of a plane section forming one of the two diverging walls, 3 feet.
$Nu_{x_b c}$	= Nusselt number including the equivalent distance from the diffuser exhaust, X_b , and corrected for unheated starting length and variation of fluid properties,

$$(hX_b/k)[1 - (\xi_b/X_b)^{.9}]^{1/9} (T_w/T_\infty)^{.4}.$$

$Nu_{x_t c}$ = Nusselt number including the equivalent distance from the diffuser throat, X_t , and corrected for the unheated starting length and variation of fluid properties,

$$(hX_t/k)[1 - (\xi_t/X_t)^{.9}]^{1/9} (T_w/T_\infty)^{.4}.$$

Pr = Prandtl number, $\rho \nu c_p/k$.

Q_c = Heat transfer rate by convection.

Q_k = Heat transfer rate by conduction.

Q_m = Measured energy transfer rate that is produced by electrical resistance heating in a spot heater.

R = Electrical resistance of spot heater.

Re_x = Reynolds number, UX/ν .

$Re_{x_t u_t}$ = $U_t X_t/\nu$.

$$Re_{x_t} = \frac{X_t}{\nu} \cdot \frac{U_t}{1 + 2(\ell/W)\sin \theta}$$

$Re_{x_b u_t}$ = $U_t X_b/\nu$.

Re_w = Throat Reynolds number, $U_t W/\nu$.

S = Aspect ratio of the semi-cylindrical entrance sections, $W/(W + D)$.

St = Stanton number, $h/U\rho c_p$.

St_{u_t} = $h/U_t\rho c_p$.

$St_{u_t c}$ = Stanton number corrected for the unheated starting length and variation of fluid properties in the boundary layer.

$$(h/U_t\rho c_p)[1 - (\xi_t/X_t)^{.9}]^{1/9} (T_w/T_\infty)^{.4}.$$

T_a	= Atmospheric temperature.
T_h	= Temperature of a spot heater.
T_w	= Temperature of the heated wall.
T_∞	= Free stream gas temperature.
U	= Local velocity.
U_d	= Velocity at the discriminating streamline.
U_m	= Maximum velocity in a plane turbulent wall jet [see Equation (6)].
U_m'	= Measured maximum velocity in the wall jet during fully-developed two-dimensional stall.
U_r	= Velocity of the reversed flow region during fully-developed two-dimensional stall.
U_t	= Throat velocity.
U_2	= $U_m/2$.
W	= Throat width.
X_t	= The equivalent distance from the diffuser throat, $\xi_t + \ell$.
X_b	= The equivalent distance from the diffuser exhaust, $\xi_b + \ell_b$.
x	= Surface distance from the beginning of the semi-cylindrical entrance surface.
x_t	= Surface distance from the beginning of the semi-cylindrical entrance surface to the edge of the adjoining plane-wall section.
λ	= An independent length variable having direction normal to the "wall of reversed flow" (see Figure 2).

δ_d	= Distance from "r" line to discriminating streamline in the η direction (see Figure 2).
δ_r	= Distance from "r" line to the "wall of reversed flow" in the λ direction (see Figure 2).
δ_{2r}	= Distance from "r" line to location of the U_2 streamline in the η direction (see Figure 2).
δ^*	= Boundary layer momentum thickness.
δ_t^*	= Momentum thickness at the junction of the semi-cylindrical and plane-wall sections.
η	= An independent length variable originating on the "r" line and having direction normal to the "wall of jet flow" (see Figure 2).
δ_{2w}	= Distance from the "wall of jet flow" to the location of the U_2 streamline in the η direction (see Figure 2).
θ	= One-half the total divergence angle.
ν	= Kinematic viscosity.
ξ_t	= Unheated starting length for boundary layer development on the diffuser entrance surface.
ξ_b	= Unheated starting length for the exhaust end of a diffuser wall subjected to reversed flow.
ρ	= Fluid density.

CONVECTION HEAT TRANSFER IN SEPARATED REGIONS - SUBSONIC DIFFUSERS

I. INTRODUCTION

A. The Problem

Predictions of heat transfer rates in separated flows (fluid stall) are important to many engineering design problems. For example, space vehicle or nuclear reactor components experiencing separated flow and relying on high heat transfer rates could fail if not sufficiently cooled. These cases provide the incentive for increased study of separated flow heat transfer during recent years.

The problem of determining convection heat transfer rates from the walls of subsonic diffusers was chosen for the present investigation because a review of the literature indicated very little information on this problem was available. Results from the present investigation should be of value to designers concerned with cases such as those mentioned in the foregoing.

B. The Selected Flow Geometry

A symmetrical, plane-wall, two-dimensional, subsonic diffuser was chosen as the configuration to be used for studying separated flow heat transfer. Predictions were made of the heat transfer coefficients for this configuration for different flow regimes

and a comparison was made with experimental results. Because the use of flow rates small enough to develop only laminar boundary layers would have allowed free convection to occur it was decided to limit the present study to turbulent flow with high enough velocity so that free convection would not be a problem.

The performance of a diffuser and the type of flow that can be developed in a diffuser depend mainly on the ratio of diffuser wall length to throat width and the total divergence angle. Consequently, an air-flow apparatus in which these parameters could be varied was designed.

In addition to providing instrumentation to determine local heat transfer coefficients on an isothermal wall, provision was made to allow for simultaneous flow visualization. Arrangements were also made for measuring fluid velocities in regions of fully-developed stall.

C. The Nature of Separated Flow

Usually, the term separated flow (stall) implies a region of vortex flow bounded by a surface called a bubble. This bubble is formed by a characteristic pattern of limiting flow streamlines. An open curve represents a streamline that is not within the stalled region or bubble, while a closed curve represents flow within the bubble. Thus, a region of fluid stall can be considered as a volume

of space enclosed by an imaginary shell-type surface which separates open-type streamline curves from closed-type.

When the methods for generating fluid stall are regarded, there are two that can be listed. The first is one in which there is a development of separation as a result of boundary layer and pressure field interactions. This concept was first introduced by L. Prandtl and involves the curvature of the fluid boundary layer at the location of stall initiation. In some cases, an adverse pressure gradient causes the boundary layer of a fluid moving along a wall to increase its thickness considerably. When the velocity gradient at the wall in a direction normal to the wall is zero, separation occurs. Associated with this there is a flow of boundary layer material into a region outside the boundary layer. The result is that the direction of flow is reversed at positions downstream from the location of zero velocity gradient. Consequently, at the location where separation begins, the pressure gradient at the wall in the direction of main flow changes from negative to positive. This occurrence may take place on geometries such as a smooth surface with large radius of curvature or on a flat plate that is sufficiently inclined to the direction of mainstream flow.

The second method for generating stall is one in which the wall has an abrupt change in curvature, such as a back step. In this instance separation occurs at the edge of the step and back flow is

present immediately downstream of the step. Also, the wall shear stress is not zero at the location of separation because of the discontinuity of the wall boundary. In the first method the velocity gradient is zero at the location where separation has initiated, so that fluid shear at the wall should also be zero, while the second method involves finite values of shear at the separation point.

Separated flow can be regarded as being influenced by three regions of flow. The region in which there is a transition from the maximum mainstream velocity to the reversed flow velocity is called the mixing region. The region of reversed flow is generally called the wake flow region. Thus, the three regions of flow are the mainstream flow region, the mixing region and the wake flow region.

Indeed, it should not be imagined that the stall bubble is always a steady phenomenon having definite size and shape. More times than not the bubble size and location are transient. When a stall bubble is being developed there is mass transfer from the main flow into the bubble, causing it to increase in size. The bubble may continue to increase in size until the dynamic forces of the mainstream cause it to be swept away and allow a new bubble to form, or its size could fluctuate by mass diffusion in and out of the bubble, or equilibrium conditions could be attained and the bubble could become relatively stationary.

A large number of attempts have been made to predict the location of stall from boundary layer equations and conditions. If the boundary layer is laminar, a prediction of the location and size of a separated flow region can usually be obtained within 20 percent of the actual values. In some cases, however, wall geometries are complicated, causing the prediction to be in error as much as 100 percent. When a turbulent boundary layer is present, predictions are much less successful. In fact, literature reviews indicate that adequate methods for predicting turbulent separations have not been developed, although a number of methods have been tried.

The accuracies stated in the foregoing statements are also valid for the predictions of the flow within a separation region. Velocity and pressure gradients for laminar flow in the separation vortex can be reasonably predicted, but the nature of turbulent separation is so complex that only very rough approximations have been made.

II. LITERATURE REVIEW

Presently available references concerned with separated flow are quite diverse. Even so, few are closely related to the configuration selected for the present investigation. However, many are useful in providing an over-all comprehension of the nature of energy and momentum transport in the subsonic diffuser. Some of these references are briefly discussed in the following.

A. Discussions of Generalized Separated Flows

Maskell (29; 30) described flow separation in three dimensions and the basic elements into which he believed separation could develop (i.e. the free vortex layer and the stall bubble). These elements were described as being created by the same conditions of flow and wall geometry, but each has different effects on the surrounding flow. It was explained that a free vortex layer is different from a bubble in that closed streamline curves do not exist in a free vortex layer, but they are present in a stall bubble. Also, streamlines forming the free vortex layer begin spiralling at some location on the fluid boundary and usually make up a large surface or sheet.

In addition, Maskell speculated that the free vortex layer can originate either on a wall surface or on the surface of a stall bubble (29, p. 11). He claimed that predictions of the qualitative nature of

separation from present theories are not satisfactory and that there is a need for theories which are more general.

Kline (22; 23) has made some timely presentations on the nature of stall. In his papers he compared the classical theory to actual cases. The physical data available on the problem of stall were reviewed. The discussion given by Kline was centered on the problem of flow in passages, particularly flow in two-dimensional subsonic diffusers. The three major types of flow patterns that can occur in a subsonic diffuser were discussed and the parameters used to classify these flow patterns were given. A discussion of these flow patterns is given in another part of the present dissertation.

B. Laminar and Turbulent Separations

An analytical development for determining the local laminar skin friction and velocity profiles in a cavity which has a wall curvature matching the streamlines of the wake flow region has been presented by Carlson (6). His method is a refinement of an earlier one developed by Chapman (7).

In Carlson's analysis a "dividing streamline" was assumed. This streamline forms the surface of a separation bubble. Carlson assumed that no fluid enters or leaves this "dead-air" region and, that for steady-state conditions, the energy transferred across this

streamline is equal to the energy transferred to the body surface.

The significant differences between Carlson's and Chapman's assumptions are that Carlson assumed that the thickness of the "dead-air" region below the "dividing streamline" is of the same order of magnitude as the thickness of the mixing region above this streamline. Chapman assumed that the surface in the separated region is an infinite distance away from the high velocity stream. In other words, the mixing-layer velocity and enthalpy profiles were assumed to be affected only slightly by the presence of the wall. In both Carlson's and Chapman's analyses, solutions were obtained by use of the integral method. Also, the results of both cases showed that the local friction coefficient is practically constant in the separated regions.

A doctoral thesis on the subject of dissipative mechanisms within separated flow regions was presented by Golik (19). Special consideration was given to turbulent, compressible, $Pr = 1$, mixing regions. With the use of integral methods he analytically solved for velocity profiles and friction coefficients in terms of a separation velocity. Experimental results from rectangular notches of various sizes were compared with analytical solutions.

Charwat, et al. (9) studied flow patterns and pressure distributions behind steps, wedges, cylinders and in notches. Analytical predictions were given and compared with experimental

measurements from compressible flow conditions. Flow patterns were observed in visual studies and were schematically described. Special attention was given to a rectangular notch.

Page (35) has estimated pressure coefficients for laminar and turbulent incipient separations with porous and non-porous walls. He suggested in his presentation that the solution of a flow field with separation involves the simultaneous interaction of the boundary layer before the separation point, the flow field after the separation point and the boundary conditions.

The generalized model which Page used is a two-dimensional wall boundary that may turn away from the main flow through an angle θ ($0^\circ < \theta < 180^\circ$) immediately at the separation point. At some location downstream from the separation point there is a pressure increase caused by either the geometry of the wall or another wall in the vicinity of the flow. Also, the wall may be curved or straight and it may be solid or porous. Through an analytical treatment, Page solved for pressure coefficients, C_p , in terms of Mach number, M , specific heat ratio, wall to mainstream temperature ratio, T_w/T_a , and the discriminating to main flow velocity ratio, U_d/U_a . The discriminating streamline was described as the boundary of the "dead-air" region (stall bubble) adjacent to the mainstream when mass does not pass across this boundary. The case of particular interest to the present study is when M

approaches zero and $T_w/T_a \cong 1$,

$$\lim_{M \rightarrow 0} (C_p) = (U_d/U_a)^2 = 0.3798 \quad (1)$$

This result was used in an analysis given in another part of the present dissertation.

C. Jets, Wakes and Mixing Regions

The case of a two-dimensional turbulent wall-jet, its velocity profile development and friction factor, has been studied experimentally and theoretically by Myers, et al. (33) and Schwartz and Cosart (46). The shearing stress, maximum velocity decay and jet thickness were predicted analytically by momentum-integral methods and compared with experimental measurements. The maximum velocity decay presented by Myers, et al., given in terms of the ratio of the distance from the jet to the jet width, was used in an analysis of diffuser flow and is given in another part of the present dissertation.

Theoretical developments for free turbulent flows in several types of jets and wakes have been presented in a text by Schlichting (45, Chap. XXIII). Velocity profiles and shear stress in the mixing regions which were estimated by theory are compared to physical measurements. Schlichting mentioned that empirical coefficients

used to predict velocities are valid only for the specific case for which they were determined. However, the parameters used in the correlation of velocities and curvature of velocity profiles in mixing regions were of general interest to the present problem of separated flow.

Sabin (42) has analytically and experimentally studied incompressible, turbulent, free shear-layers of two fluid streams having arbitrary velocities and arbitrary pressure gradients that have been brought together. Velocity profiles and mixing coefficients were given from theory and compared to measurements in water flow. The theory was an extension of the one given in the text by Schlichting (45, Chap. XXIII).

D. Boundary Layer Transition and Separation

The importance of the location of boundary layer transition on pressures in separated flow regions has been examined by Chapman, et al. (8). They considered the cases of pure laminar, pure turbulent and transitional separations (i.e. when the boundary layer becomes turbulent downstream of the reattachment point, upstream of the separation point or between these points). They have suggested that pressure distributions in pure laminar separation can be predicted from theory with less than ten percent error, but that errors of predictions for turbulent separation are excessive. Several geometries for inducing separation were studied

experimentally and it was found that: (a) Pressures up to the separation point do not depend on the mode of separation, (b) turbulent separations depend only slightly on Reynolds number and (c) transitional separations are very unsteady.

E. Heat Transfer Effects on Separation

Effects of heat transfer on the separation of laminar boundary layers in supersonic flow were considered theoretically and experimentally by Gadd (17). His theory indicated that cooling the wall reduces the extent of the region of separation and increases the pressure gradient, while heating the wall has opposite effects. It was shown that experimental results confirm these predictions.

F. Subsonic Diffusers

During the past decade several investigations have been carried out at Stanford University under the direction of S. J. Kline for the purpose of studying the characteristics of two-dimensional subsonic diffusers. Initially, pressure recovery, flow regimes and velocity distributions were determined for straight-wall diffusers, with and without vanes, by using separate water and air-flow experiments (11; 23; 24; 32). (These references were used extensively for determining the design and operation of the apparatus used for the present investigation.) The parameters having the greatest influence

on the diffuser flow regimes were listed as wall length to throat width ratio, total divergence angle and inlet turbulence level.

Figures 1a through 1d illustrate the flow regimes developed in the diffuser.

Additional tests were conducted with an air-flow apparatus (52) for the purpose of determining the effects of inlet conditions on diffuser flow regimes. Generally, a slight effect on diffuser flow regimes was detected by varying inlet boundary layer thickness or turbulence level. This is contrary to the observations from earlier water flow tests (32), but reasons for the difference were not given.

In addition, these same types of studies were conducted on two-dimensional, subsonic, curved diffusers (16). Curved diffusers were found to have the same general performance characteristics as the plane-wall diffusers.

Kline has discussed the structure of small transitory stall that was observed by dye studies in a subsonic diffuser (23, p. 32). In another writing (26) Kline and Runstadler described the wall layers of the turbulent boundary layer in an adverse pressure gradient as noted from dye studies. The pressure gradient was created by flow in a subsonic diffuser having the same configuration as the one Kline used to develop small transitory stall. They did not observe stall bubbles, which might be expected but, instead, transient vortex filaments. Their description of the filaments is as follows:

The pattern or flow model appears to consist of an array of 'islands of hesitation' and longitudinal vortexes which impart a wispy appearance to the flow; these are interspaced with areas of faster moving fluid. The islands of hesitation appear as long stretched filaments in the direction of flow which move downstream more slowly than the surrounding fluid. The vortexes apparently originate as a breakup or roll-up along the edges of the islands of hesitation. The primary orientation of the vortex elements is longitudinal, that is, in the flow direction, but each vortex stands at a slight angle to the wall so that its distance from the wall increases as it moves downstream. After the vortex element reaches a certain critical distance from the wall, . . . , it breaks up into a typical turbulent hash by a process too rapid for the eye to follow.

Runstadler, et al. (41) have presented more information on the turbulent wall layer structure in a recent presentation.

Persh and Bailey (36) experimentally investigated a 23 degree, conical, air-flow diffuser that was found to behave much like the plane-wall diffuser. Velocity profiles, momentum thicknesses and pressures were determined. Persh and Bailey found that a surface roughness applied a short distance downstream of the diffuser throat had very definite stabilizing effects on the flow. That is, experimental results could be more closely duplicated.

G. Heat Transfer in Separated Regions

Carlson (6) and Chapman (7) have theoretically analyzed heat transfer through cavities. (These references are the same ones that were discussed on page 7.) Larson (28) tested the validity of

Chapman's theory by experimental measurements. The theory was found to agree very well with results from cases of laminar flow, but it agreed poorly with results from cases of turbulent flow.

Larson stated that the average heat transfer for both turbulent and laminar separated flow in his model were approximately 30 to 50 percent less than the case having equivalent attached boundary layers. Chapman's theory indicated that the turbulent separated flow heat transfer should be approximately six times greater than for laminar flow.

Larson measured temperatures across the cavity during turbulent flow and found that the temperature on the cavity side of the mixing region was between the wall temperature and the free stream temperature. One of Chapman's assumptions was that the temperature on the cavity side of the mixing region is equal to the wall temperature.

Carlson's analysis was for laminar separations, but effects of the mixing region on energy transport were included. Predicted and experimental heat transfer values were compared in Carlson's presentation and good agreement was shown. However, the agreement appeared to be only slightly better than the comparison between Chapman's theory and Larson's data.

A discussion of heat and mass transfer in turbulent separated flows has been given by Richardson (39). He concluded that these

transport phenomena are proportional to the $2/3$ power of Reynolds number. He determined this relation from experimental results for flow past spheres, cylinders and bluff bodies.

Experimental measurements of heat transfer in subsonic flows downstream of a surface step were made by Seban, et al. (47). They found that heat transfer depends on the 0.8 power of velocity in the separated region and that heat transfer rates are a maximum at the point of boundary layer reattachment.

Heat transfer, heat diffusion and flow patterns in rectangular notches of various sizes were experimentally investigated by Charwat, et al. (10). They found that heat transfer in the cavity when a thin boundary layer was present at the separation point was less than when there was a thick boundary layer.

Miles (31) has extended the work of Golik (19) by predicting and measuring Stanton numbers in notches and cavities. He showed that the local Stanton number is inversely proportional to the local Reynolds number to the 0.2 power.

H. Heat Transfer in Nozzles and Jets

A convergent-divergent nozzle was tested by Saunders and Calden (43) at subsonic and supersonic flows. They found that the Nusselt number depended approximately on the 0.8 power of the Reynolds number when the length involved in these parameters was

the distance from the nozzle entrance. Ragsdale and Smith (37) made the same measurement in another nozzle and found the same relationship.

An approximate solution of the heat transfer for compressible turbulent boundary layers in convergent-divergent nozzles has been developed by Bartz (2). The heat transfer coefficient was given in terms of the boundary layer thickness and had to be solved numerically. A good agreement between coefficients predicted by Bartz's method and coefficients from experimental results has been shown in the presentation by Ragsdale and Smith (37).

Myers, et al. (34) have theoretically and experimentally studied the problem of heat transfer from the plane turbulent wall jet. They found that the Nusselt number depends not only on the 0.8 power of the jet Reynolds number, but also on the ratio of the distance from the jet nozzle to the nozzle width.

I. Heat Transfer Correlations for Flat Plates

The predictions of heat transfer measurements obtained from the present investigation were determined with the aid of a correlation expressing heat transfer from a flat plate. A method of correlation that was useful was given in a recent article presented

by Reynolds, et al. (38). Correlations were given for turbulent heat transfer from non-isothermal flat plates. In particular, the case of an isothermal plate with an unheated starting length and a step temperature rise was of interest.

III. FLOW IN SUBSONIC DIFFUSERS

Before presenting predictions of heat transfer from the diffuser walls, the regimes of flow that may occur will be described. As mentioned on page 7, Kline, et al., have defined the flow regimes for straight-wall diffusers as governed by wall length to throat width ratio, L/W , and total angle of divergence, 2θ . These regimes are illustrated in Figure 1a and are called, respectively, beginning from the bottom of the figure: No "appreciable" separation, large transitory stall, fully-developed two-dimensional stall and jet flow. Figures 1b through 1d illustrate streamlines that occur during these flows.

The nature of flow expected to occur in the diffuser during each flow regime is as follows:

No "Appreciable" Separation -- This is the region lying below curve a-a in Figure 1a. In this region dye streamers always show an apparently unseparated flow, but close observations of the wall layers reveal that small isolated spots of separation are sometimes present even to very low divergence angles. The spots occur individually and are greatly affected by mainstream disturbances. They are transient and have a very short duration, but as the divergence angle of the diffuser is increased they grow steadily in size and duration. It is believed that this type of separation involves only the

wall layers of the fluid boundary layer (sublayer and buffer layer) and is apparently an inherent part of the structure of a turbulent boundary layer with moderate and strong adverse pressure gradients (22, p. 308)(see page 13). The terminology - no "appreciable" separation - implies that the small spots of stall do not affect the mainstream flow.

Another aspect of the line a-a is that it nearly corresponds to the conditions required for maximum pressure recovery (22, p. 310).

Large Transitory Stall -- As the divergence angle is increased from the line a-a, in Figure 1a, into the large transitory stall regime, the separations become more persistent. In other words, they are not as readily washed away by the main flow. The small areas of stall accumulate into large areas of stall, forming stall bubbles that persist for relatively long periods of time. As the stall bubble grows in size it moves upstream considerable distances before being washed away. As one might expect, the average size of stall bubbles when near the no "appreciable" separation regime shown in Figure 1a is usually smaller than when near the fully-developed two-dimensional stall regime. The large transitory stall regime is thus characterized by large-scale unsteadiness that is three-dimensional in nature and involves at least a major portion of the entire flow.

Fully-Developed Two-Dimensional Stall -- The flow pattern for this regime is that of an asymmetrical, fully-developed, steady

stall as shown in Figure 1d. The particular wall on which stall occurs is arbitrary and is determined by some very small initial effect that is very difficult to distinguish. The location of the stall bubble is bistable in that it remains indefinitely on the side on which it was formed until it is forced to change position by a change in flow geometry.

The flow in this type of stall is only relatively steady. That is, the flow is transient but has much less fluctuation than the flow in a large transitory stall. The fully-developed stall bubble may fluctuate in size, but it does not collapse as does the transitory stall bubble. Some unsteadiness is developed in the mixing region between the reversed and main flow areas. However, separation becomes increasingly more stable as the divergence angle is increased toward the center of the fully-developed two-dimensional stall regime (22, p. 308).

In conical diffusers the stall area is reasonably stable in axial movements, but since there are no side walls to contain the stall bubble, it rotates about the centerline of the diffuser. Streamlines representing the flow in this case become spiral vortices.

It has been speculated (23, p. 49) that the fully-developed stall is the result of the unstable growth of a spot of stall. In other words, the time average rate of production of stall over a given area of wall exceeds the average ability of the locally available momentum of the

mainstream to remove the stalled fluid. Once such an action commences it can be expected to continue until a large region of stall or wake area is developed. When the size of the separation area becomes stabilized, the rate at which stalled fluid is produced equals the rate at which it is swept away. This description agrees with observations of flow past airfoils and in diffusers.

Jet Flow -- This flow pattern is also relatively stable. However, the main flow is no longer attached to either of the diverging walls after emerging from the diffuser throat. Steady stall regions exist on both walls of the plane-wall diffuser, or, in the case of a conical diffuser, steady stall completely encompasses the main flow. A rather large hysteresis zone exists for transition from fully-developed stall to jet flow. When the divergence angle is increased, the transition to jet flow occurs at a larger angle than when shifting from jet flow to fully-developed stall by decreasing the divergence angle.

The position of the transition lines given in Figure 1a is expected to be dependent upon variables other than those used for the axes of the graph. When Reynolds number, based on throat width and mean throat velocity, ranges from 6000 to 300,000, flow regimes are only weakly dependent on parameters such as Mach number, throat aspect ratio and Reynolds number. Other than the variables 2θ and L/W , inlet turbulence level has been found to have the greatest effect

on the establishment of the flow regimes. A study of this effect has been made in a water-flow apparatus, but not in an air-flow apparatus (51). The effect of an increase of turbulence level in the diffuser is to broaden the large transitory stall regime at the expense of the no "appreciable" separation regime and the steady two-dimensional stall regime. Apparently the transport of momentum toward the wall from the central core of the flow caused by large scale disturbances in the main-flow has the effect of aiding spots of stall to develop (32, p. 63).

Because the lines drawn in Figure 1a were established by an observer deciding which type of flow was present, it might seem that the results from one individual would be different from the results of another individual. However, the flow regime chart developed by Kline, et al. was determined from data given by several observers and the results were always essentially the same.

IV. PREDICTIONS OF TURBULENT HEAT TRANSFER IN STRAIGHT-WALL TWO-DIMENSIONAL DIFFUSERS

The present investigation is concerned with predicting the heat transfer coefficients in three of the regimes of flow that are encountered in subsonic diffusers and verifying such predictions.

These regimes, no "appreciable" separation, large transitory stall and fully-developed two-dimensional stall, are discussed in the foregoing section. Because the fluid movement in a diffuser is established by the regimes of flow, heat transfer predictions are presented for each regime.

A. Non-Separated Flow (No "Appreciable" Separation)

When the divergence angle of the diffuser is such that no separation occurs, then the local heat transfer is expected to be expressible in a Colburn type correlation. That is,

$$St = aRe_x^{-b} \quad (2)$$

The value of "b" for a turbulent boundary layer is listed at 0.2 in References 37 and 43 which present the results of experiments conducted on nozzles. Saunders and Calden (43) found the value of "a" to be 0.0285 when Reynolds number was based on the distance from the nozzle throat and the mean local velocity. However, Ragsdale and Smith (37) found the value of "a" to be 0.0292 when the

Reynolds number included the distance from the nozzle entrance and the mean local velocity. In either case, when these values for "a" and "b" are applied to Equation (2) it closely resembles the equation predicting the heat transfer coefficients for a flat plate with a turbulent boundary layer. From these considerations, it is believed that when there is no "appreciable" separation in the diffuser, heat transfer from the walls may be closely approximated with the equation representing heat transfer from a turbulent flat plate if the change in mainstream velocity is taken into account.

The results of a recent study of heat transfer from a turbulent flat plate given in Reference 38 are correlated to include effects of Prandtl number, a non-isothermal wall condition and the variation of fluid properties in the boundary layer. The relations given in Reference 38 were used to predict heat transfer in a diffuser during non-separated turbulent flow. For the case of a step temperature rise on an isothermal wall the equation is:

$$\text{Nu}_{x_t} (T_w/T_\infty)^{.4} [1 - (\xi_t/X_t)^{.9}]^{1/9} = .0296 \text{Pr}^{.6} \text{Re}_{x_t}^{.8}$$

or

$$\text{St} \text{Pr}^{.4} (T_w/T_\infty)^{.4} [1 - (\xi_t/X_t)^{.9}]^{1/9} = .0296 \text{Re}_{x_t}^{-.2} \quad (3)$$

It must be understood that the velocity in the above equation should be the mean local velocity. For the present straight-wall two-dimensional diffuser having a small angle of divergence this

velocity was determined by

$$U = \frac{U_t}{1 + 2(\ell/W) \sin \theta} \quad (4)$$

B. Fully-Developed Two-Dimensional Stall

During a condition of fully-developed two-dimensional stall the main fluid stream entering the diffuser through its throat attaches to one of the two divergent walls in a manner very similar to a plane wall jet (see Figures 1d, 2a and 2b). The other divergent wall encounters stall or fluid moving in a direction reversed to the main flow. Heat transfer from these two walls is therefore influenced by two separate fluid flows. Consequently, separate predictions of the heat transfer coefficient for the two walls should be determined for each wall. The wall exposed to fluid entering the diffuser through its throat is referred to as the "wall of jet flow." The wall exposed to the stalled fluid is referred to as the "wall of reversed flow." The "wall of jet flow" will be discussed first.

As mentioned on page 17 of the foregoing, Myers, et al. presented predictions for heat transfer coefficients (34) and velocity distributions (33) for a plane turbulent wall jet. Experimental data taken by Myers, et al. showed that their prediction of heat transfer coefficients was too large for ratios of distance from the jet exhaust to the jet nozzle width (ℓ/W) less than 25. Their prediction of the

maximum velocity along the wall states that the maximum velocity along the wall does not change between the jet nozzle exhaust and $\ell/W = 7$, but beyond the position $\ell/W = 7$ it decreases. The prediction of the maximum velocity at positions downstream from $\ell/W = 7$ agreed well with experimental data.

Because the flow along the "wall of jet flow" appeared to be much like jet flow past a flat plate, it was assumed that the maximum velocity variation along the diffuser wall was the same as in the case of the wall jet. It was assumed that heat transfer from the diffuser "wall of jet flow" was like heat transfer from a flat plate. Using these assumptions as a basis, the correlation of heat transfer from a turbulent flat plate was used to predict heat transfer coefficients for the diffuser, taking into account the decrease in the maximum velocity. Equation (3) was again used and written as

$$Nu_{x_t} (T_w/T_\infty)^{.4} [1 - (\xi_t/X_t)^{.9}]^{1/9} = .0296 Pr^{.6} Re_{x_t}^{.8} U_m \quad (5)$$

Wherein the maximum velocity along the "wall of jet flow," U_m , was introduced and determined by Myers', et al. predicting Equation (32). Their equation is expressed as

$$U_m/U_t = \left\{ \begin{array}{ll} 1 & \text{for } \ell/W < 7 \\ [1 + .381(\ell/7W - 1)]^{-1/2} & \text{for } \ell/W > 7 \end{array} \right\} \quad (6)$$

The reason the wall jet correlation given by Myers, et al. should not be used to predict heat transfer coefficients in the diffuser is that the largest value for l/W in the diffuser used for the present study was 18. As discussed by Myers, et al. (34) the presence of large-scale turbulence in a wide mixing region, when far downstream from the jet nozzle, causes the ratio of the thermal eddy diffusivity to the momentum eddy diffusivity to be larger than for a flat plate. At wall positions near the jet nozzle this ratio is nearly the same as for a flat plate because the width of the mixing region is less and the mixing region is farther from the wall. Consequently, the heat transfer should be more closely predicted by a flat plate correlation than by a wall jet correlation.

Flow over the "wall of reversed flow" was also similar to flow over a flat plate. Thus, it was assumed that the heat transfer from this wall could be predicted by the correlation for heat transfer from a turbulent flat plate providing the velocity of the reversed flow could be approximated.

A theoretical determination of the reversed flow velocity was not made because of the lack of information concerning fluid shear stresses and pressure forces in the diffuser. Instead, an integral approach was made using expressions for an experimentally determined nondimensional velocity profile. Experimental results from the present investigation showed that for a given diffuser geometry

the reversed flow velocity appeared to be nearly constant throughout the separation region. Also, the velocity profile in the mixing region within the separation bubble was a linear function of the distance into the mixing region. The details of the prediction are given in the following:

A control volume, as shown in Figure 2b, was selected and a surface integral of the conservation of mass during steady two-dimensional flow was written for this control volume. The resulting integral equation was:

$$\oint^{cv} \rho \mathbf{U} \cdot d\mathbf{A}_f = 0$$

Fluid density in the stall region was essentially constant, therefore the density term, ρ , was eliminated. Also, by making use of the parameters shown in Figure 2b, the foregoing equation was written

$$\int_0^{\delta_d} U d\eta = \int_0^{\delta_r} U d\lambda \quad (7)$$

The variable η has its origin on the "r" line and its direction is normal to the "wall of jet flow." The direction of λ is normal to the "wall of reversed flow" and begins on the "wall of reversed flow."

An expression for the velocity profile in the mixing region was needed for the left hand side of Equation (7). This profile could not

be predicted because the prediction required an expression for fluid shear stress which included empirical parameters. Such information on velocity profiles in subsonic diffusers with fully-developed stall could not be found in the literature. Consequently, the velocity profile in the mixing region was determined from velocity measurements in the diffuser used for the present study. It was found that for any location along the "wall of jet flow," the mixing region velocity profile within the separation bubble (see Figure 10) can be expressed as

$$U/U_m = .5\eta/\delta_{2r} \quad (8)$$

Equation (6) was used to predict the value of the maximum velocity of the flow along the "wall of jet flow," U_m , required in Equation (8) in order to solve for the velocity U . The term δ_{2r} is the distance from the "r" line to the velocity vector U_2 in the η direction. The velocity U_2 is defined as $U_m/2$, while the "r" line is a line separating reversed flow streamlines from mixing region streamlines (see Figure 2a).

The magnitude of δ_{2r} was determined from velocity measurements in the diffuser and was expressed as

$$\delta_{2r}/D = .093l/D + .063 \quad (9)$$

The "d" line, also called the discriminating streamline (35, p.566) separates streamlines passing through the diffuser throat from all other streamlines representing flow in the diffuser. The

results of an analysis presented by Page (35) were used to predict the velocity on the discriminating streamline, U_d , at the diffuser exhaust (refer to page 9). At this location a sudden pressure increase resulted from the wall geometry, which was a necessary condition for establishing Equation (1). Thus, Equation (1), as written in the following, was used to predict U_d , at the diffuser exhaust.

$$U_d/U_m = 0.616 \quad (1)$$

Equation (6) was used to predict the value of U_m required in Equation (1) after substituting L for ℓ . This substitution changes Equation (6) to

$$U_m/U_t \Big|_{\ell=L} = \left\{ \begin{array}{ll} 1 & \text{for } L/W < 7 \\ [1 + .381 (L/7W - 1)]^{-1/2} & \text{for } L/W > 7 \end{array} \right\} \quad (10)$$

The magnitude of δ_d , the distance from the "r" line to the "d" line in the η direction (when $\ell = L$) was approximated by changing η to δ_d and U to U_d in Equation (8) and then substituting the relations for U_d and δ_{2r} from Equations (9) and (1) into Equation (8). The resulting expression is

$$\delta_d/D = .1146 L/D + .0776 \quad (11)$$

The left hand side of Equation (7), when the relation for U is

taken from Equation (8) and U_d and δ_d are determined from Equations (1) and (11), becomes:

$$\begin{aligned} \int_0^{\delta_d} U d\eta &= U_d \delta_d / 2 \\ &= (.0353 L + .0239 D) U_m \end{aligned} \quad (12)$$

The boundary layer thickness on the "wall of reversed flow" near the diffuser exhaust was small when compared to δ_r , thus the right hand side of Equation (7) was approximated by writing

$$\int_0^{\delta_r} U_r d\lambda \cong U_r \delta_r, \quad (13)$$

wherein U_r is the reversed flow velocity outside the wall boundary layer.

Equations (12) and (13) were equated to give the following results:

$$U_r / U_m = (.0353 L + .0239 D) / \delta_r \quad (14)$$

The length of δ_r was related to other known lengths in the diffuser (see Figure 2c). Specifically,

$$W + [L + (\delta_{2w} + \delta_{2r}) \tan \theta] 2 \sin \theta = (\delta_r + \delta_{2r} + \delta_{2w}) / \cos \theta$$

or (15)

$$\delta_r = \{W + [L + (\delta_{2w} + \delta_{2r}) \tan \theta] 2 \sin \theta\} \cos \theta - (\delta_{2r} + \delta_{2w})$$

All of the quantities in this equation, except δ_{2w} , have been

discussed. Myers, et al. (32) predicted the value of δ_{2w} for the plane turbulent wall jet. Their results were used to predict δ_{2w} in the flow past the "wall of jet flow." For large values of throat Reynolds number ($Re_w > 10^4$) Myers', et al. prediction is

$$\delta_{2w}/W = 1.33(U_m/U_t)^{-2} \quad (16)$$

Equation (14) was written as a functional relationship:

$$\frac{U_r}{U_t} = f \left[\frac{W}{L}, \frac{D}{L}, \theta \right]$$

$$= \frac{(.0353 + .0239 \frac{D}{L}) [1 + .381 (\frac{L}{7W} - 1)]^{-1/2}}{\left\{ \frac{W}{L} + [1 + (.1654 + .063 \frac{D}{L} + .8233 \frac{W}{L}) \tan \theta] 2 \sin \theta \right\} \cos \theta - .1654 - .063 \frac{D}{L} + .8233 \frac{W}{L}}$$

for $\frac{L}{W} > 7$ (17)

$$= \frac{(.0353 + .0239 \frac{D}{L})}{\left\{ \frac{W}{L} + [1 + (.093 + .063 \frac{D}{L} + 1.33 \frac{W}{L}) \tan \theta] 2 \sin \theta \right\} \cos \theta - .093 - .063 \frac{D}{L} + 1.33 \frac{W}{L}}$$

for $\frac{L}{W} < 7$

(See Figure 13b for a graphical presentation of $f(W/L, D/L, \theta)$).

The ratio D/L was a constant for the apparatus used in the present investigation. Therefore, Equation (17) was reduced to the following:

$$\frac{U_r}{U_t} = \frac{.03769[1 + .381(\frac{L}{7W} - 1)]^{-1/2}}{\left\{ \frac{W}{L} + [1 + (.182 + .8233 \frac{W}{L}) \tan \theta] 2 \sin \theta \right\} \cos \theta - .182 + .8233 \frac{W}{L}}$$

for $\frac{L}{W} > 7$

$$\frac{.03769}{\left\{ \frac{W}{L} + [1 + (.1096 + 1.33 \frac{W}{L}) \tan \theta] 2 \sin \theta \right\} \cos \theta - .1096 + 1.33 \frac{W}{L}}$$

for $\frac{L}{W} < 7$

Heat transfer from the "wall of reversed flow" was predicted in terms of the foregoing equation and the throat velocity, U_t .

$$Nu_{x_b} (T_w/T_\infty)^{.4} [1 - (\xi_b/X_b)^{.9}]^{1/9} = .0296 Pr^{.6} [Re_{x_b} U_t f(\frac{W}{L}, \frac{D}{L}, \theta)]^{.8} \quad (18)$$

Note that the function $f(W/L, D/L, \theta)$ effectively causes the Reynolds number to be in terms of the reversed flow velocity, U_r . The quantities X_b and ξ_b are distances from the diffuser exhaust (or bottom) in the direction parallel to the "wall of reversed flow."

C. Large Transitory Stall

A prediction of heat transfer for the case of unsteady separating boundary layers cannot be accomplished unless time-dependent values such as the location of the stall bubbles, the velocities in the

stall bubbles and the mass transfer rate into the stall bubbles are known. Because transitory separations are random in frequency and position, a rigorous analysis could not be made.

During conditions of very rapid development and elimination of stall areas, the development of the wall boundary layers was interrupted. Because of this interruption, it was believed that heat transfer coefficients for large transitory stall conditions would be greater than they would be if flow had been achieved in the same geometry without separation.

V. EXPERIMENTAL PROGRAM

A. Scope

An apparatus was constructed to allow both heat transfer and fluid flow studies in two-dimensional air-flow diffusers. The design of an air-flow apparatus developed by Cochran and Kline (11, p. 94) was closely approximated. The diffuser used for the present study had longer diverging walls than Cochran and Kline's apparatus. Also, screens and honeycomb were placed above the diffuser entrance.

The geometry of the diffuser was adjustable so that values of L/W could range from 6 to 18 and the total divergence angle could be set between zero and 45 degrees. Reynolds number based on throat velocity and throat width ranged from approximately 40,000 to 300,000.

Heat transfer measuring devices were used for determining both time averaged and time dependent values. Flow visualization techniques and velocity measurements were carried out to verify flow regimes and velocity distributions inside the diffuser.

B. Experimental Apparatus

Over-all Description:

Schematic diagrams showing nominal dimensions are given in Figures 3a and 3b. The complete system, beginning at the air inlet,

consisted of honeycomb flow straightener, screens, diffuser assembly, a large plenum, piping, flow measuring orifice, axial flow fan, small plenum, centrifugal fan and exhaust.

Flow was visualized by means of tufts attached to the diffuser walls and by smoke streamers that were initiated above the diffuser inlet.

One of the diverging walls contained instruments for measuring heat transfer rates. This wall was a 3/8-inch thick aluminum plate heated by ten electrical strip-heaters. The devices for measuring heat transfer rates were inserted in 1/2-inch diameter holes located between these heaters.

Descriptions of the equipment is given in more detail in the following:

Diffuser Assembly:

The diffuser was formed principally from two parallel, 1/2-inch thick plexiglass walls and two diverging walls. One of the diverging walls was a 1/2-inch thick plexiglass plate and the other was a 3/8-inch thick aluminum plate with heat transfer equipment attached.

The diverging walls were 24-inch by 36-inch plane sections with a 9 1/2-inch diameter semi-cylindrical section attached to the top end and a four-inch diameter semi-cylindrical section attached

to the bottom end of each. The semi-cylindrical sections were made of rolled 18-gauge sheet metal and each was joined to one of the plane sections so that the surface of the plane section was tangent to the surface of the semi-cylindrical section at the line of contact. Thus, a smooth transition was formed. Cracks in the joints were filled with cement and then sanded down in order to attain a smooth surface.

The diverging walls were pivoted about shafts positioned at the axial centerline of each semi-cylindrical entrance section. These shafts were held by bearing mounts that could be positioned horizontally in order to change the throat dimension. Divergence angles could be changed without disturbing the throat dimension.

Results of preliminary tests on the diffuser indicated that when the laminar boundary layer on the entrance section made an early transition to a turbulent one, the flow in the diffuser was somewhat stabilized and test results were more repeatable. Without this stabilizing effect the lines separating the regimes of diffuser flow in Figure 1a were not very definite. Several methods of "tripping" the boundary layer were investigated, such as attaching wires, tapes and narrow strips of sand grains that were adjustable in position. The best configuration was found when the entire surface of both semi-cylindrical entrance sections, except a two-inch wide strip preceeding the plate-cylinder joints, were covered with 20 by 30 mesh, Ottawa Standard sand grains at an average surface density of approximately

300 grains per square inch. These grains were attached by first applying varnish to the surface, then sprinkling on the sand grains. After the varnish had hardened more varnish was brushed on. The sand grains projected approximately .015 to .020 inches above the surface.

Near the bottom end of the diffuser, sliding panels were butted against the outer surface of the diverging walls to allow air to enter only through the throat. All edges of the diverging walls and sliding panels were fitted with rubber strips in order to help form an air-tight seal. Tie rods which passed through the parallel diffuser walls were tightened to complete the seal.

The air that discharged from the diffuser then passed through a two-foot by four-foot section that was two feet long. Two sides of this section were a continuation of the parallel plexiglass walls of the diffuser.

Flow Control Equipment:

Above the inlet of the diffuser there was a 72-inch by 30-inch section containing six screens, spaced two-inches apart, and a section of aluminum honeycomb on top of the screen assembly. The bottom screen was placed 14 inches above the topmost part of the semi-cylindrical sections which formed the diffuser inlet. The screens were enclosed with paneling in order to channel the flow of

air. The aluminum honeycomb section was 2 1/2-inches thick with 3/8-inch wide cells and the screens were 0.010-inch diameter fiberglass filaments spaced at 250 mesh per square inch.

The size of the section containing the screens was established so that the Reynolds number based on filament diameter and mean air velocity between the filaments was always less than 55, assuring that no large disturbances were produced.

Before the screens and honeycomb were installed on the diffuser an examination of smoke filaments which originated several feet above the diffuser entrance showed that large-scale disturbances in the atmosphere, caused possibly by convection currents or physical obstructions to flow, created highly turbulent flow inside the diffuser. After the screens and honeycomb were added these disturbances were very greatly reduced.

The large plenum on which the diffuser section rested was 6 1/2-feet high and was five feet by five feet in cross section. Across the middle of it, in a horizontal direction, there were two layers of 250-mesh fiberglass screen, having a four-inch spacing. These screens were used to reduce the effect of the outlet duct location on the diffuser discharge (see Figure 3a).

An 18-inch diameter metal air-duct was attached to the plenum by a fairing section. On the centerline of the duct inside the plenum was a large cone-shaped device that could be moved in or out of the

fairing section for fine control of flow. Near the entrance of the air duct a bundle of three-inch diameter by 30-inch long aluminum tubes was inserted to form flow straighteners.

The length and diameter of the air duct were determined in accordance with A.S.M.E. Fluid Meter Codes (1, 49), as was the design and calibration of the flange-tap, flat plate, sharp-edged orifice plates. Three orifice plates (3-, 7 1/2- and 13-inch hole diameters) were available so that one could be selected for developing a pressure drop of at least 1/2-inch water but yet so the diameter was large enough to allow the required flow rate to occur.

Connected to the exhaust of the air-duct system were a 24-inch I.D. vane-axial fan, a four-foot cube plenum chamber, a centrifugal fan and an exhaust duct leading to a window. The small plenum was installed so that a separate air-flow apparatus, not concerned with the present experiment, could be operated by the centrifugal fan. Air was exhausted outside the building so that during flow visualization tests the atmosphere would not become congested with smoke.

Heat Transfer Equipment:

The aluminum wall of the diffuser was heated with ten 2 1/2-inch wide by 3/8-inch thick by 24-inch long electrical strip heaters which were positioned laterally and separated by one-inch wide by 3/8-inch thick by 24-inch long aluminum bars. All joining surfaces

of these items were heavily coated with varnish before assembly in order to reduce their thermal contact resistance. They were clamped to the aluminum plate by cap screws (see Figure 4).

The separation of the strip heaters by the aluminum bars caused a temperature variation of the aluminum plate surface exposed to the airflow. This variation (in the direction of flow) was estimated by measurements with an electrical analog. The results of the analog study, illustrated in Figure 7, were determined for an extreme case of cooling. The graph shows that the surface temperature should not vary more than 0.8 percent of the gross temperature difference between the plate and the air. This difference was small enough so that the plate could be considered isothermal.

Spot heaters, which measured steady-state heat transfer rates, were positioned in holes drilled through the aluminum bars and plate so that they were flush with the plate's surface on the flow side (see Figure 5). These heaters were located in 28 positions (see Figure 4) so that experimental data from them could be studied for variations in the heat transfer coefficient with respect to lateral and longitudinal positions on the wall.

The spot heaters were made by wrapping ten feet of 0.010-inch diameter constantan wire on a cylindrical copper mandrel (see Figure 5). (Constantan wire was used because it has a very low temperature coefficient of electrical resistivity.) The heater wire

was heavily covered with electrical varnish while being wrapped on the copper mandrel and then later oven-baked in order to assure a good thermal bond to the copper mandrel.

Twelve inches of 0.008-inch diameter coiled copper lead wire was attached to each end of the constantan wire. A copper-constantan thermocouple junction with 12 inches of coiled lead wires was soldered to the copper mandrel. Cotton wool and a Teflon holder were used to provide insulation between the heater and the aluminum plate. The heater and thermocouple lead wires were coiled inside the Teflon holder in order to reduce the heat loss along these wires.

A thermocouple junction was placed near each spot heater in the aluminum plate. Their locations are indicated by a "+" in Figure 4. Additional details are shown in Figure 5. Also, ten thermocouple junctions were placed in the plate at the intersections of the plate centerline and the strip heater centerline. The use of these thermocouples allowed temperature surveys of the plate to be made so that the power to each strip heater could be adjusted until a nearly isothermal condition was obtained.

The a.c. voltage supplied to each strip heater was controlled by an individual auto-transformer, and the d.c. voltage supplied to each spot heater was controlled by a 50-ohm rotary voltage divider. Two six-volt wet-cell storage batteries, connected in parallel, supplied power to these voltage dividers. The d.c. voltage applied to

each spot heater was measured by a null-balance, millivolt potentiometer through a fixed voltage divider. Thermocouple outputs were measured with the same instrument. Temperatures associated with thermocouple outputs included: The difference between the aluminum plate temperature under each strip heater and the ambient air temperature, the difference between each spot heater temperature and the ambient air temperature and the difference between each spot heater temperature and the temperature indicated by the thermocouple placed adjacent to each spot heater in the aluminum plate. All the electrical meters and controls were mounted on a single control panel (see Figure 3c).

Transient heat meters were fashioned according to the descriptions given in Reference 18 (see Figure 5). A 0.002-inch thick constantan foil was attached on the end of a copper cylinder with a low temperature solder. The 0.010-inch diameter copper lead wire attached to the center of the foil was peened to approximately .001-inch thickness, then trimmed to 1/32-inch width before spot welding to the foil. This was done to keep the mass affected by transient temperatures small. The thickness of the foil and diameter of the hole in the copper cylinder were pre-determined so that the millivolt output of each heat meter was large enough to be recorded by the metering equipment. These dimensions limited the time constant of the heat meters to approximately one second. The meters

were located in five positions so that variations in heat transfer in different areas of the plate could be compared (positions 2, 11, 15, 19 and 26 in Figure 4).

Flow Visualization Equipment:

Smoke streamers and tufts were used to observe flow patterns in the diffuser. The tufts were fashioned according to a suggestion given by Shapiro (48). They were made of white cotton string tied loosely to wire loops that were normal to the wall and the direction of flow. These loops were fastened down with plastic tape. The two free ends of the string were approximately one-inch long and could point freely in either the upstream or downstream direction without restrictions. These tufts were located at 54 positions on each diverging wall (see Figure 3c).

Smoke was produced by a specially designed generator (see Figure 6) which worked very successfully. Mineral oil was used instead of the usual kerosene, because it is less toxic and less combustible. The mineral oil smoke was as visible in all respects as the kerosene smoke.

The smoke traveled through three long tubes to the inlet of the apparatus where it was discharged through 1/8-inch diameter steel tubes which were placed against the top screen of the flow inlet assembly. (The tubes can be seen positioned above the diffuser inlet in Figure 3c.) Also, smoke was injected at the exhaust of the diffuser

in order to observe reversed flow during fully-developed stall.

Continuous lighting of the smoke streamers was provided by a light box containing four 300-watt reflector spot lamps. The light box was positioned on one of the sliding panels so that light could pass through the plexiglass diverging wall. Photographs of the smoke streamers were recorded with a 35 mm, single lens reflex camera. This was done at night so that daylight reflections would not interfere. Kodak Royal-X film having an ASA rating of 1200 was used, developed and printed according to standard procedures supplied by the film manufacturer.

C. Experimental Procedures

Flow Studies:

Tuft movements were noted in order to establish the lines that separate flow regimes shown in Figure 1a. When the tufts pointed steadily downstream the flow was recorded as no "appreciable" separation and when they pointed steadily upstream the flow was recorded as a steady stall. Unsteady movements of the tufts in any direction were considered as an indication of transitory stall.

The diffuser flow regimes were established, during both heated and unheated wall conditions, when Reynolds number based on throat width and throat velocity ranged from approximately 40,000 to

300,000. For each setting of divergence angle and throat width the flow rate was started from zero, and the tufts were observed for several minutes before recording observations. The tufts on both diverging walls were removed before heat transfer measurements were made.

A fluid stall condition was recorded when smoke streamers were noted to be skewing or bending. Smoke studies were made both before and during heat transfer tests, but the light box lamps were not used at this time.

Velocity measurements were made during fully-developed two-dimensional stall by traversing a 1/8-inch diameter pitot-static tube across the non-separated flow region in a direction normal to the "wall of jet flow" along the wall centerline at four locations ($\ell = 6, 12, 18$ and 29 inches). The shaft of the pitot-static tube passed through holes drilled in the plexiglass diverging wall and pressures were read with a micromanometer. After these measurements were completed the reversed flow region was shifted to the plexiglass wall and traverses were made in the stalled region at the same four locations with a hot-wire type anemometer.

Heat Transfer Measurements:

Steady state heat transfer measurements were accomplished as follows:

1. The heated plate was brought to an isothermal condition by adjusting the power to each strip heater until the temperatures of the aluminum plate beneath each strip heater were all nearly equal.

2. The d.c. voltage supplied to each spot heater was adjusted until the temperature of each spot heater minus the temperature indicated by the thermocouple located adjacent to the spot heater was nulled.

3. The voltage applied to each spot heater and the difference between each spot heater temperature and atmospheric air temperature were recorded.

Transient heat transfer measurements were obtained by first accomplishing Step One of the foregoing. The outputs of the transient meters were amplified by two Hewlett Packard Model 413A d.c. amplifiers and recorded on a two-channel Sanborn chart recorder. The outputs of all possible combinations of two meters were recorded simultaneously for periods of at least five minutes in order to establish any relation between pairs of meter locations and varying heat transfers.

Both the transient heat meters and spot heaters were calibrated before testing. The method of calibration is discussed in Appendix A. The spot heaters were calibrated to establish a relationship between the electrical energy supplied to them and the thermal energy transferred directly from them to the diffuser flow. The transient meters

were calibrated to determine the relationship between their voltage output and heat flux.

The fluid velocity in the diffuser throat was not allowed to be less than ten feet per second while heat transfer data were being recorded. As discussed in Appendix D, a throat velocity less than this might have allowed free convection to have an appreciable effect on the results.

During all tests the temperature difference between the heated wall and the atmospheric temperature was kept less than approximately 40°F . This condition limited the bulk temperature rise of the air passing through the diffuser to less than approximately $1/2^{\circ}\text{F}$. All temperature differences measured by thermocouples were referenced to the atmospheric air at the diffuser inlet.

Procedures used for computing heat transfer results are discussed in Appendix E.

VI. RESULTS

The following discussion is a presentation of the results of the fluid flow and heat transfer studies. The flow studies include smoke and tuft observations made in the three flow regimes encountered (no "appreciable" separation, large transitory stall and fully-developed two-dimensional stall) and velocity measurements in two-dimensional stall. Heat transfer results were taken in the three flow regimes.

A. Flow Studies

A description of the observations of smoke and tuft movements in the present study is not given. Smoke and tuft movements indicated the flow patterns in the diffuser were almost identical to those described by Kline, et al. (11, p. 31; 16; 32, p. 51). Little can be added to the descriptions they have given for tuft movements at different conditions of diffuser geometry. Consequently, the reader is referred to these references for a detailed explanation.

The lines a-a and b-b for the present investigation (Figure 1a) are very close to the lines taken from Reference 11 for high turbulence. It is speculated that the reason for the differences is the turbulence generated by the diffuser entrance. A change in throat Reynolds number did not affect the position of the transition lines

shown in Figure 1a. However, it is believed that the turbulence level was great enough to cause the shift of the lines a-a and b-b for the present test compared to those of Reference 11. The transition lines which were taken from Reference 16 lie even farther from the lines taken from Reference 11. It is mentioned in Reference 16 that this difference was caused by a higher turbulence level rather than changes in throat Reynolds number.

Photographs of smoke streamers are shown in Figures 1b through 1d. All of these photographs had an exposure of 1/120 second, except the photograph in Figure 1d, which shows smoke injected at the diffuser exhaust. This last photograph had a 1/4 second exposure and, therefore, showed an integrated or average smoke pattern rather than an instantaneous one.

The results of velocity traverses in the diffuser during fully-developed two-dimensional stall are presented in Figures 9 through 11. Data are given for δ_{2r} , δ_{2w} , U_m , U_r and velocities in the mixing region. The mixing region velocities and δ_{2r} were used in the prediction of U_r . (See Figure 2 for an illustration of δ_{2r} , δ_{2w} , U_m and U_r .) The throat Reynolds number for these data ranged from 50,000 to 300,000. However, there was no indication of any relationship between throat Reynolds number and the parameters listed in the foregoing. In addition, there was no apparent indication

that a change in L/W or 2θ affected the values of δ_{2r} , δ_{2w} or U_m . The experimental uncertainty of the data from these velocity measurements is \pm five percent.

Measurements of the length δ_{2r} were originally correlated as

$$\delta_{2r} = .093l + .6 \text{ inches} \quad (19)$$

The constant term extends the mixing region to its virtual origin. Because δ_{2r} was not affected by changes in L/W or 2θ , the location of the virtual origin was assumed related only to the diameter of the semi-cylindrical entrance section. This relation was based on the assumption that the separation point always occurred at the same angular position on the entrance section. If this were the case, the distance from the virtual origin to the actual origin would be directly proportional to the diameter D . The value of D was 9.5 inches, thus this distance can be written as $0.063 D$. When this value is substituted for the constant term in the foregoing equation and the equation is divided by D , a dimensionless equation in the following form results:

$$\delta_{2r}/D = .093l/D + .063 \quad (9)$$

The non-dimensional relationship has not been experimentally investigated because the diameter of the semi-cylindrical entrance section

for the present study was constant. Nevertheless, it is expected that Equation (9) will closely predict the magnitude of δ_{2r} in other two-dimensional, straight-wall diffusers having cylindrical entrance sections for the reasons indicated in the foregoing.

Velocities measured in the mixing region of the fully-developed two-dimensional stall are given in Figure 10. The major portion of the velocity data fall within \pm three percent of the equation

$$U/U_m = .5 \eta / \delta_{2r} \quad (8)$$

The dependency of the velocity ratio U/U_m on the ratio η/δ_{2r} is consistent with information given by Schlichting (45, p. 607). Also, the linearity of the velocity profile agrees with velocity measurements taken in the mixing region of a plane turbulent wall jet (33).

A correlation of the measured values of the maximum velocity along the "wall of jet flow," U'_m , is given in Figure 11. These data points agree within approximately \pm four percent of the values determined by

$$U'_m / U_t(S)^{.1} = \left\{ \begin{array}{ll} 1 & \text{for } \ell/W < 7 \\ [1 + .381 (\ell/7W - 1)]^{-1/2} & \text{for } \ell/W > 7 \end{array} \right\} \quad (20)$$

The difference between this equation and the one given by Myers, et al. (33) is the addition of the parameter S (aspect ratio) to the minus .1 power. The manner in which S is used in Equation

(20) was established empirically. An explanation for the appearance of S in the correlation of U_m' is that the separation point is affected by the geometry of the diffuser entrance. For the case of flow past two parallel cylinders in a direction normal to a plane intersecting the axes of the cylinders, the separation point moves downstream as the aspect ratio of the cylinders is decreased. Because the entrance of the diffuser was made of portions of cylinders, it is suspected that the separation point moved downstream when the aspect ratio was decreased. The width of the region bounded by the "wall of jet flow" and the "d" line (see Figure 2a) at $l = 0$ was greater than the width of the throat because the separation point was located downstream from the throat. Consequently, U_m' was less than the prediction for U_m given by Myers, et al. (33).

The measured values of δ_{2w} are presented in Figure 12. (See Figure 2 for an illustration of δ_{2w} .) An explanation for the inclusion of the parameter S in the correlation of δ_{2w} is the same as the explanation given in the foregoing for the appearance of S in the correlation of U_m' .

Experimental velocity data showed that the reversed flow velocity was uniform throughout the region between the wall boundary layer and the "r" line. This uniformity was found for traverses normal to the wall and parallel to the wall between the diffuser exhaust and $l = 6$ inches. The measured reversed flow velocity as

affected by the diffuser configuration is plotted in Figure 13 and compared to the predicting line that has been derived. There is a large discrepancy between measured and predicted values of reversed flow velocity. In addition, there is a large scatter of the data. A study of the results showed that this scatter did not appear to be related to variations in flow rates or diffuser configuration. There was some variation in U_r with respect to time during one test run, but its variation from one test run to another was even greater, even though flow rate and diffuser configuration were repeated. The reason for this variation cannot be explained.

An empirical improvement of the correlation of U_r is shown in Figure 14. When the functional relation $f(W/L, D/L, \theta)$ [see Equation (17)] is divided by $\tan 2\theta$, a new function which is in closer agreement with measured values of U_r/U_t is obtained. This indicates that there is an additional effect of the angle 2θ which is not considered in the prediction of U_r .

From the way that the screens in the middle of the plenum deflected during fully-developed two-dimensional stall, it is concluded that the reversed flow in the diffuser started near the bottom of the plenum (see Figure 3a).

B. Heat Transfer

The discussion of heat transfer data presented in the following

paragraphs is subdivided according to the regimes of diffuser flow encountered. All of the graphical data, with the exception of Figures 20a and 20b, were obtained by measurements with spot heaters. Due to their large thermal time constant, the spot heaters gave steady state data which represent time averaged values. The experimental uncertainty for the heat transfer data encountered generally ranged from ± 3 percent to ± 22 percent. The smallest uncertainty value corresponds to the largest convection coefficient value and the largest uncertainty corresponds to the smallest convection coefficient value.

Heat transfer rates were measured at a sufficient number of locations on the diffuser wall to detect variations of the convection coefficient in directions of the width and length of the wall. However, in all cases, the magnitude of experimental uncertainty was larger than any indication of a variation of the coefficient in the direction of the wall width. Consequently, this aspect has not been considered in the presentation of experimental results.

No "Appreciable" Separation Flow Regime:

Heat transfer data taken in the diffuser flow regime indicated by the area beneath line a-a in Figure 1a are presented in Figure 16. Approximately 90 percent of the data points in Figure 16 lie within ± 13 percent of the prediction line. This departure is within the

experimental uncertainty of most of the data points. It is possible that velocity profiles outside the boundary layer and near the diffuser exhaust were not uniform as assumed. The mainstream velocity near the wall might have been less than assumed. This circumstance causes the data points to lie below the predicting line by a larger degree.

A line faired through the data given in Figure 16 can be expressed as

$$(hX_t/k)[1-(\xi_t/X_t)^{.9}]^{1/9}(T_w/T_\infty)^{.4} = .0283 \text{ Pr}^{.6} \left[\frac{X_t}{\nu} \cdot \frac{U_t}{1+2(\ell/W)\sin\theta} \right]^{.8} \quad (21)$$

This line departs from the data by less than \pm nine percent.

Fully-Developed Two-Dimensional Stall:

The results shown in Figure 17a represent the heat transfer data taken from the "wall of jet flow." The Reynolds number in this graph includes the maximum velocity along the wall from the correlation given by Myers, et al. (33)[see Equation (6)] for a plane turbulent wall jet. The main reason the data points lie below the predicting line is that the measured maximum velocity of the mainstream along the wall, U_m' , was less than the velocity that was computed from Equation (6)(see Figure 11). Figure 17b shows the data with Reynolds number including the velocity U_m' from Equation (20) which is a correlation of the data in Figure 11. A line that represents the

predicting equation [see Equation (5)] using this Reynolds number is drawn on the graph.

Data points for Reynolds number less than 100,000 lie above the predicting line much more than other data points. The reason for this occurrence is not known, however, the validity of these data was verified by repeating test conditions and comparing results. Corresponding Nusselt numbers were nearly identical.

A line faired through the data given in Figure 17b lies within ± 14 percent of more than 90 percent of the data points and is expressed as:

$$(hX_t/k)[1 - (\xi_t/X_t)^{.9}]^{1/9} (T_w/T_\infty)^{.4} = .0277 \text{ Pr}^{.6} (X_t U'_m/\nu)^{.8}, \quad (22)$$

where

$$U'_m/U_t(S)^{.1} = \left\{ \begin{array}{ll} 1 & \text{for } \ell/W < 7 \\ [1 + .381(\ell/7W - 1)]^{-1/2} & \text{for } \ell/W > 7 \end{array} \right\} \quad (20)$$

Heat transfer measurements from the "wall of reversed flow" are shown in Figures 18a and 18b. The Reynolds number in Figure 18a includes the reversed flow velocity predicted from Equation (17). The Reynolds number in Figure 18b includes the predicted reversed flow velocity divided by $\tan 2\theta$. The experimental uncertainty of these heat transfer data (± 13 percent to ± 22 percent) is generally

greater than the experimental uncertainty of the heat transfer data from other diffuser flow regimes because of the low values of the convection coefficient.

It was found by empirical means, that when the factor $1/\tan 2\theta$ was applied to the function predicting the reversed flow velocity, the scatter of data plotted in Figure 18a was reduced. This can be seen by comparing Figures 18a and 18b. Also, the improvement in the correlation of reversed flow velocity can be seen in Figures 13 and 14.

A reason for the data scatter, other than the experimental uncertainty, is that reversed flow velocities were not consistent. That is, they were not always repeatable from test to test when the diffuser geometry was not changed. This was discussed in an earlier part of the Results.

A line faired through the data plotted in Figure 18b and represented by

$$\begin{aligned} (hX_b/k)[1 - (\xi_b/X_b)^{.9}]^{1/9} (T_w/T_\infty)^{.4} = \\ .0325 \text{Pr}^{.6} \{(X_b U_t/\nu) f(W/L, D/L, \theta)/\tan 2\theta\}^{.8} \end{aligned} \quad (23)$$

departs from more than 90 percent of the data points by less than ± 30 percent. The functional relation, $f(W/L, D/L, \theta)$ is given in Equation (17).

As pointed out on page 15, the heat transfer coefficients in the

stall region of bluff bodies have been correlated as (39):

$$\text{Nu} = m\text{Re}^{2/3}$$

Although the present configuration is not that of a bluff body, the measured heat transfer coefficients for the "wall of reversed flow" were plotted against the throat velocity on log-log coordinates. A line was drawn through each set of points having the same throat width, divergence angle and wall position. The average slope of all the lines through all sets of points was found to be 0.770. The slope of individual lines ranged from 0.625 to 0.910 because of the experimental uncertainty of the heat transfer data. Therefore, it seems that the Nusselt number would not be dependent on the $2/3$ power of the Reynolds number for the diffuser configuration.

Large Transitory Stall:

Data from the large transitory stall regime are plotted in Figures 19a and 19b. The Reynolds number used in Figure 19a is based on the mean velocity that is computed by:

$$U = \frac{U_t}{1 + 2(\ell/W)\sin\theta}$$

while the Reynolds number used in Figure 19b is based on the throat velocity.

Heat transfer measurements in the regime of large transitory

stall could not be estimated by predictions. However, as explained on page 35, it is expected that, depending upon the frequency of stall development and elimination, heat transfer coefficients might be greater than they would be if flow could be achieved in the same geometry without separation. This is verified in Figure 19a, which shows the results of measurements compared with a line representing the heat transfer that would be expected for non-separated flow conditions. In most cases, at wall positions near the diffuser throat the heat transfer coefficients nearly agree with the non-separated flow condition, but at locations further downstream the Nusselt numbers are larger than for the non-separated flow condition. Apparently, the transitory stall bubbles develop and collapse more rapidly in the region near the downstream end of the wall than in the region near the throat.

The transitory stall data are better correlated by plotting Nusselt number against Reynolds number based on the length X_t and the throat velocity. This is demonstrated in Figure 19b. A line faired through the data points in this graph, expressed as

$$(hX_t/k)[1-(\xi_t/X_t)^{.9}]^{1/9}(T_w/T_\infty)^{.4} = .0181 Pr^{.6}(X_t U_t/\nu)^{.8}, \quad (24)$$

is within ± 30 percent of more than 90 percent of the data points.

The data given in Figure 20a and Table III were obtained with the transient heat meters. These data give the greatest difference

between maximum and minimum heat rates during a time period of at least five minutes at the conditions indicated and at a single position on the diffuser wall. In nearly all cases, this difference was the same for all wall positions tested.

Figure 20a indicates that the parameter $(h_{\max} - h_{\min})/h_{\text{av}}$ was dependent on throat Reynolds number. Other variables might have an effect on this parameter, but, because the study made with the transient heat meters was only exploratory in nature the effect of all diffuser flow variables on the parameter $(h_{\max} - h_{\min})/h_{\text{av}}$ was not determined.

A study was also made of the variations of each transient meter's output relative to the other meters. The frequencies of the recorded data were always random with no apparent correspondence between meters. Periods were estimated to range from a little more than one cycle per minute to one cycle per second. These variations could be found in the case of every meter and in nearly every test run. It must be realized, however, that the time constant of the transient heat meters was approximately one second.

The average value of the film coefficient, h_{av} , was found to be nearly equal to the mean value in all cases. This was determined by using a planimeter to measure the integrated area under curves of recorded transient meter output.

A calibration of the transient meters showed that their voltage

output was a function of the isothermal wall convection coefficient in addition to the temperature variation along the foil (see Figure 5).

It was discussed in Reference 18 that if the foil temperature variation had been sufficiently small, in comparison to the wall-air temperature difference, then the dependency of the meter voltage output on the isothermal wall convection coefficient would be negligible. That is, the measured heat flux would have been equal to a constant times the foil temperature variation. The reason the heat meter calibration was dependent on the wall coefficient is that a non-isothermal wall condition causes the convection coefficient to be different than an isothermal coefficient. Because the temperature variation along the foil was large, some variation of the meter calibration with wall convection coefficient would be expected.

Nusselt numbers based on the average value of the heat transfer coefficient, h_{av} , determined from recorded transient meter data are plotted in Figure 20b. The line faired through the data in Figure 19b is also shown and illustrates that the data given in Figure 20b are in agreement with the data given in Figure 19b.

It should be noted that there was a condition during which it was decided not to record steady-state test data. At a diffuser geometry of $L/W = 18$, $2\theta = 8$ degrees and the high flow rate, vibrations of the walls of the large plenum and diffuser were so violent

that it was feared that because of this resonant condition some physical damage might occur if the test were continued.

Additional Observations:

Figure 21 is given to briefly summarize all of the heat transfer data collected and to illustrate the effect of changing the divergence angle, 2θ , the wall length, L , and the throat width, W . Stanton number with throat velocity and Reynolds number based on throat velocity and distance from the throat, X_t , are the coordinates. All the curves share the same throat velocity.

All the curves in Figure 21, with the exception of the curve for a shorter length of the "wall of reversed flow," were determined by plotting the results of experimental data as Stanton number against Reynolds number and then fairing a line through the data points. The line illustrating the effect of a shorter length of the "wall of reversed flow" was determined by assuming that the Stanton number at the diffuser exhaust does not change as L is shortened and other variables are held constant, and that the slope of the curve is the same as the slope of the other curves for the "wall of reversed flow."

The scales have been purposely left off the coordinates of the graph in Figure 21 because the curves represent only qualitative data and not all the curves were established directly from experimental data. Graphical data which has previously been described

should be used to predict heat transfer coefficients.

Figure 21 illustrates that when the angle of divergence is increased from zero degrees the heat transfer decreases. The curve for large transitory stall intersects with some of the lines for no "appreciable" separation because of the diverging flow during no "appreciable" separation. The highest heat transfer rates occur when the divergence angle is zero degrees and the lowest rates occur at large angles of divergence and large L/W values on the "wall of reversed flow. "

VII. CONCLUSIONS

The following conclusions have been obtained from heat transfer and fluid flow measurements in the diffuser. They pertain to only plane-wall two-dimensional diffusers having turbulent fluid boundary layers.

A. Flow Studies

1. Diffuser flow regimes closely agree with the descriptions given by Moore and Kline (32, p. 120). The effect of varying the level of inlet turbulence was not investigated, but the discussions given in References 16 and 32 indicate that turbulence should be expected to have an effect on the vertical position of lines a-a and b-b in Figure 1a.

2. Velocity traverses in the diffuser during fully-developed two-dimensional stall have shown that the velocity profile in the portion of the mixing region lying between the "d" and "r" lines can be expressed as

$$U/U_m = .5\eta/\delta_{2r}$$

Also, the width of the region lying between the streamline for $1/2$ the maximum velocity and the "r" line, δ_{2r} , can be written

$$\delta_{2r}/D = .093 \ell/D + .063$$

3. The magnitude of the measured maximum velocity in flow past the "wall of jet flow" during fully-developed two-dimensional stall, U'_m , can be determined from

$$U'_m / U_t(S)^{.1} = \left\{ \begin{array}{ll} 1 & \text{for } \ell/W < 7 \\ [1 + .381 (\ell/7W - 1)]^{-1/2} & \text{for } \ell/W > 7 \end{array} \right\}$$

This expression is Myers,¹ et al. (33) correlation modified by the inclusion of the aspect ratio, S.

4. The fluid velocity in the region of reversed flow during fully-developed two-dimensional stall is not consistent. That is, this velocity is not repeatable from test to test even though the diffuser throat velocity and geometry are not changed. The reversed flow velocity can vary as much as \pm ten percent of the mean value of the range of reversed flow velocities encountered when the diffuser geometry and throat velocities are unchanged. The following expression predicts reversed flow velocities within \pm 20 percent of the true velocity when straight-wall diffusers having a sudden pressure rise at their exhaust, caused by wall geometry, are used:

$$U_r / U_t = f(W/L, D/L, \theta) / \tan 2\theta$$

The functional relation $f(W/L, D/L, \theta)$ is defined in Equation (17).

B. Heat Transfer

1. In the regime of no "appreciable" separation, predictions of heat transfer coefficients developed from a turbulent flat plate correlation [Equation (3)] were within approximately ± 13 percent of the measured coefficients. Equation (21), which represents a line faired through the experimental data, lies within ± 9 percent of the data and improves the correlation.

2. Heat transfer coefficients measured on the "wall of jet flow" during fully-developed two-dimensional stall were within ± 30 percent of the coefficients predicted by Equations (5) and (6). Equation (5) was developed from a turbulent flat plate heat transfer correlation. A correlation which is within ± 14 percent of the data is expressed as Equations (20) and (22) and was found by fairing a line through the data.

3. Heat transfer coefficients on the "wall of reversed flow" during fully-developed two-dimensional stall are within approximately 200 percent of the coefficients predicted by the flat plate type of heat transfer correlation given in Equation (18). If the Reynolds number based on the predicted reversed flow velocity is divided by $\tan 2\theta$ and plotted against Nusselt number, a line that lies within ± 30 percent of the data can be faired through the points. Equation (23) represents this line.

4. Heat transfer coefficients for large transitory stalls have been correlated so that a line faired through the data and expressed as

$$(hX_t/k)[1 - \xi_t/X_t]^{.9}]^{1/9} (T_w/T_\infty)^{.4} = .0181 Pr^{.6} (X_t U_t/\nu)^{.8}$$

lies within ± 30 percent of the data.

5. The values of $(h_{\max} - h_{\min})/h_{\text{av}}$ during large transitory stalls were as large as 0.50. This occurred at large L/W values and angles of 2θ near the line b-b shown in Figure 1a. It is possible that the parameter $(h_{\max} - h_{\min})/h_{\text{av}}$ might have been even larger at frequencies of transient heat transfer which were greater than one cycle per second. The time constant of the transient heat meters used in the present study was equal to approximately one second.

6. Heat transfer rates from plane-wall two-dimensional channels are greatest when the angle of divergence is zero degrees. When the angle of divergence is increased, heat transfer rates decrease. The lowest rates are obtained on the "wall of reversed flow" during fully-developed two-dimensional stall and large angles of divergence.

VIII. RECOMMENDATIONS

1. Diffuser entrance and exit configurations different from those used in the present study should have an effect on heat transfer rates in the diffuser. Even though these changes should not have a great effect on the location of flow regimes, as explained in Reference 52, variations in fluid boundary layer thickness at the throat, or at the exit when reversed flow occurs, should affect the heat transfer coefficient. When diffuser geometries are different from those used in the present study, heat transfer coefficients can be predicted with the present results by adjusting the length values in Nusselt and Reynolds number to the proper quantity. The method discussed in Appendix B is suggested.

An experiment which determines the effects of diffuser entrance and exhaust configurations is recommended. In many instances, the entrance and exhaust of a diffuser are connected to flow ducts. This establishes continuous walls at these junctions, instead of discontinuous walls as was the case in the present experiment.

2. It is recommended that transient heat meters having a faster response than those used in the present experiment be used to make measurements of the unsteady heat transfer rates. Variations at high frequencies could not be detected in the present

experiment due to the large time constant (one second) of the meters, but it is possible that a correlation of such results could be made with diffuser configuration and flow parameters.

3. As explained in Reference 11, diffuser performance at large angles of divergence can be improved by adding straightening vanes. It might be worthwhile to study heat transfer rates in the diffuser when these vanes are installed.

4. Divergence angles sufficiently large to develop jet flow could not be obtained. However, the results of heat transfer measurements on the "wall of reversed flow" during fully-developed two-dimensional stall should be useful for predicting heat transfer coefficients for the jet flow condition. The correspondence between throat and reverse flow velocities is expected to be approximately the same for these two types of flow when one-half the total divergence angle for jet flow is compared to the total divergence angle for two-dimensional stall. If one imagined a plane down the center of the jet flow, then the flow between this plane and one of the diverging walls would be much like fully-developed two-dimensional stall. Consequently, convection coefficients for the "wall of reversed flow" during fully-developed two-dimensional stall are believed to be nearly the same as coefficients for jet flow. One-half the total divergence angle for jet flow should be used in the correlation of heat transfer

coefficients for the "wall of reversed flow" during two-dimensional stall.

5. It is recommended that spot heaters which have smaller conduction heat losses than those used in the present investigation be used. The thermal resistance of the conducting heat path needs to be increased.

IX. BIBLIOGRAPHY

1. American Society of Mechanical Engineers. Fluid meters, their theory and application. A report of the American Society of Mechanical Engineers Research Committee on Fluid Meters. 5th ed. 1959. 203 p.
2. Bartz, D. R. An approximate solution of compressible boundary-layer development and convective heat transfer in convergent-divergent nozzles. Transactions of the American Society of Mechanical Engineers, 77:1235-1245. 1955.
3. Bloom, M. H. and A. Pallone. Shroud tests of pressure and heat transfer over short afterbodies with separated wakes. Journal of Aero-Space Sciences 26:626-634. Oct. 1959.
4. Bradshaw, P. and M. T. Gee. Turbulent wall jets with and without an external stream. London, Her Majesty's Stationery Office, 1962. 49 p. (Aeronautical Research Council R&M No. 3252)
5. Bursnall, W. J. and L. K. Loftin. Experimental investigation of localized regions of laminar-boundary layer separation. Langley Field, Va., April, 1951. 57 p. (NACA TN2338)
6. Carlson, W. O. Heat transfer in laminar separated and hydraulic wake flow regions. In: Proceedings of Heat Transfer and Fluid Mechanics Institute. Stanford, Stanford University Press, 1959. p. 140-155.
7. Chapman, Dean R. A theoretical analysis of heat transfer in regions of separated flow. Moffett Field, California, Oct. 1956. 47 p. (NACA TN3792)
8. Chapman, Dean R., D. M. Kuehn and H. K. Larson. Investigation of separated flows in supersonic and subsonic streams with emphasis on the effect of transition. Moffett Field, California, 1958. 40 p. (NACA Report 1356)
9. Charwat, A. F. et al. An investigation of separated flows. Part I. The pressure field. Journal of Aero-Space Sciences 28(6):457-470. June 1961.

10. Charwat, A. F. et al. An investigation of separated flows. Part II. Flow in the cavity and heat transfer. Journal of Aero-Space Sciences 28(7):513-527. July 1961.
11. Cochran, D. L. and S. J. Kline. Use of short flat vanes for producing efficient wide-angle two-dimensional subsonic diffusers. Stanford, Sept. 1958. 135 p. (Stanford University. NACA TN4309)
12. Crocco, L. and L. Lees. A mixing theory for the interaction between dissipative and nearly isentropic streams. Journal of Aeronautical Sciences 19:649-676. Oct. 1952.
13. Curle, N. Heat transfer and laminar boundary layer separation in steady compressible flow past a wall with non-uniform temperature. London, Her Majesty's Stationery Office, 1961. 16 p. (Aeronautical Research Council R&M No. 3179)
14. Curle, N. and S. W. Skan. Approximate method for predicting separation properties of laminar boundary layers. Aeronautical Quarterly 8:257-268. Aug. 1957.
15. Eckert, E. R. G. and Robert M. Drake, Jr. Heat and mass transfer. New York, McGraw-Hill, 1959. 530 p.
16. Fox, R. W. and S. J. Kline. Flow regimes in curved subsonic diffusers. Transactions of the American Society of Mechanical Engineers, Ser. D 84:303-312. Sept. 1962.
17. Gadd, G. E. Boundary layer separation in the presence of heat transfer. Paris, April 1960. 13 p. (NATO AGARD Report 280)
18. Gardon, R. An instrument for the direct measurement of intense thermal radiation. Review of Scientific Instruments 24:366-370. May, 1953.
19. Golik, R. J. On dissipative mechanisms within separated flow regions (with special consideration to energy transfer across Turbulent, compressible, $Pr = 1$, mixing regions). Ph.D. thesis. Urbana, University of Illinois, 1962. 111 numb. leaves. (Microfilm)
20. Ihrig, H. K., Jr. and H. H. Korst. Quasi-steady aspects of the adjustment of separated flow regions to transient external

- flows. American Institute of Aeronautics Journal 1:934-935. 1963.
21. King, Hartley H. The diffusion of injected gas in separated flow. Journal of Aero-Space Sciences 29:473-474. April 1962.
 22. Kline, S. J. On the nature of stall. Transactions of the American Society of Mechanical Engineers, Ser. D 81:305-320. Sept. 1959.
 23. Kline, Stephen J. Some new mechanisms and conceptions of stall including the behavior of vaned and unvaned diffusers. Stanford, March 1957. 112 p. (Stanford University. Progress Report MD-1 under NACA Contract NAW-6500)
 24. Kline, S. J., D. E. Abbott and R. W. Fox. Optimum design of straight-walled diffusers. Transactions of the American Society of Mechanical Engineers, Ser. D 81:321-329. Sept. 1959.
 25. Kline, S. J. and F. A. McClintock. The description of uncertainties in single sample experiments. Mechanical Engineering 75:3-8. Jan. 1953.
 26. Kline, S. J. and P. W. Runstadler. Some preliminary results of visual studies of the wall layers of the turbulent boundary layer. Transactions of the American Society of Mechanical Engineers, Ser. E 81:166-173. June 1959.
 27. Knudsen, James G. and Donald L. Katz. Fluid dynamics and heat transfer. New York, McGraw-Hill, 1958. 576 p.
 28. Larson, Howard K. Heat transfer in separated flows. Journal of Aero-Space Sciences 26: 731-738. Nov. 1959.
 29. Maskell, E. C. Flow separation in three dimensions. Farnborough, England, Nov. 1955. 20 p. (Royal Aircraft Establishment Report No. Aero 2565)
 30. Maskell, E. C. The significance of flow separation in the calculation of general fluid flow. In: Proceedings of Ninth International Congress for Applied Mechanics, University of Bruxelles. Paris, 1957. p. 226-231.

31. Miles, John Bruce. Stanton number for separated turbulent flow past relatively deep cavities. Ph.D. thesis. Urbana, University of Illinois, 1963. 99 numb. leaves. (Microfilm)
32. Moore, Carl A., Jr. and Stephen J. Kline. Some effects of vanes and of turbulence in two-dimensional wide-angle subsonic diffusers. Stanford, June 1958. 139 p. (Stanford University. NACA TN4080)
33. Myers, G. E., J. J. Schauer and R. H. Eustis. Plane turbulent wall jet flow development and friction factor. Transactions of the American Society of Mechanical Engineers, Ser. D 85: 47-53. March 1963.
34. Myers, G. E., J. J. Schauer and R. H. Eustis. The heat transfer to plane turbulent wall jets. Transactions of the American Society of Mechanical Engineers, Ser. C 85:209-214. Aug. 1963.
35. Page, R. H. A theory for incipient separation. In: Developments in Mechanics. Vol. 1. Proceedings of Seventh Midwestern Mechanics Conference held at Michigan State University. Sept. 6-8, 1961. New York, Plenum Press, 1961. p. 563-577.
36. Persh, Jerome and Bruce M. Bailey. Effect of surface roughness over the downstream region of a 23° conical diffuser. Langley Field, Va., Jan. 1954. 55 p. (NACA TN3066)
37. Ragsdale, W. C. and J. M. Smith. Heat transfer in nozzles. Chemical Engineering Science 11:242-251. Jan. 1960.
38. Reynolds, W. C., W. M. Kays and S. J. Kline. A summary of experiments on turbulent heat transfer from a non-isothermal flat plate. Transactions of the American Society of Mechanical Engineers, Ser. C 82:341-348. Nov. 1960.
39. Richardson, P. D. Heat and mass transfer in turbulent separated flows. Chemical Engineering Science 18:149-155. Jan. 1963.
40. Roos, J. N. and A. F. Charwat. The effect of an external pressure gradient on a separated region. Journal of Aero-Space Sciences 29:370-371. March 1962.

41. Runstadler, P. W., S. J. Kline and W. C. Reynolds. An experimental investigation of the flow structure of the turbulent boundary layer. Stanford, June 1963. 308 p. (Stanford University. Dept. of Mechanical Engineering. Report MD-8, Thermosciences Division)
42. Sabin, C. M. An analytical and experimental study of the plane incompressible turbulent free shear layer with arbitrary velocity ratio and pressure gradient. Stanford, Oct. 1963. 113 p. (Stanford University. Dept. of Mechanical Engineering. Report MD-9, Thermosciences Division)
43. Saunders, O. A., and P. H. Calden. Some experiments on the heat transfer from a gas flowing through a convergent divergent nozzle. In: Proceedings of Heat Transfer and Fluid Mechanics Institute. Stanford, Stanford University Press, 1951. p. 91-106.
44. Savage, Stuart B. The effect of heat transfer on separation of laminar compressible boundary layers. Pasadena, June 1962. 43 p. (California Institute of Technology. Separated Flow Project. Technical Report No. 2)
45. Schlichting, Hermann. Boundary layer theory. New York, McGraw-Hill, 1960. 647 p.
46. Schwartz, W. H. and W. P. Cosart. The two-dimensional turbulent wall jet. Journal of Fluid Mechanics 10:480-495. June, 1961.
47. Seban, R. A., A. Emery and A. Levy. Heat transfer to separated and reattached subsonic turbulent flows obtained downstream of a surface step. Journal of Aero-Space Sciences 26:809-814. Dec. 1959.
48. Shapiro, Ascher H. Design of tufts for flow visualization. American Institute of Aeronautics and Astronautics Journal 1:213-214. Jan. 1963.
49. Spink, Leland Kenneth. Principles and practice of flow meter engineering. Foxboro, Massachusetts, Foxboro Company, 1958. 549 p.

50. VanSant, James H. and Milton B. Larson. Heat transfer from a semi-infinite strip. Transactions of the American Society of Mechanical Engineers, Ser. C 85:191-192. May 1963.
51. von Karman, Th. and C. B. Millikan. On the theory of laminar boundary layers involving separation. Pasadena, 1934. 22 p. (California Institute of Technology. NACA Report No. 504)
52. Waitman, B. A., L. R. Reneau and S. J. Kline. Effects of inlet conditions on performance of two-dimensional subsonic diffusers. Transactions of the American Society of Mechanical Engineers, Ser. D 83:349-359. Sept. 1961.

APPENDICES

APPENDIX A

DETERMINATION OF CONDUCTION HEAT LOSSES
FROM THE SPOT HEATERS

If the thermal energy which passes directly from the copper mandrel of the spot heaters into the moving air stream is known, in addition to a temperature difference and surface area, then a convection coefficient may be calculated. Specifically,

$$h = \frac{Q_c}{A_h (T_h - T_a)} \quad (1A)$$

The measured electrical power supplied to each spot heater, Q_m , includes the convection heat transfer in the foregoing equation, Q_c , and the heat transfer lost by conduction, Q_k . That is,

$$Q_m = Q_c + Q_k \quad (2A)$$

The conduction heat loss term can be broken down into the following categories:

- a. Transfer through the edge of the Teflon insulation sleeve and into the gas stream.
- b. Conduction along the electrical and thermocouple lead wires.
- c. Conduction from the spot heater to the aluminum plate.

Heat transfer through the edge of the Teflon, Q_{k_e} , can be estimated from the solution of the semi-infinite strip problem which has

been presented by the author and M. B. Larson in Reference 50. For a relatively small range of h , this heat transfer rate can be written in the form

$$Q_{k_e} = Ah^B (T_h - T_a) \quad (3A)$$

However, the constants A and B depend on variations of thermal contact resistance between the aluminum plate and the Teflon and between the copper mandrel and the Teflon. Also, a variation of the heat transfer coefficient on the end of the Teflon sleeve exposed to the gas stream affects these constants.

Steady-state heat conduction out the lead wires depends mainly on the thermal properties of the wires and a temperature difference. The influencing temperatures would be the spot heater temperature, T_h , and the atmospheric temperature, T_a . Consequently, this heat loss can be written as

$$Q_{k_w} = C' (T_h - T_a) \quad (4A)$$

Even though the power to the spot heater was adjusted until its temperature matched the aluminum plate temperature, there was heat transfer between the two because the outer windings of the resistance wire were at a temperature slightly higher than the measured temperature of the copper mandrel. This slight temperature difference caused some heat transfer between the heater and aluminum wall.

Also, it is suspected that the temperature of the aluminum plate on the periphery of the Teflon was not absolutely isothermal. The reason for this temperature variation is that each spot heater was located between two strip heaters. The thermocouple junctions used to measure the aluminum plate temperatures near each spot heater were located midway between the strip heaters. Thus, these junctions gave the minimum temperature of the aluminum plate. As a result, it is likely that some heat was conducted from the plate to the spot heaters when the plate and spot heater thermocouple temperature difference was nulled.

The transfer of heat from the plate to the spot heaters also depended mainly on measured temperatures and the thermal properties of the materials involved. Thus, this heat loss can be written

$$Q_{k_p} = C'' (T_h - T_a) \quad (5A)$$

The total conduction heat loss is determined by adding equations 3A, 4A and 5A which gives the following:

$$Q_k / (T_h - T_a) = Ah^B + C \quad (6A)$$

C is the combination of the constants C' and C'' .

The constants A, B and C were determined by calibrating each individual spot heater. This was accomplished by operating the heaters under conditions in which the heat transfer rates were

reasonably well known and by using Equation (2A) to determine the heat loss values.

When determining heat loss values at values of h greater than $1.0 \text{ Btu/Hr-Ft}^2 - ^\circ\text{F}$, the diffuser walls were set parallel and at their widest spacing ($L/W = 6$). For this arrangement it is expected that fluid boundary layers developed as if on a flat plate in an infinite medium. Equation (3) was used when calculating heat transfer rates expected for this condition.

Heat losses at values of h less than $1.0 \text{ Btu/Hr-Ft}^2 - ^\circ\text{F}$ were obtained by allowing natural convection conditions on the heated plate. This wall was set vertical in the apparatus, a sharp edge was attached to its bottom edge, both sliding panels were removed, an access door on the side of the plenum was opened and the opposite plexiglass wall was removed. Temperatures on the heated plate were maintained at low enough values to allow only a laminar boundary layer. The equation used for calculating the expected heat transfer rates was (15, p. 315)

$$\text{Nu}_{l_b} = 0.378 \text{ Gr}_{l_b}^{\frac{1}{4}} \quad (7A)$$

Heat loss values were expressed as $Q_k / (T_h - T_a)$ and plotted against h . The constants A , B and C were then determined from a line faired through the data. Figure 15 shows a typical calibration curve obtained from heat loss data.

Table I lists the values of A , B and C along with some other parameters for each spot heater. The negative values of the constant C are assumed to be caused by heat flow from the aluminum plate to the spot heater, as discussed in the foregoing.

TABLE I

Spot Heater Parameters

$$Q_k / (T_h - T_a) = Ah^B + C$$

Position No.	R ohms	l inches	A	B	C
1	40.26	7.5	.00043	1.000	-.00120
2	40.01	14.6	.00075	0.901	-.00152
3	40.25	21.5	.00073	1.020	-.00160
4	40.16	28.5	.00040	1.033	-.00059
5	39.93	4.0	.00069	0.909	-.00069
6	40.26	11.0	.00004	1.445	.00020
7	40.12	18.0	.00043	1.062	-.00165
8	39.92	25.0	.00075	1.083	-.00113
9	40.15	32.0	.00020	1.074	-.00038
10	40.11	0.5	.00021	1.094	.00212
11	39.76	4.0	.00041	1.056	-.00076
12	39.90	7.5	.00066	0.987	-.00179
13	40.10	11.0	.00033	1.059	-.00061
14	39.91	14.5	.00030	1.098	-.00066
15	39.91	18.0	.00036	1.045	-.00079
16	40.28	21.5	.00051	1.002	-.00110
17	40.20	5.0	.00059	1.045	-.00129
18	39.84	28.5	.00052	1.005	-.00139
19	39.80	32.0	.00060	0.894	-.00055
20	40.10	4.0	.00054	0.843	-.00119
21	39.84	11.0	.00024	1.061	-.00088
22	40.23	18.0	.00048	0.919	.00022
23	39.86	25.0	.00055	0.823	-.00061
24	39.91	32.0	.00031	0.948	-.00015
25	39.91	7.5	.00055	0.908	.00005
26	39.78	14.5	.00068	0.891	-.00188
27	39.89	21.5	.00091	0.877	-.00170
28	39.92	28.5	.00080	0.827	-.00010

APPENDIX B

EVALUATION OF THE UNHEATED ENTRANCE LENGTH

A condition which affected the thermal boundary layer development at positions that were downstream of the diffuser throat was the adiabatic curved inlet surface of the diffuser.

Correlations of heat transfer data from all the regimes of diffuser flow that were investigated included a correction factor for this step function of surface temperature. The correction factor, $[1 - (\xi/X)^{.9}]^{1/9}$ was obtained from Reference 38 and includes the unheated length, ξ , which must correspond to a length on a flat surface having a constant mainstream velocity along its length.

The method employed for determining the unheated starting length was the equating of the momentum thickness that occurred at the diffuser throat to the momentum thickness that would have occurred on a flat plate having length ξ and a constant mainstream velocity equal to the diffuser throat velocity. The momentum thickness for a turbulent boundary layer on a two-dimensional body with a pressure gradient can be expressed as

$$\delta^* = \frac{0.037 \nu^{0.2}}{U^{3.29}} \left[\int_0^x U^{3.86} dx \right]^{0.8} \quad (1B)^+$$

+ Taken from lecture notes presented by Prof. W. M. Kays for the course Mechanical Engineering 238B at Stanford University, 1963.

The variation of U on the diffuser entrance surface was obtained from a flux plot of streamlines developed by an electrical analog field plotter. This variation, when the total divergence angle is zero degrees, is given in Figure 8.

The value of δ_t^* was determined by using Equation (1B) and a method of numerical integration which employed the Trapezoid Rule to small lengths of x . Then δ_t^* was equated to the expression for the momentum thickness for a turbulent boundary layer on a flat plate (15, p. 144) having a velocity U_t . This expression is

$$\delta_t^* = 0.037 \xi^{0.8} \left[\frac{\nu}{U_t} \right]^{0.2} \quad (2B)$$

The foregoing analysis gave a value for ξ_t of approximately 2.5 inches for the diffuser used in the present investigation.

Actually, the boundary layer was not turbulent at the leading edge of the curved entrance section. Transition occurred between the leading edge and the throat. If the momentum thickness for a laminar boundary layer with arbitrary pressure variation is determined from

$$\delta^* = \frac{0.67 \nu^{0.5}}{U^3} \left[\int_0^x U^5 dx \right]^{0.5} \quad (3B)^+$$

+ Ibid.

and equated to Equation (2B) the value of ξ_t for the present study becomes approximately 2.0 inches. The variation of ξ_t between the two extremes of 2.0 and 2.5 inches does not have a pronounced effect on heat transfer correlations. Also, sand grains were attached to the surface of the curved entrance surface to make the position of boundary layer transition as near the leading edge as possible. Consequently, the value of 2.5 inches was used for ξ_t when the divergence angle of the diffuser was set at zero degrees. When the divergence angle was increased, the starting edge of the heated plate moves downstream from the throat and the leading edge of the curved surface moved nearer the throat, thus causing the length of ξ_t to change. Equations (1B) and (2B) were still used to determine the effective unheated starting length for this case but the variation of velocity over the unheated surface was again determined from an electrical analog with the changed positions of the leading edges of the heated and unheated surfaces taken into account.

APPENDIX C

EVALUATION OF EXPERIMENTAL ACCURACIES

Uncertainties of the test data were estimated by the method of Kline and McClintock (25) on the basis of 20 to 1 odds. These uncertainties are listed in Table II in terms of an interval or percentage, depending on which is appropriate.

The worst case for heat transfer parameters corresponds to the smallest film coefficients measured and the best case corresponds to the largest coefficients.

TABLE II
Experimental Uncertainties

Symbol	Variable	Interval
V	D. C. volts	0.002 volts
R	Resistance	0.01 ohms
W	Throat width	0.02 inches
-	Parallel walls spacing	1/32 inches
P _a	Barometric pressure	0.005 inches Hg.
t _a	Atmospheric temperature	1/2 degree F.
ν	Kinematic air viscosity	1.0 percent
k	Air thermal conductivity	1.0 percent
-	Air flow rate equation	2.0 percent
-	Orifice pressure drop	0.005 inches H ₂ O
2 θ	Total divergence angle	1/2 degree
L	Diverging wall length	1/32 inch
λ	Wall position	1/32 inch
T _h - T _a	Wall-air temp. difference	0.1 degree F.
Q _k /(T _h - T _a)	Heat loss parameter	0.0003 Btu/(Hr-°F)
A _h	Convection heat transfer area	0.001 inches ²

Symbol	Variable	Percentage	
		Best Case	Worst Case
-	Air Flow Rate	2.0	2.1
Re _x	Local Reynolds number	2.2	2.4
Nu _x	Local Nusselt number	3.0	22.0
St	Stanton number	3.6	23.0
Q _m	Measured heat transfer	0.2	0.2
h	Film coefficient (spot heater)	2.9	21.8
(h _{max} - h _{min})/h _{av}	Variation measured by trans. meter	5.0	5.0

APPENDIX D

CONSIDERATION OF MIXED FREE AND FORCED CONVECTION

Predictions of heat transfer discussed in this presentation are generally considered to be uninfluenced by free convection effects. Also, when a calibration of the spot heaters was being performed, it was essential that free convection heat transfer effects did not occur so that it could be assumed the coefficients predicted by the turbulent flat plate heat transfer correlation were equal to the coefficients occurring during calibration.

Any fluid that has a density which varies with temperature experiences buoyancy forces when it is part of a heat transfer path. However, when the dynamic forces of the fluid are great enough, buoyancy forces may be neglected. A discussion of this phenomenon is presented in a text by Eckert and Drake (15, p. 331). The separation of the regimes of forced flow and free convection is influenced by a large number of parameters, but Eckert and Drake present graphical data for the case of forced flow in the same direction as buoyancy forces in a tube and show that when the Grashof number is less than 10^{10} and the Reynolds number is greater than 10^4 buoyancy forces should be sufficiently small.

The foregoing information was used to predict a minimum velocity of 0.5 feet per second and a maximum wall-air temperature

difference of 50°F for the "wall of reversed flow" in fully-developed two-dimensional stall. Figure 13 shows that the smallest value of reversed flow velocity was approximately seven percent of the throat velocity. Thus, the minimum throat velocity, based on the 0.5 feet per second reversed flow velocity, was estimated to be approximately seven feet per second.

For the "wall of jet flow" (which had buoyancy forces in a direction opposite to dynamic forces) a conservative estimate of the minimum velocity was determined by equating the buoyancy force, F_b , to the dynamic pressure force, F_p .

$$F_b = L(1/\rho_a - 1/\rho_h)$$

$$F_p = \rho U^2/2g$$

When the temperature difference between the wall and the fluid stream is equal to 50°F, this procedure gives a minimum velocity of approximately five feet per second.

A velocity of 10.0 feet per second was selected as the smallest throat velocity to be permitted in the diffuser during all tests so that natural convection need not be considered.

APPENDIX E

COMPUTING TECHNIQUE

All calculations for spot heater calibrations and heat transfer results were performed on an IBM 1620 digital computer. The machine was given, for each spot heater, values of electrical resistance (R), length (ℓ), applied voltage (E), heat transfer temperature difference in millivolts ($T_h - T_a$) and the calibration coefficients (see Table I). Also, flow metering orifice size, orifice pressure drop, atmospheric pressure and temperature, throat width and total diffuser angle data were given.

Flow rates were computed according to the formula developed for gas flow measurements in Reference 49 (p. 400). Discharge coefficients for sharp-edged flat-plate orifices with flange pressure taps were taken from the tables provided (49, p. 416-421).

The measured energy transfer rate to each spot heater, Q_m , was computed by the electrical power formula $Q_m = E^2/R$. A constant which corrected Q_m for the power loss in lead wires was applied. Voltage measurements were made several feet from the test apparatus.

The technique used for computing the convection heat transfer coefficients, h , is an algorithm commonly known as the Newton-Raphson Method. This method is for finding the roots of any

equation written as a polynomial and having a single independent variable.

Equation (2A) (Appendix A) which expresses the terms involved in a heat balance of the spot heaters can be written as

$$Q_m = (hA_h + Ah^B + C)(T_h - T_a)$$

or

$$f(h) = (hA_h + Ah^B + C)(T_h - T_a) - Q_m = 0$$

The values of all the parameters in the foregoing equation, except h , are known from experimental data, thus the required value of h is a root of this equation. An arbitrary value for the error of the computed value of h was selected as 0.005. The algorithm for computing h was as follows:

$$h_1 = \frac{Q_m}{A_h(T_h - T_a)}$$

$$1: f(h_1) = (h_1 A_h + Ah_1^B + C)(T_h - T_a) - Q_m$$

$$\frac{df(h_1)}{dh_1} = (A_h + ABh_1^{B-1})(T_h - T_a)$$

If the absolute value of $\left[\frac{f(h_1)}{df(h_1)/dh_1} \right] \leq \text{Error}$ go to 2:

$$h_2 = h_1 - \frac{f(h_1)}{df(h_1)/dh_1}$$

$$h_2 = h_1$$

go to 1:

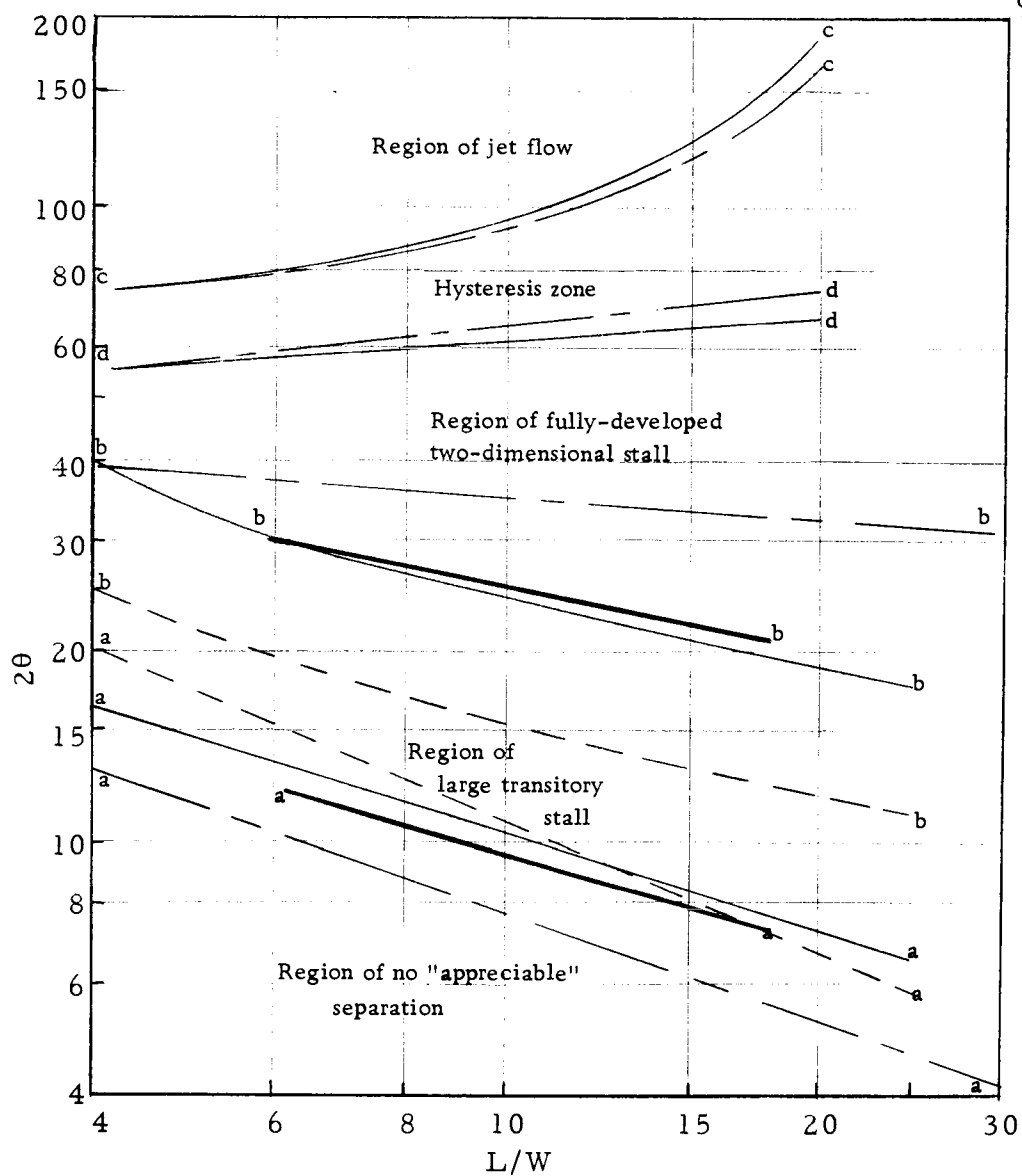
2: h_1 is the result

Nusselt, Stanton and Reynolds numbers, heat transfer temperature difference and measured heat rate for each spot heater were computed and listed. Nusselt and Stanton numbers included corrections for the unheated starting length and variation of fluid properties in the boundary layer.

Throat velocities, U_t , were determined by the ratio of air-flow rate measured by the metering orifice to throat cross-sectional area.

APPENDIX F

FIGURES



- — — Reference 16
- Reference 11, p. 92 ("high turbulence")
- — — Reference 11, p. 92 ("low turbulence")
- Results of the present study
- a - a Line of appreciable separation
- b - b Transition between transitory and two-dimensional stall
- c - c Transition from two-dimensional stall to jet flow
- d - d Transition from jet flow to two-dimensional stall

Figure 1a. Flow regimes in two-dimensional straight-wall diffusers.

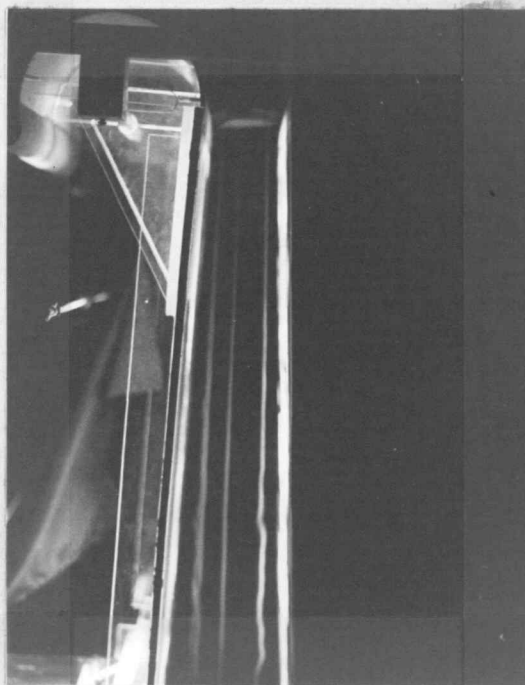
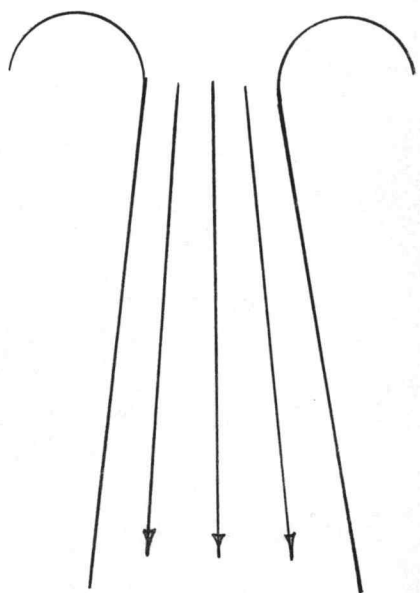


Figure 1b. Illustrations of no "appreciable" separation ($2\theta = 7^\circ$, $L/W = 9$) (below line a-a in Figure 1a).

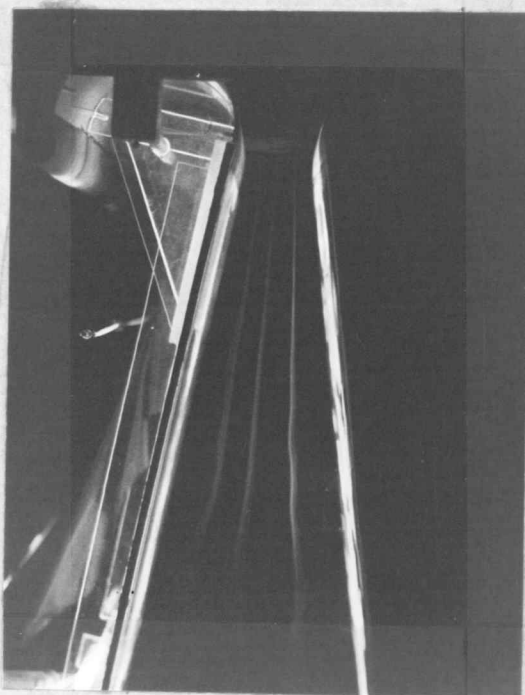
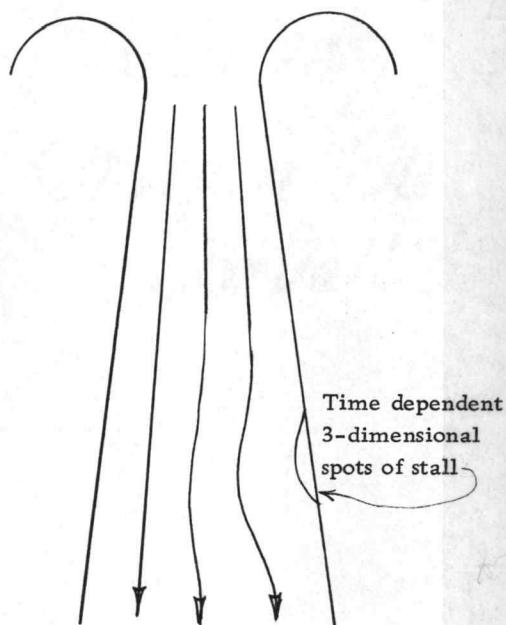
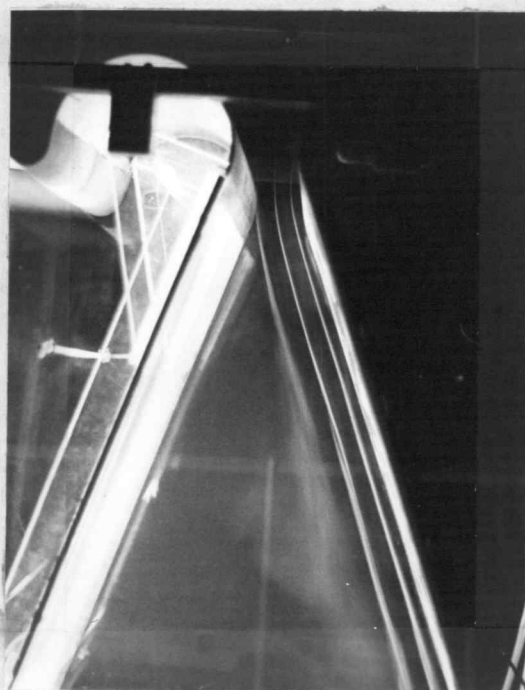
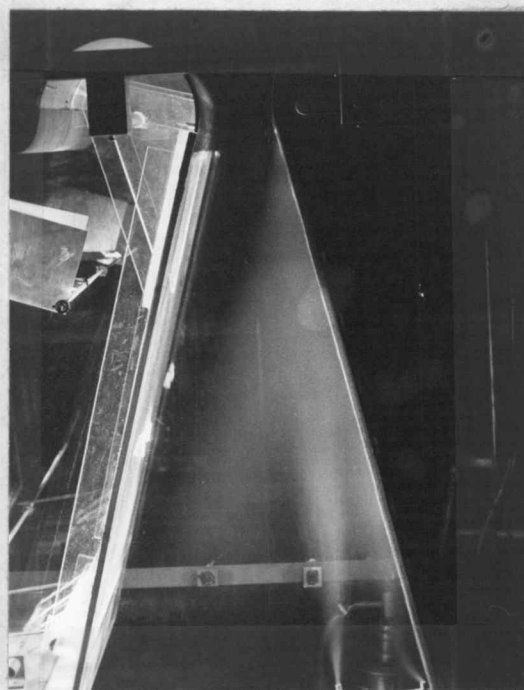


Figure 1c. Illustrations of large transitory stall ($2\theta = 18^\circ$, $L/W = 9$) (above line a-a and below line b-b in Figure 1a).



$2\theta = 40^\circ$
 $L/W = 12$
 Smoke injected above
 inlet



$2\theta = 30^\circ$
 $L/W = 12$
 Smoke injected into
 stalled fluid from below.

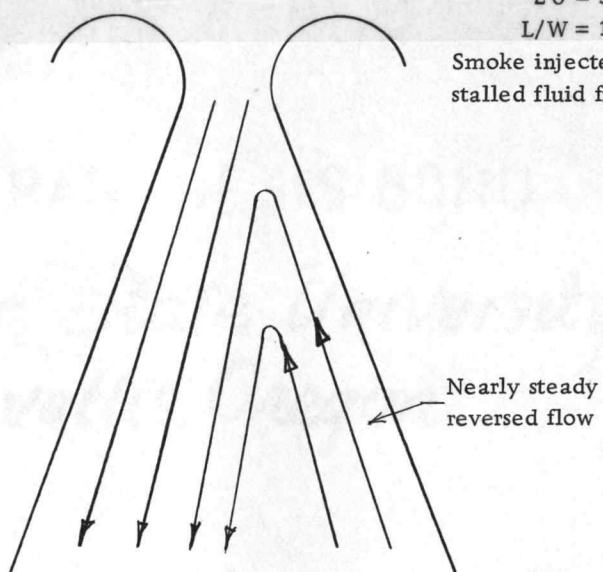


Figure 1d. Illustrations of fully-developed two-dimensional separation (above line b-b and below c-c in Figure 1a).

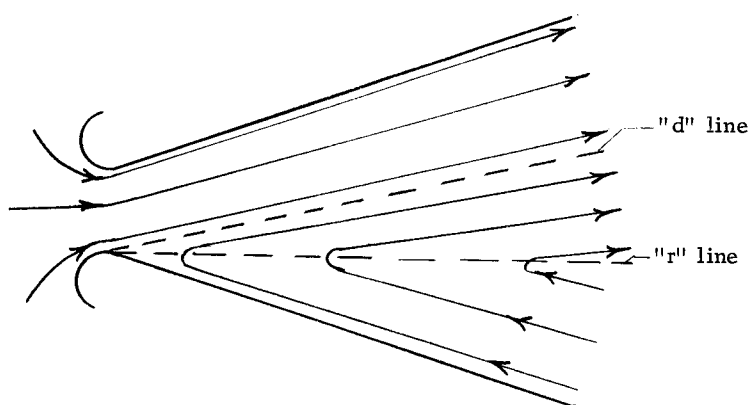


Figure 2a. An illustration of streamlines in a subsonic diffuser during fully-developed two-dimensional stall.

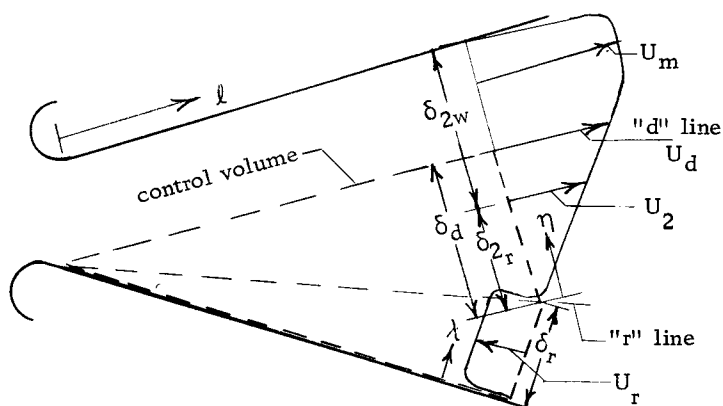


Figure 2b. An illustration of velocity profiles in a subsonic diffuser during fully-developed two-dimensional stall.

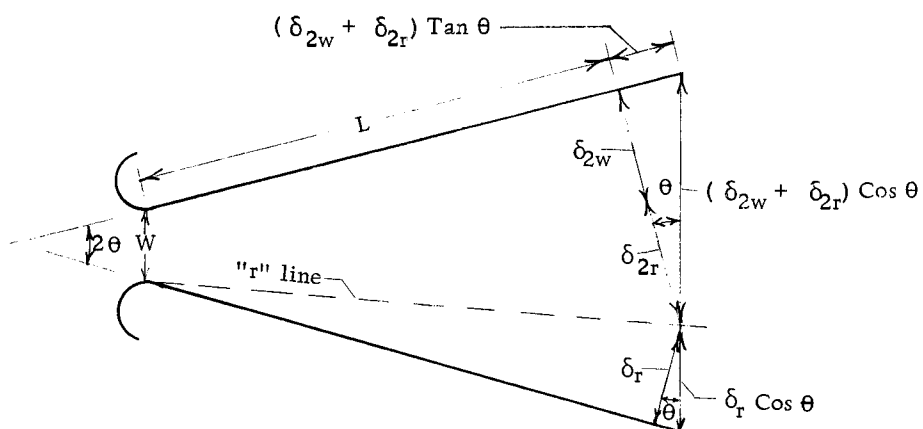


Figure 2c. An illustration of parameters used in Equation (15).

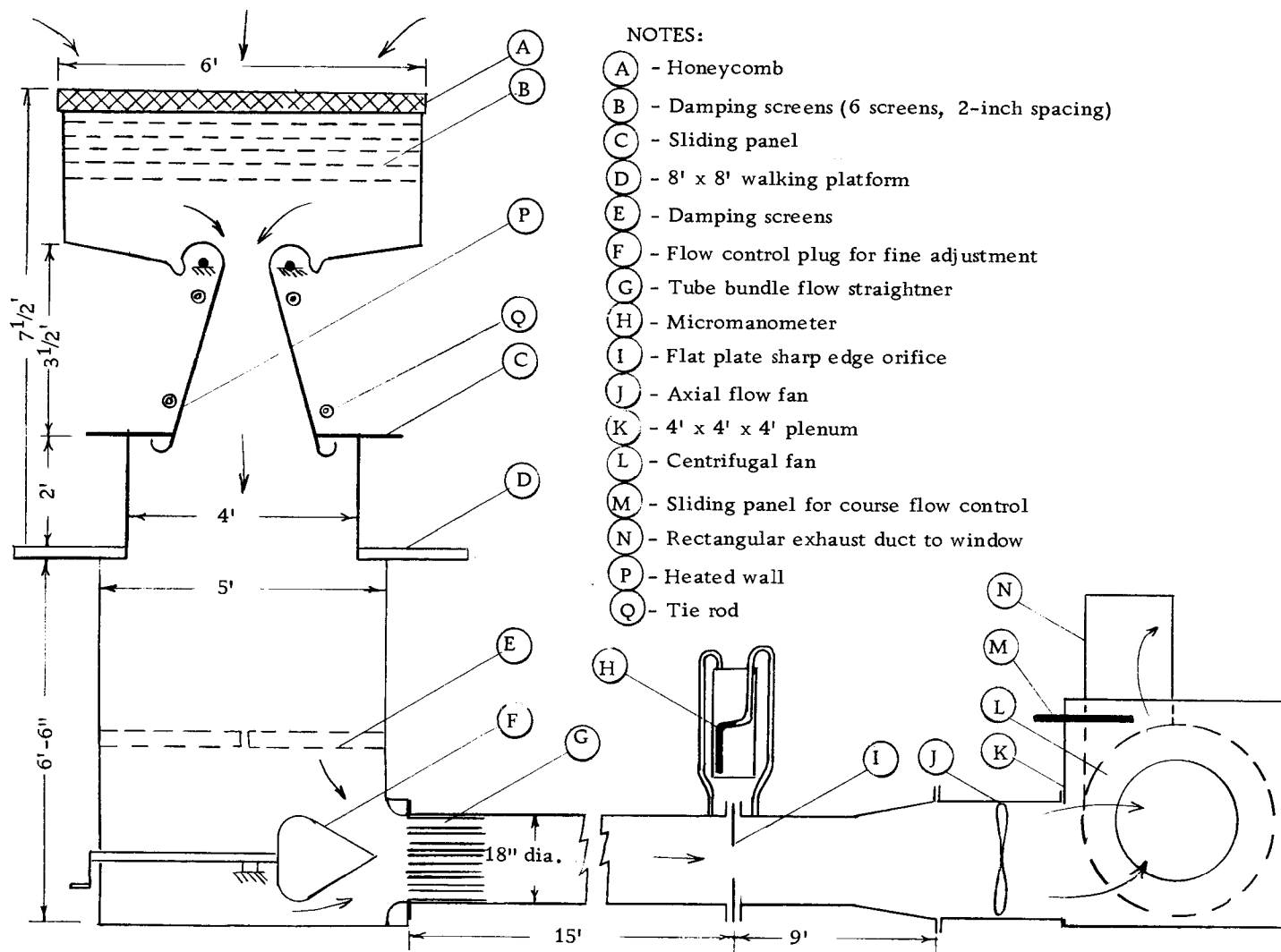


Figure 3a. Schematic side view of test apparatus.

Notes: (continued from Figure 3a)

- (R) - Motor
- (S) - Wall boundary
- (T) - Diffuser entrance

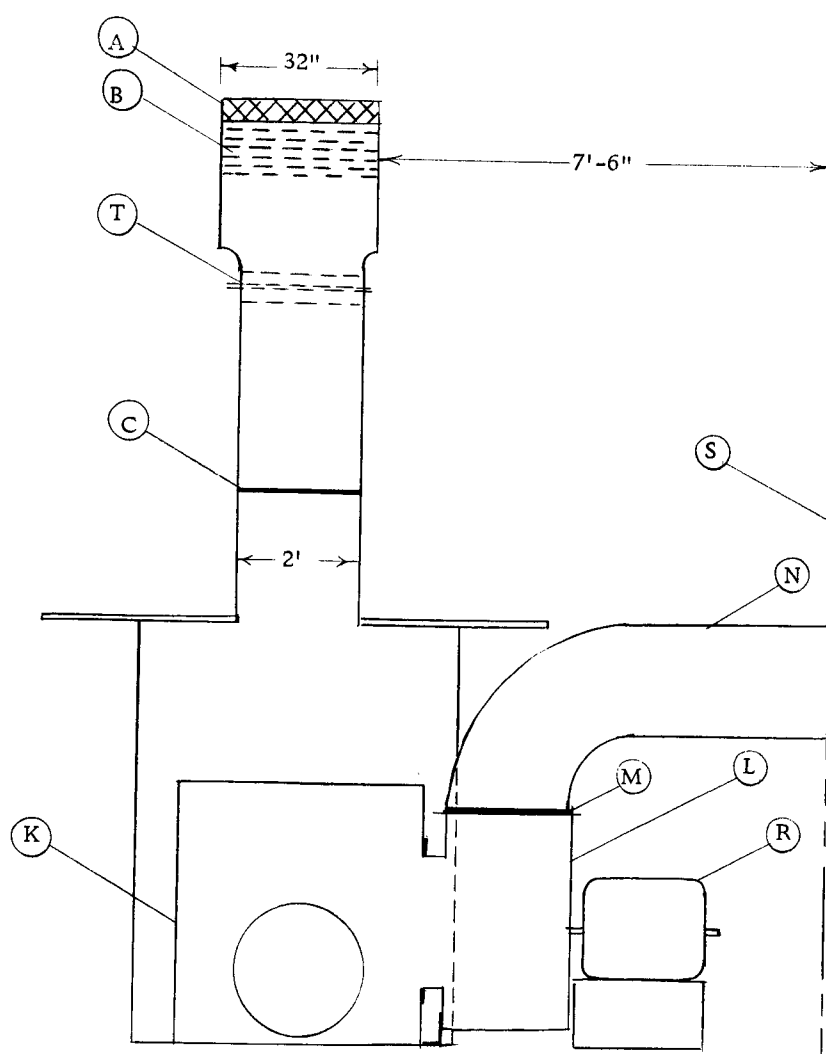
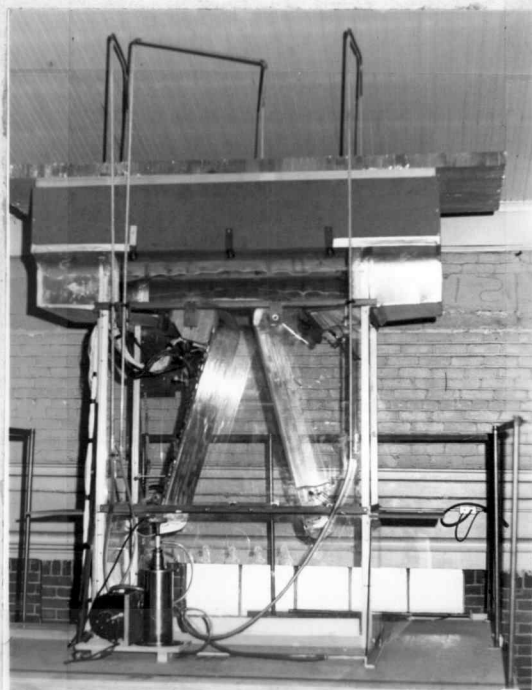
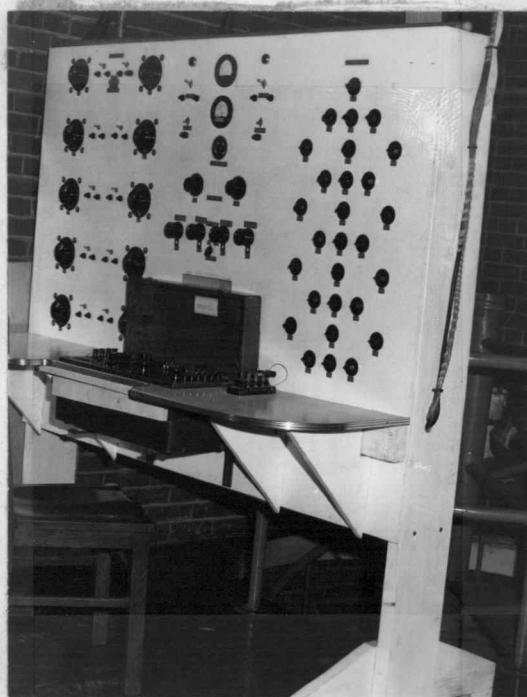


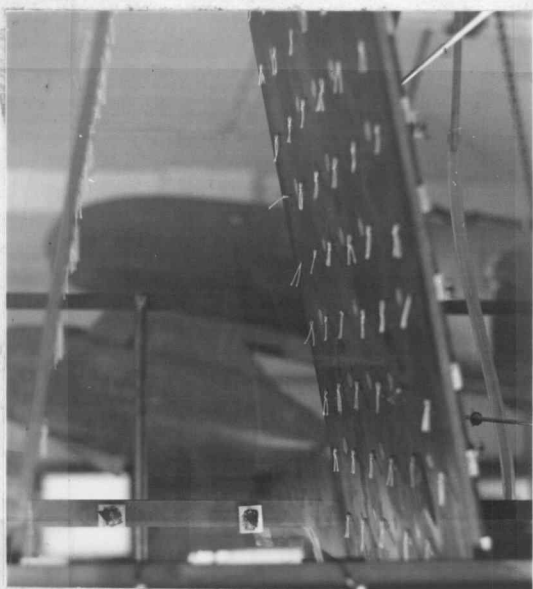
Figure 3b. Schematic end view of test apparatus.



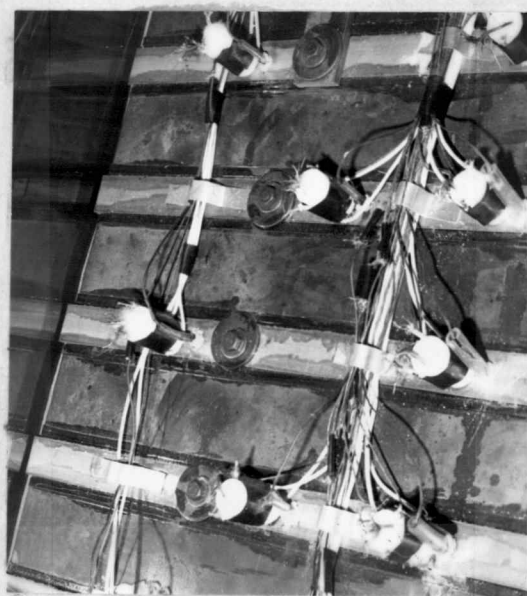
Side View of Test Apparatus Showing
Smoke Probes



Control Console



Arrangement of Tufts



Heater Side of Heated Plate

Figure 3c. Photographs of experimental equipment.

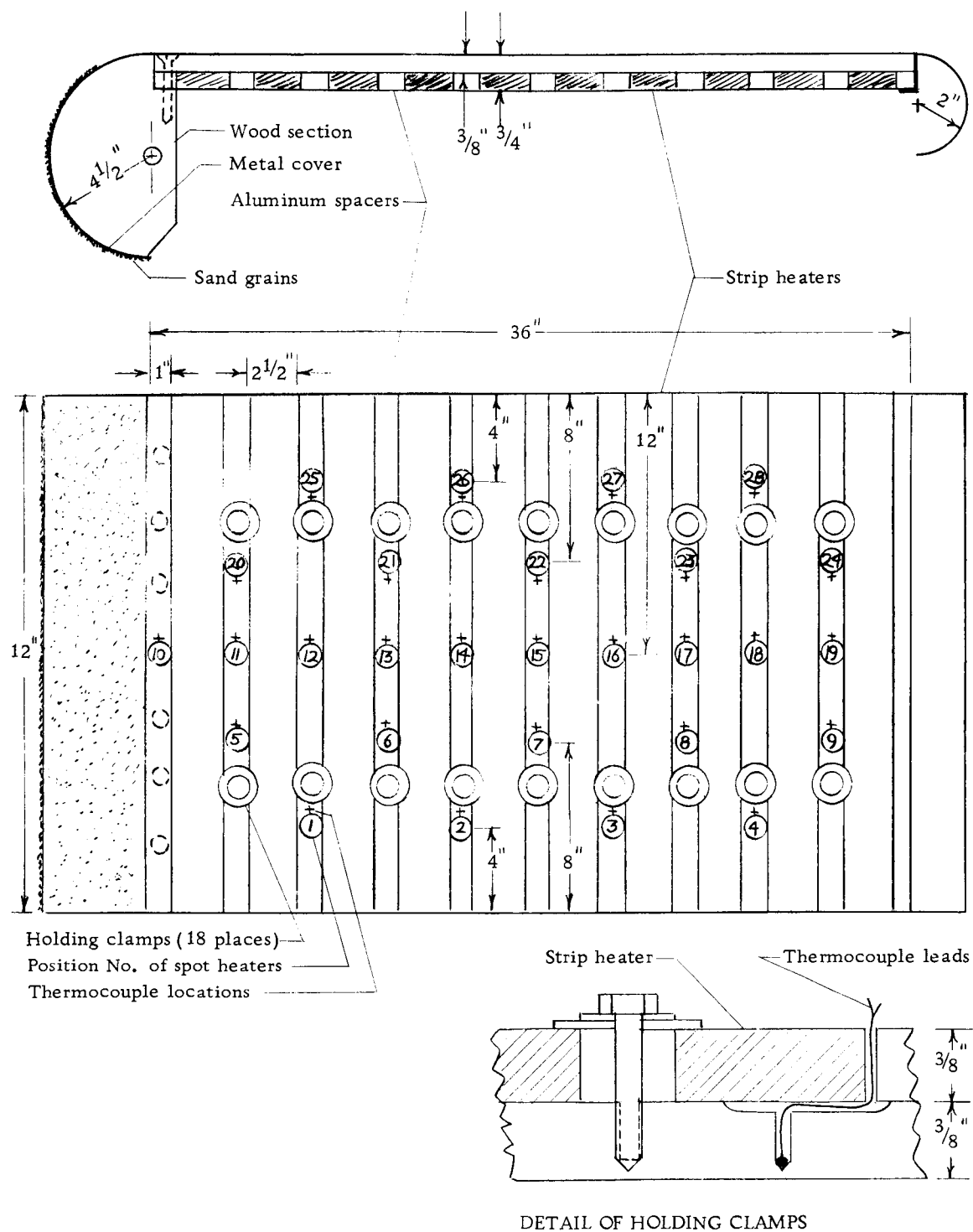
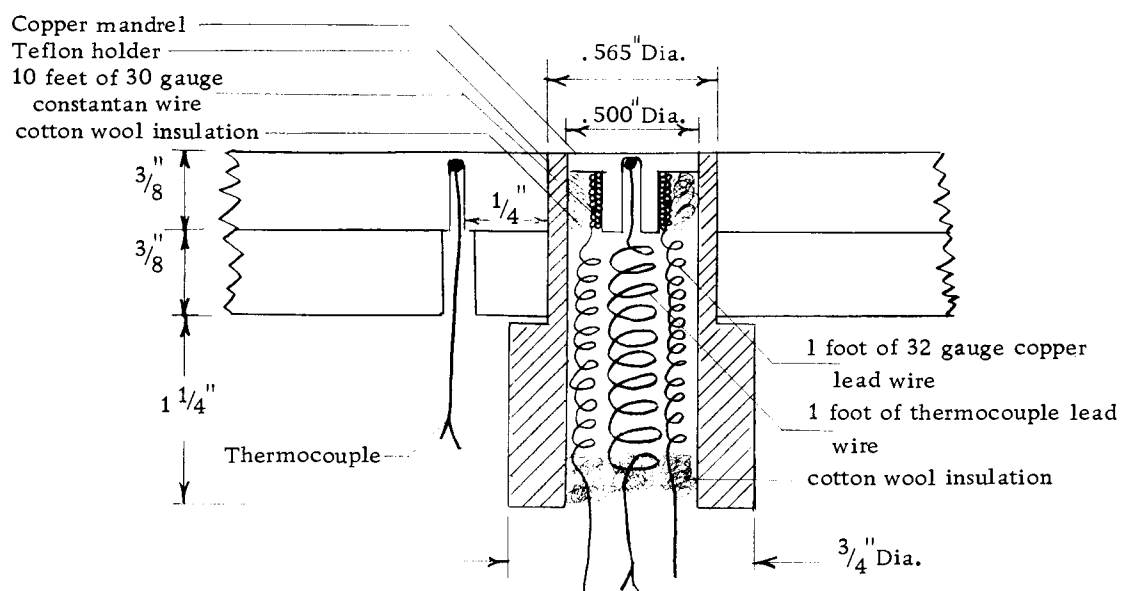
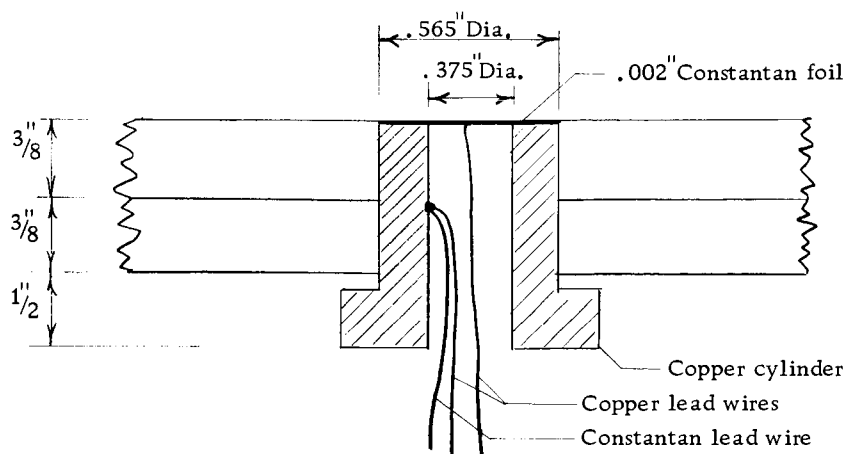


Figure 4. Schematic drawing of heated plate assembly.



SPOT HEATER ASSEMBLY



TRANSIENT HEAT METER ASSEMBLY

Figure 5. Schematic drawings of heat transfer measuring devices.

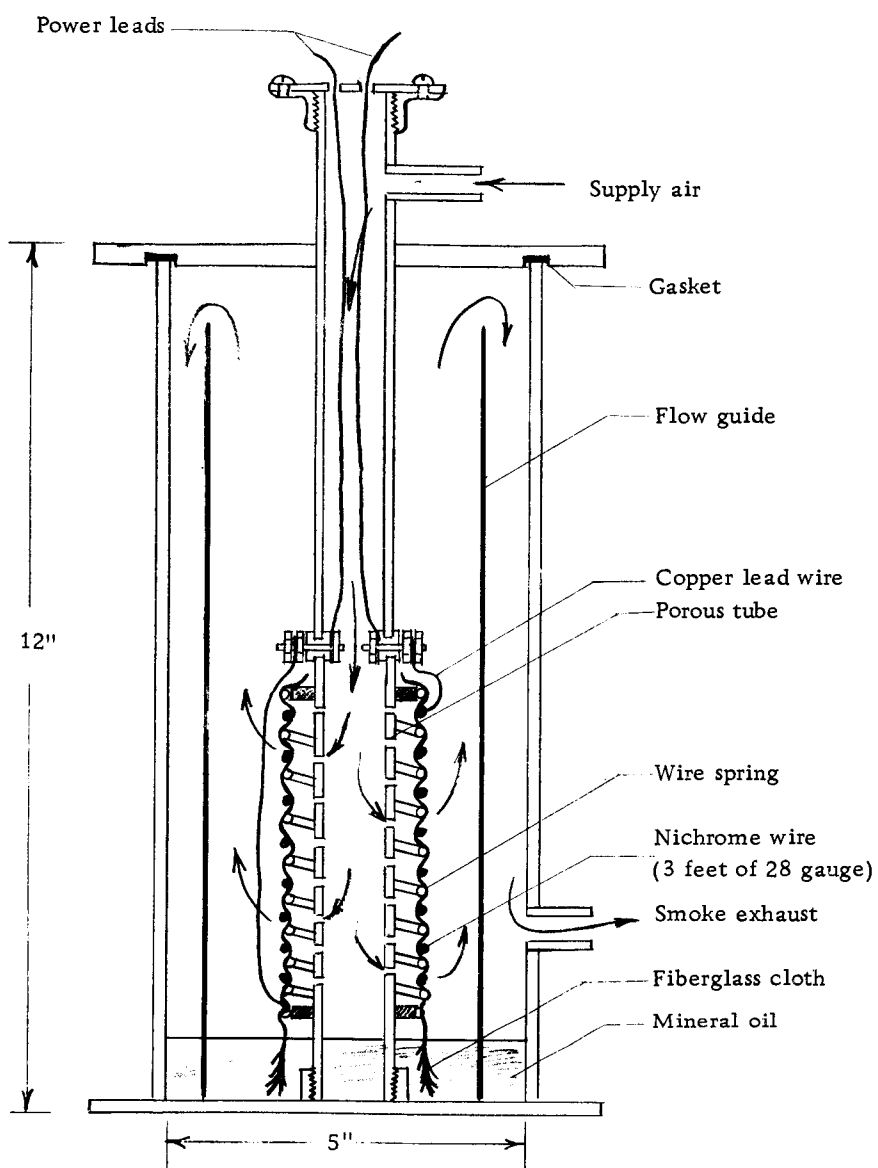


Figure 6. Schematic drawing of smoke generator.

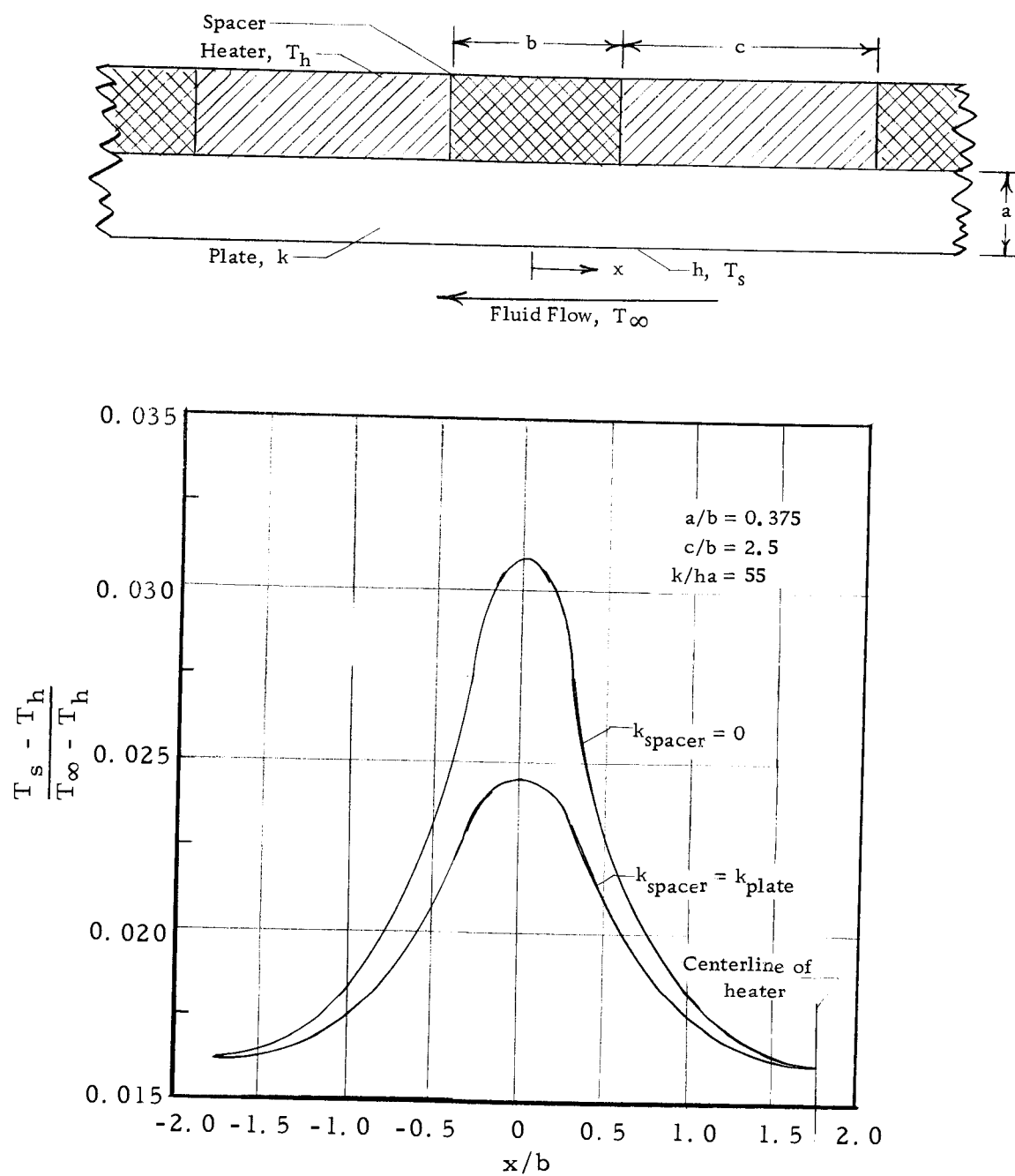


Figure 7. Variation of surface temperature on the heated plate as found by electrical analog.

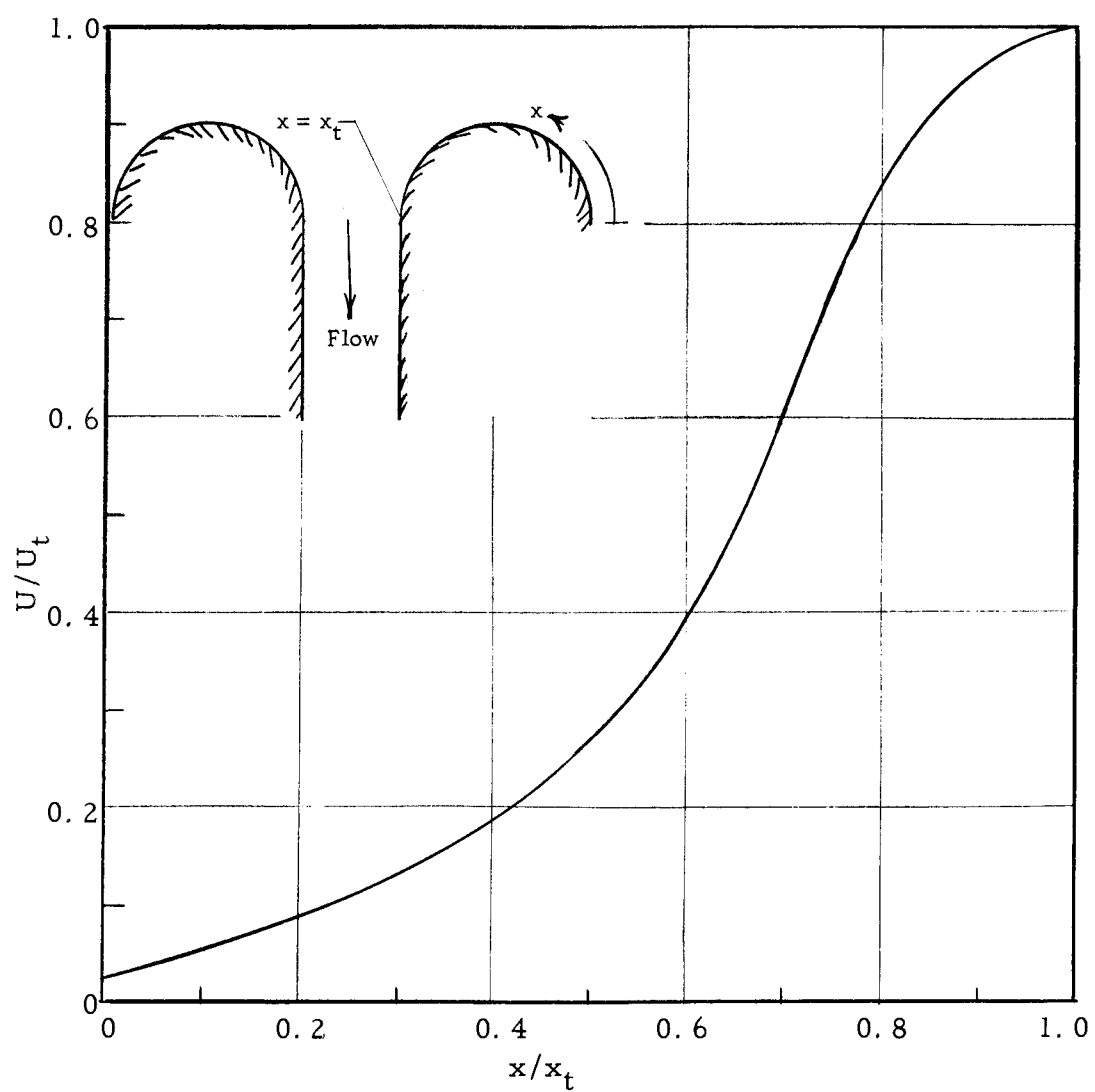


Figure 8. Velocity variation over the diffuser entrance surface from a flux plot ($2\theta = 0^\circ$).

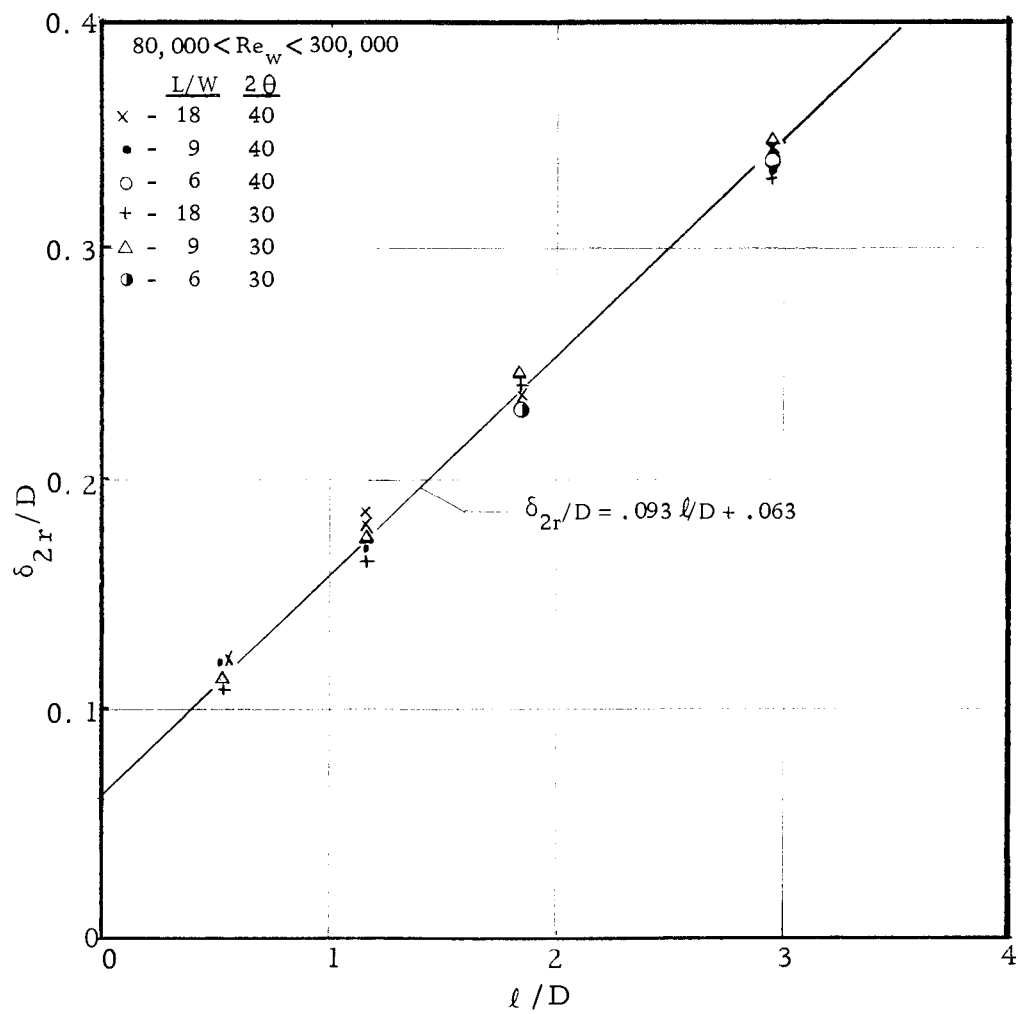


Figure 9. Correlation of δ_{2r} from velocity data.

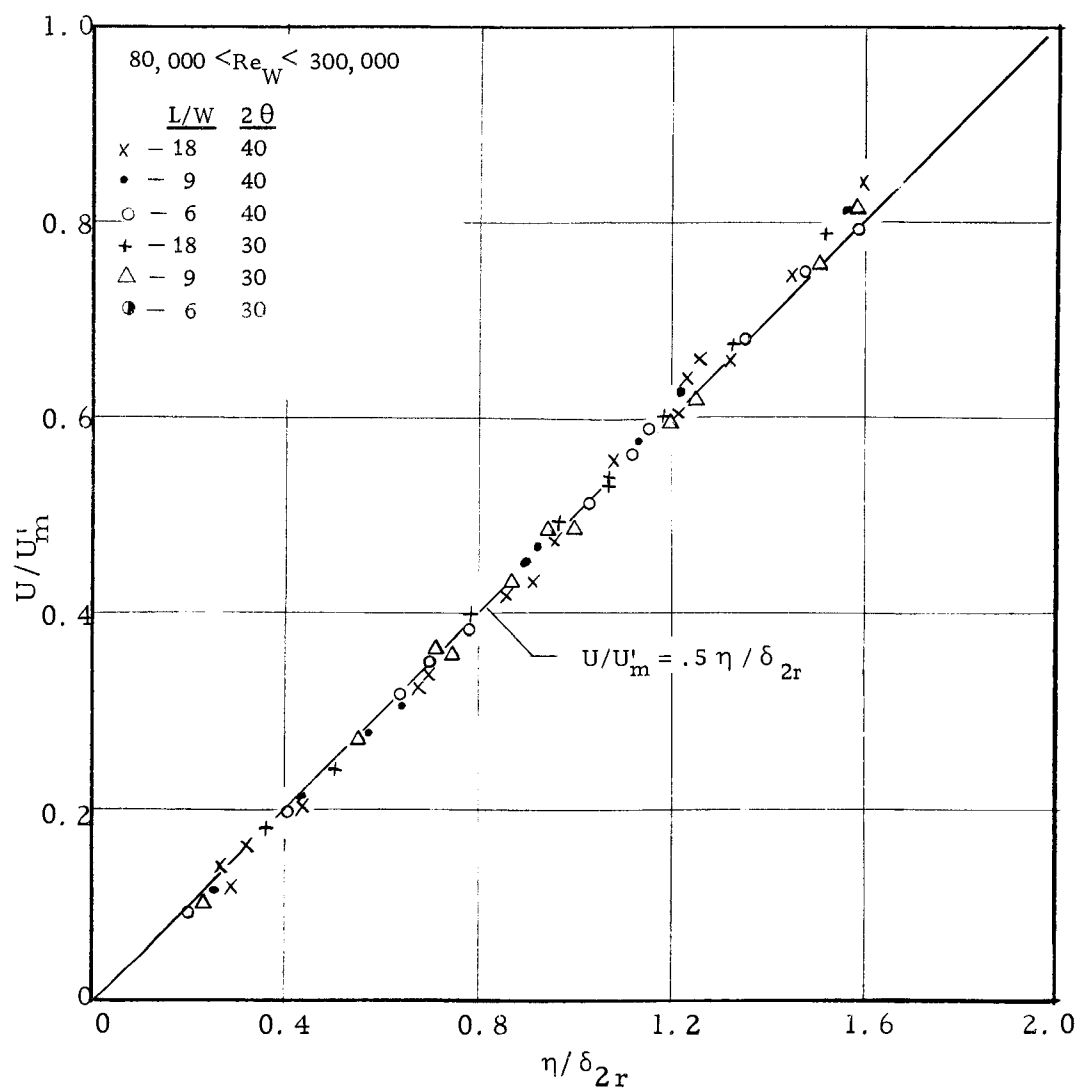


Figure 10. Velocity distribution in the mixing region during fully-developed two-dimensional stall.

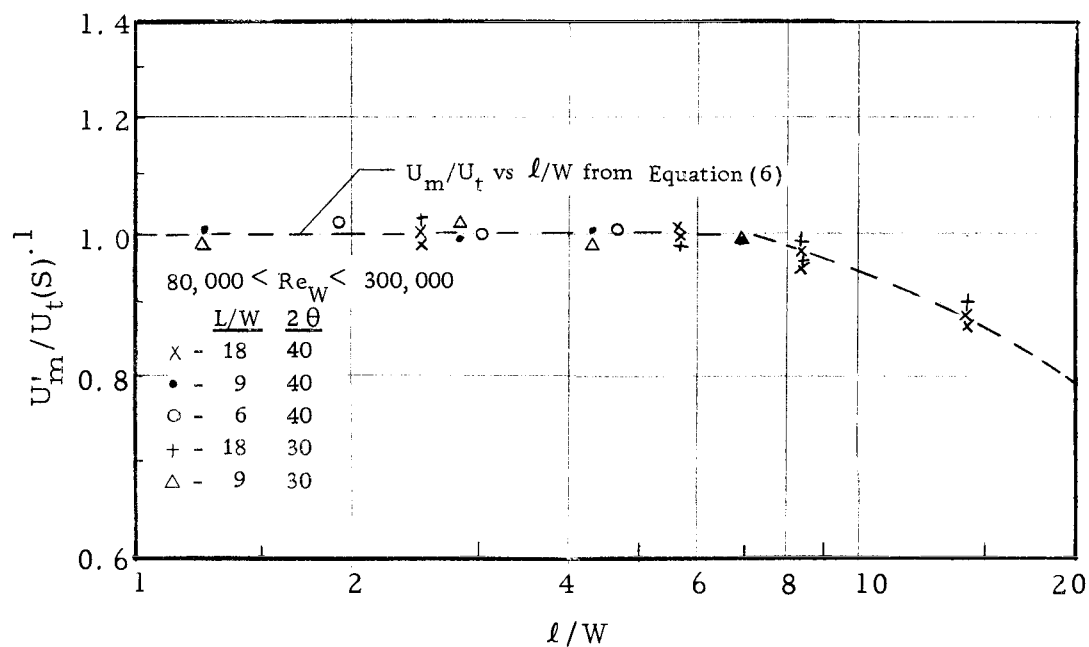


Figure 11. Correlation of the maximum velocity along the "wall of jet flow" during fully-developed two-dimensional stall.

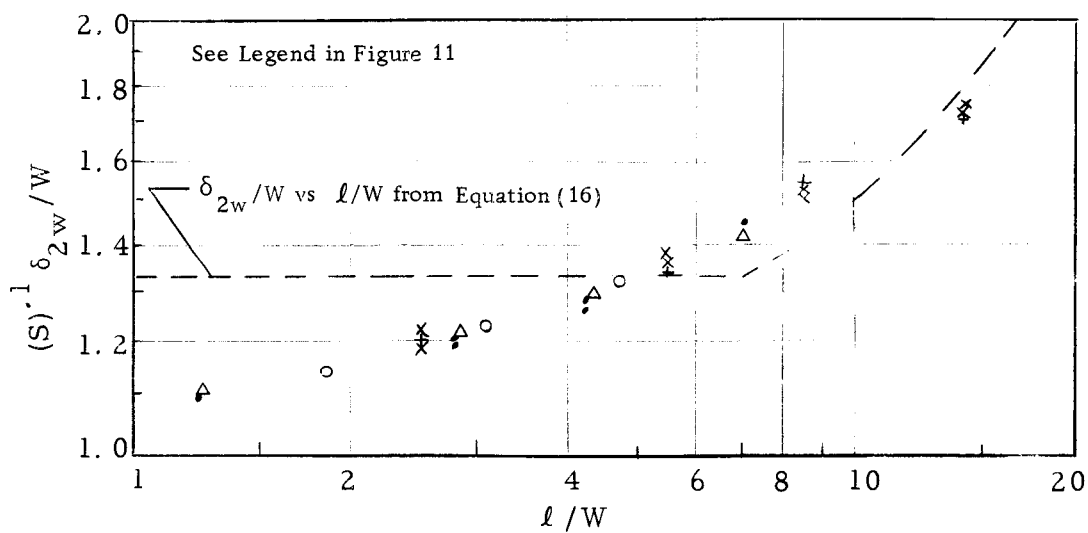


Figure 12. Correlation of δ_{2W} along the "wall of jet flow" during fully-developed two-dimensional stall.

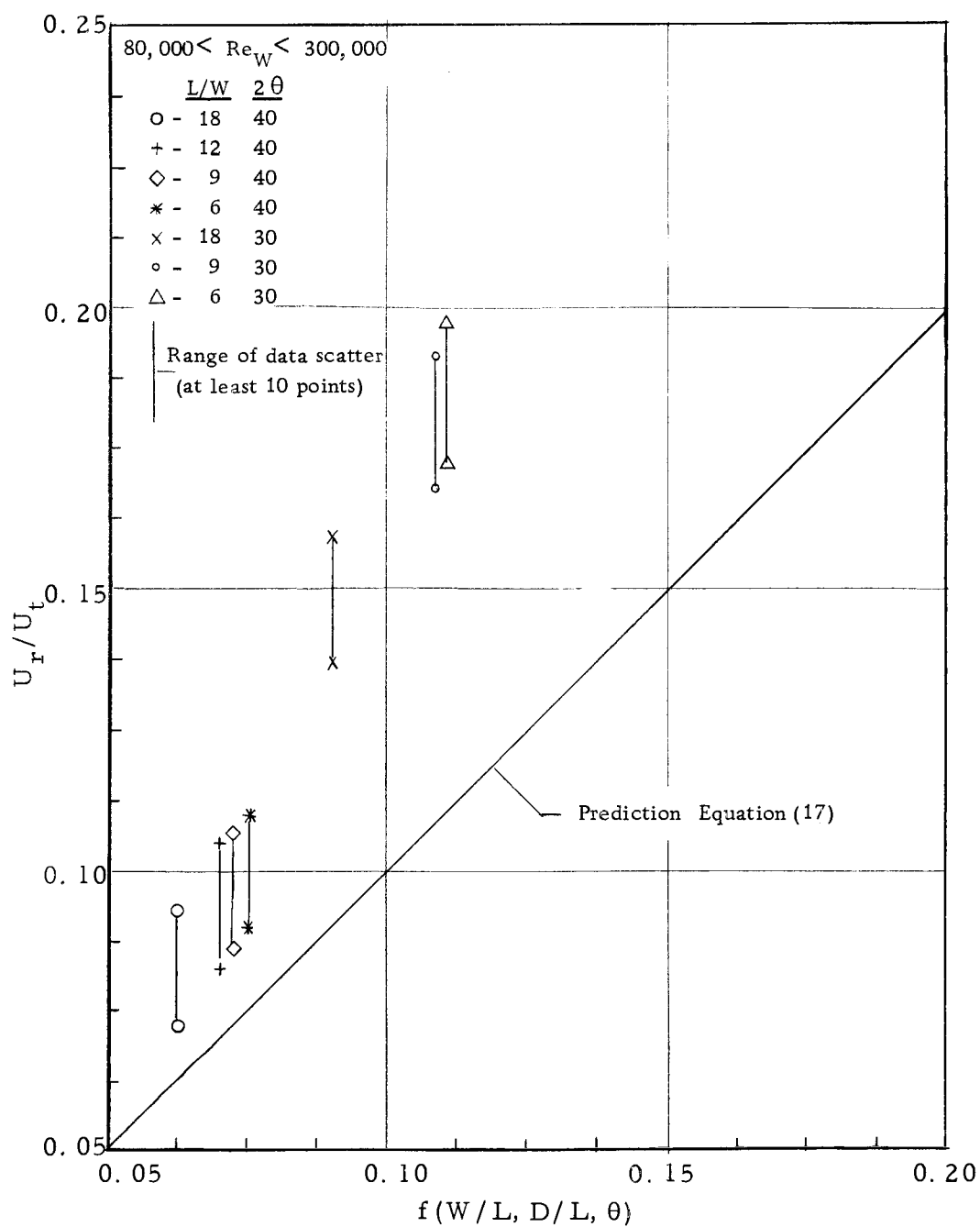


Figure 13a. Comparison of measured and predicted reversed flow velocities in fully-developed two-dimensional stall.

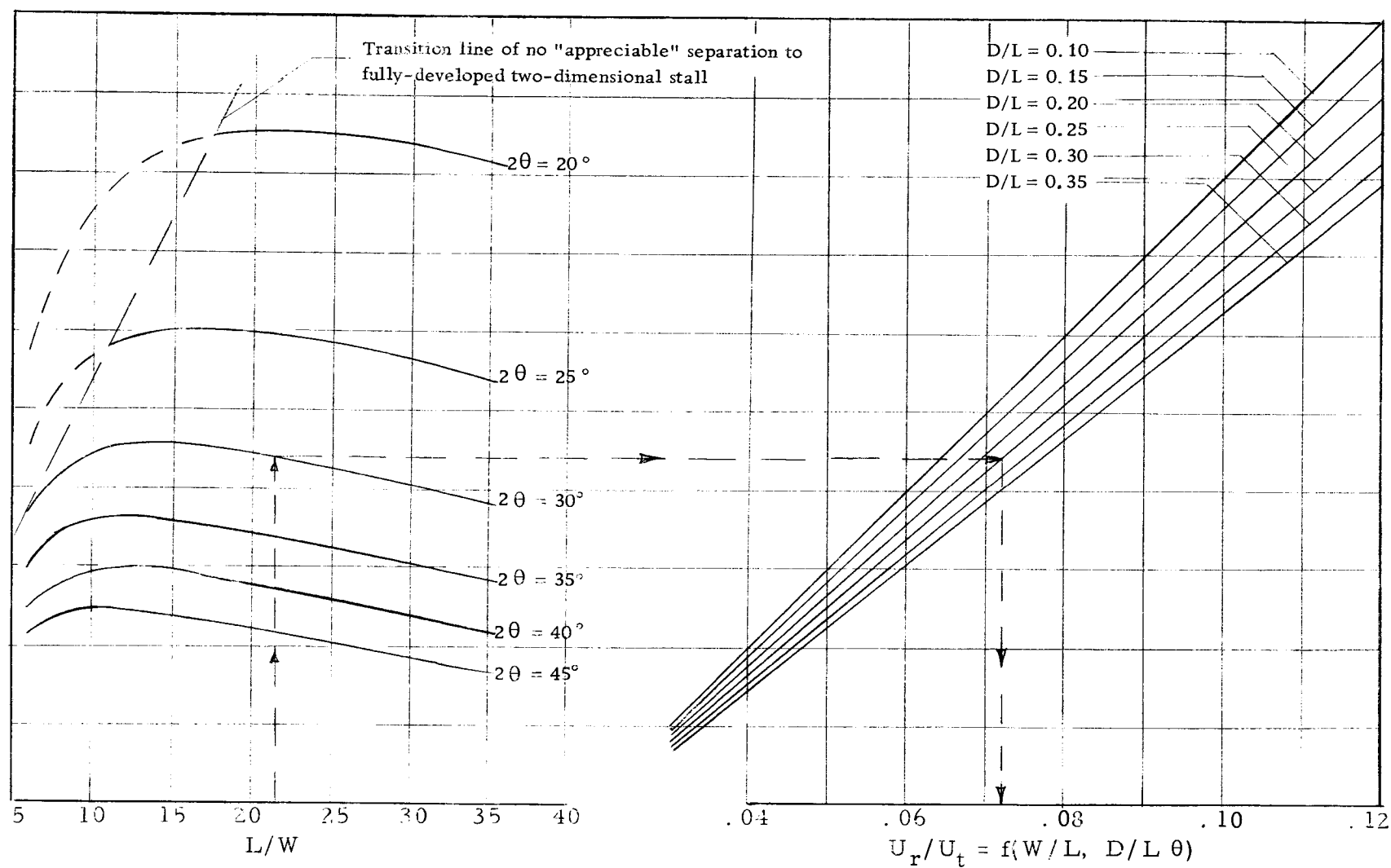


Figure 13b. A graphical presentation of the prediction of U_r/U_t [see Equation (17)].

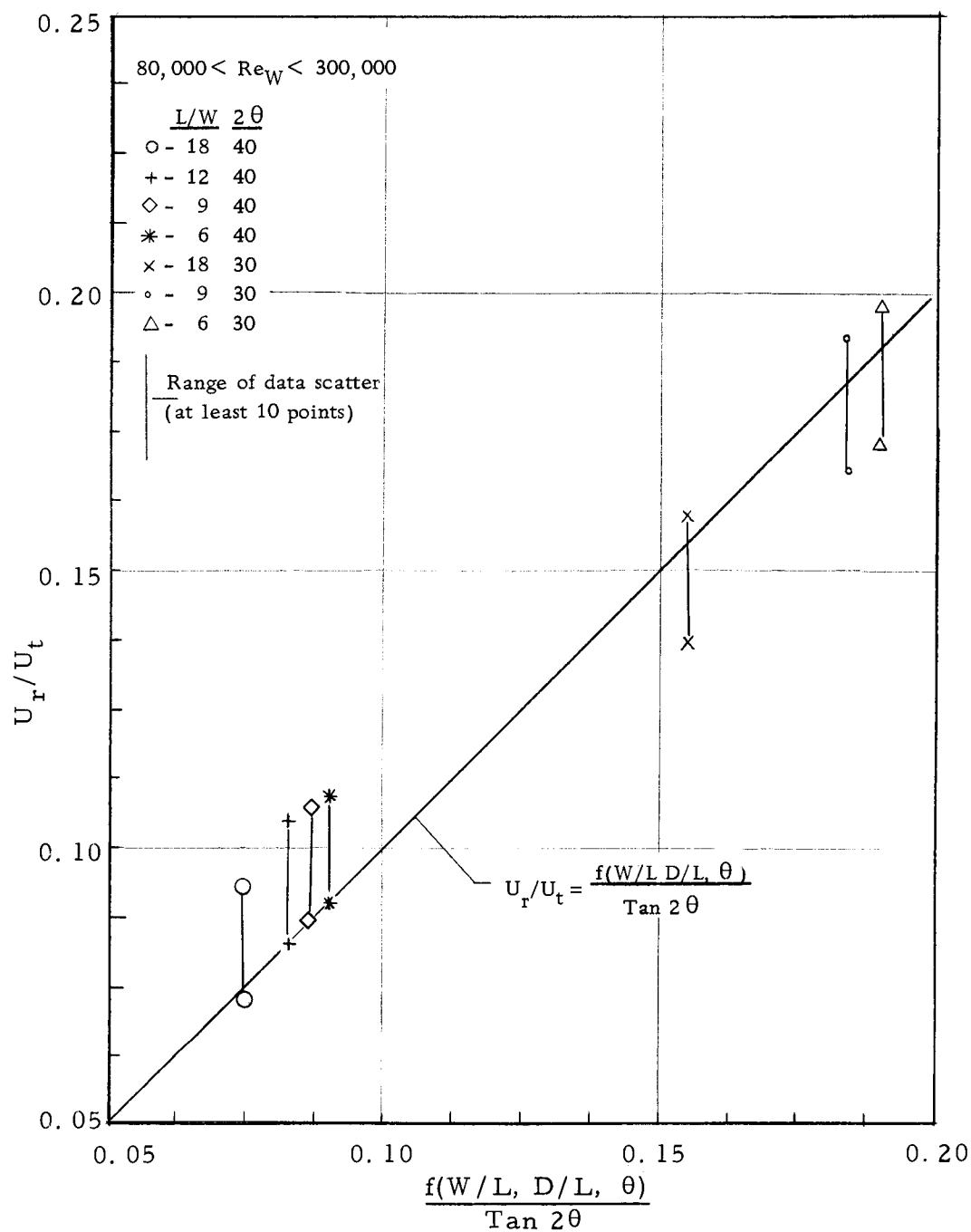


Figure 14. Correlation of measured reversed flow velocities in fully-developed two-dimensional stall.

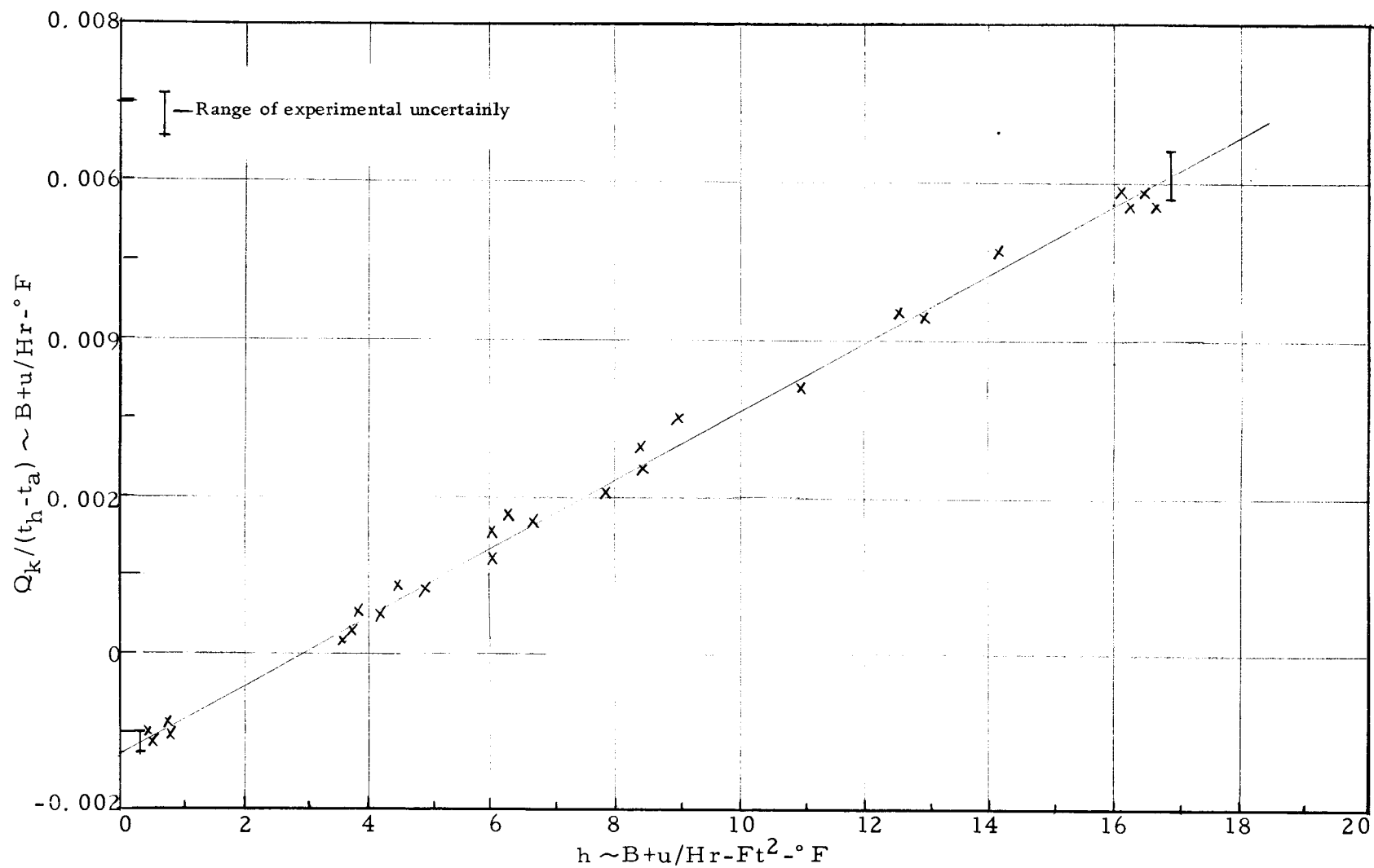


Figure 15. A typical calibration curve for spot heater conduction losses (position no. 1).

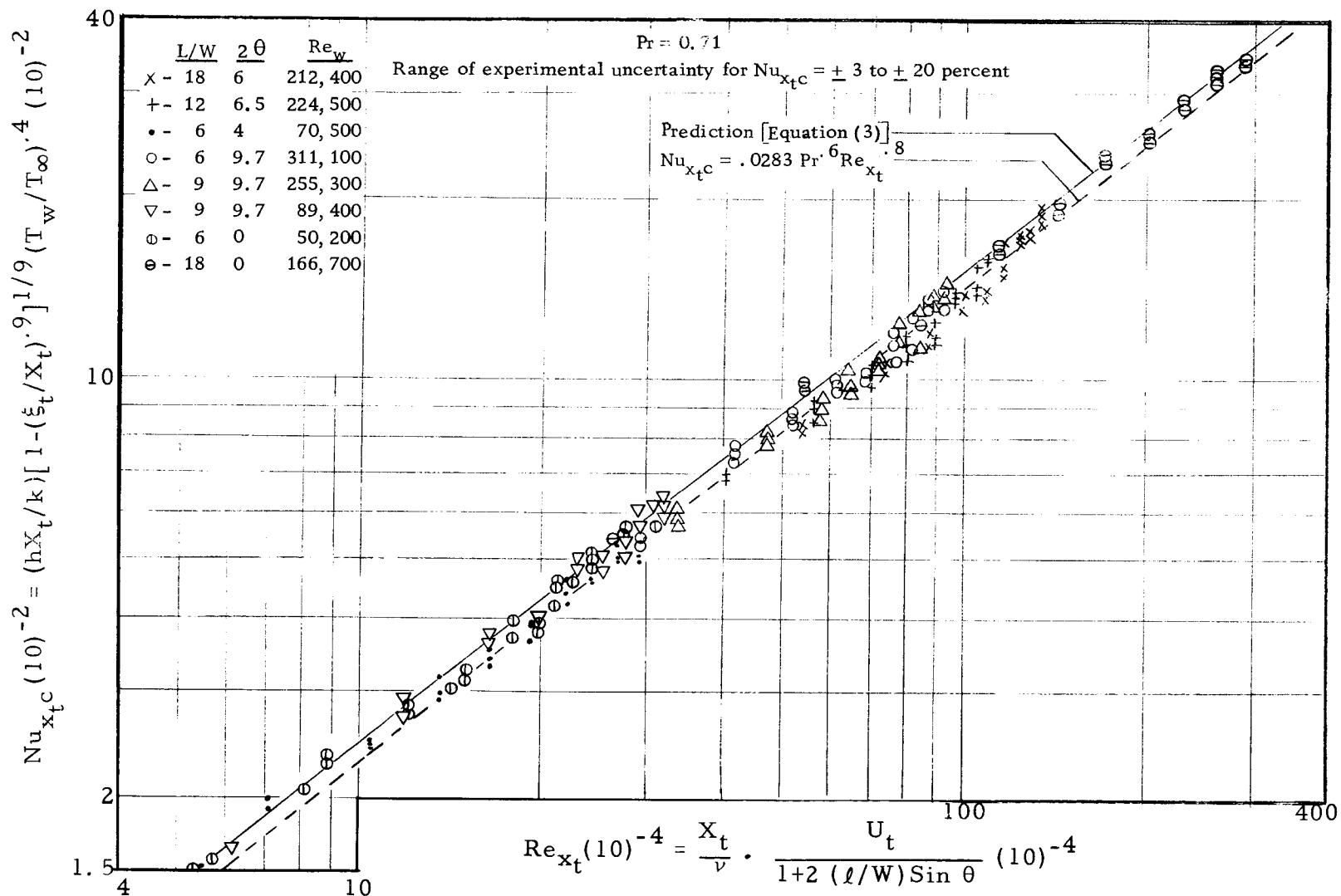


Figure 16. Results of heat transfer measurements during no "appreciable" separation.

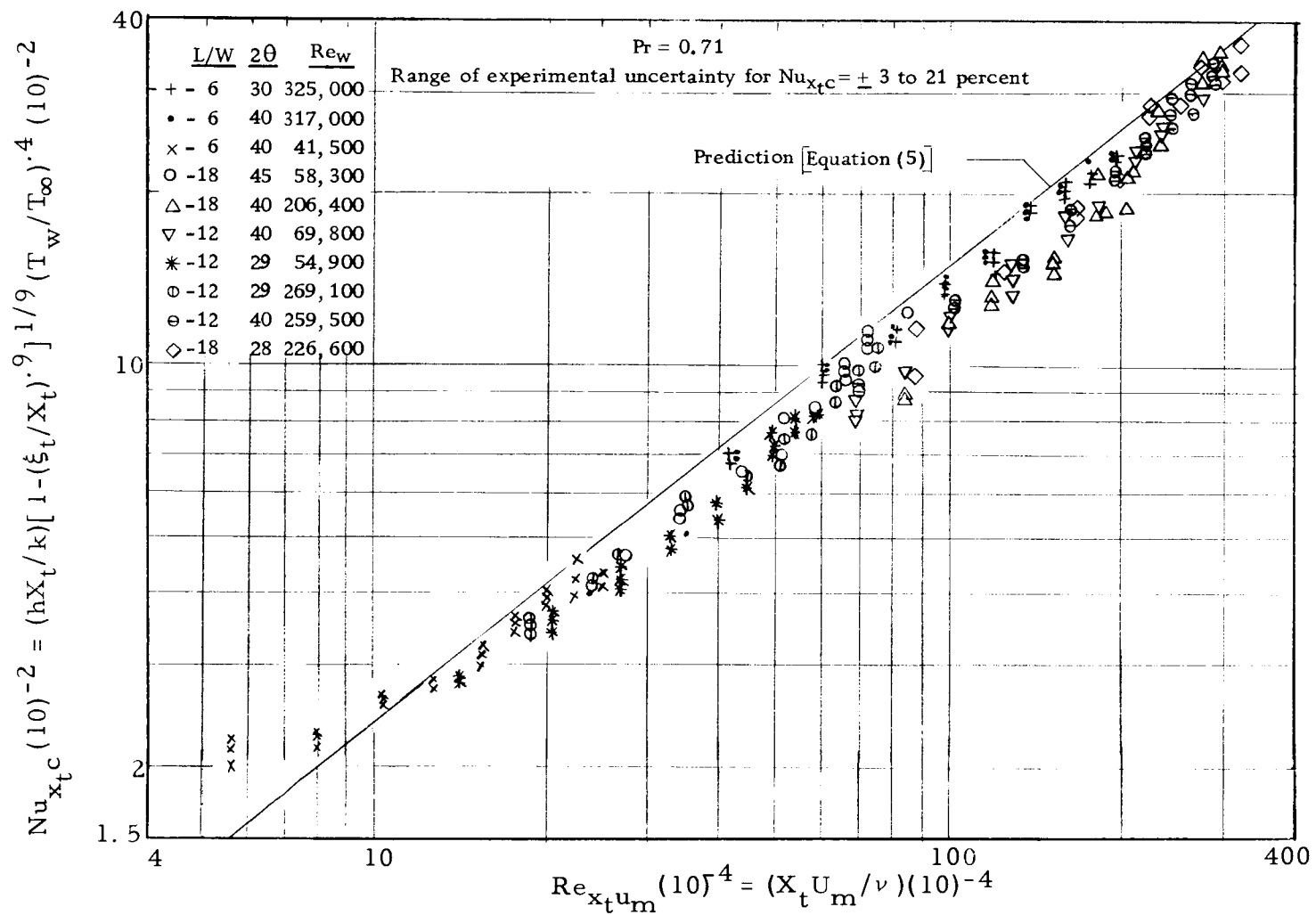


Figure 17a. Results of heat transfer measurements on the "wall of jet flow" during fully-developed two-dimensional stall [U_m determined from the correlation for a plane turbulent wall jet given by Myers, et al. (33)].

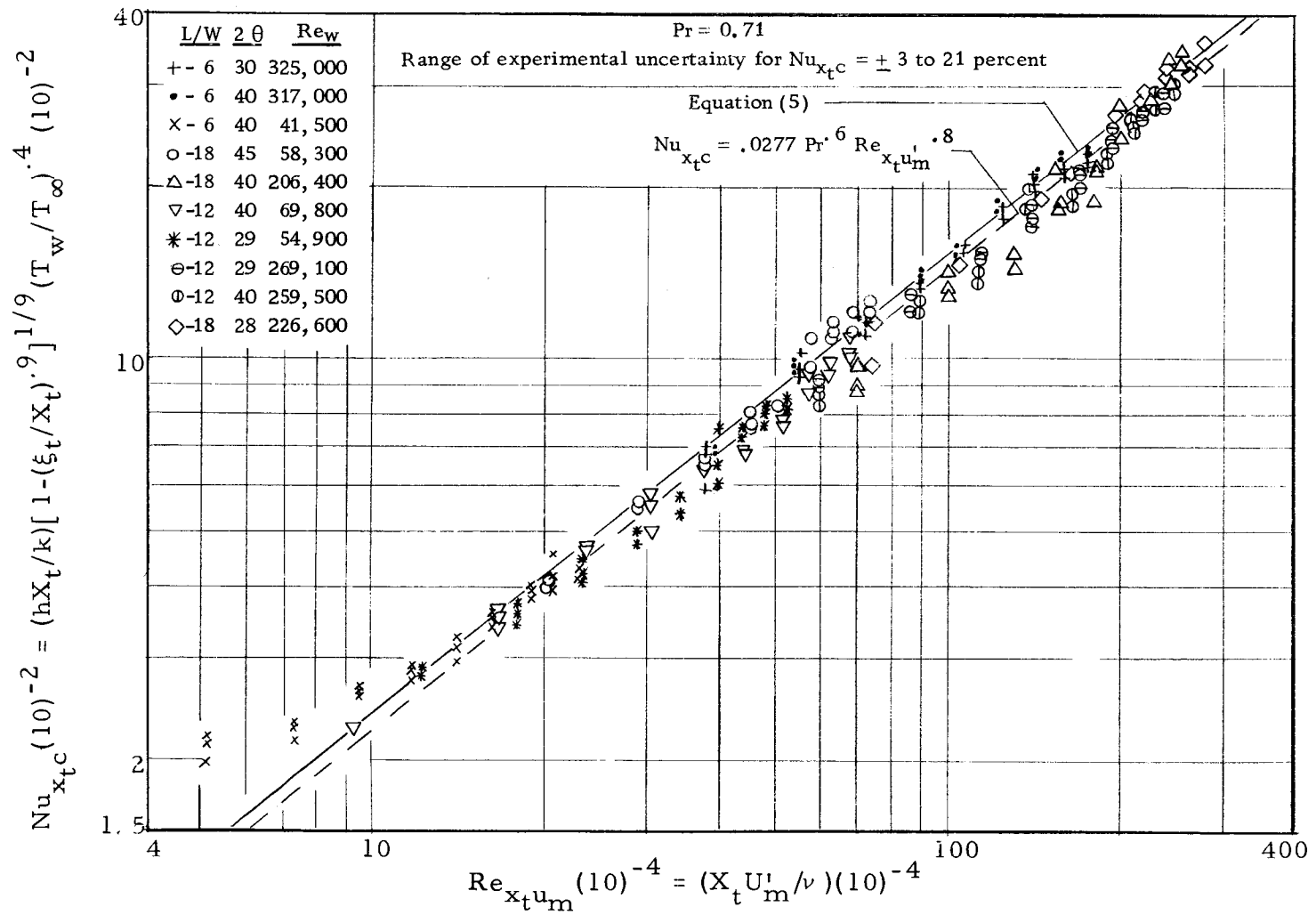
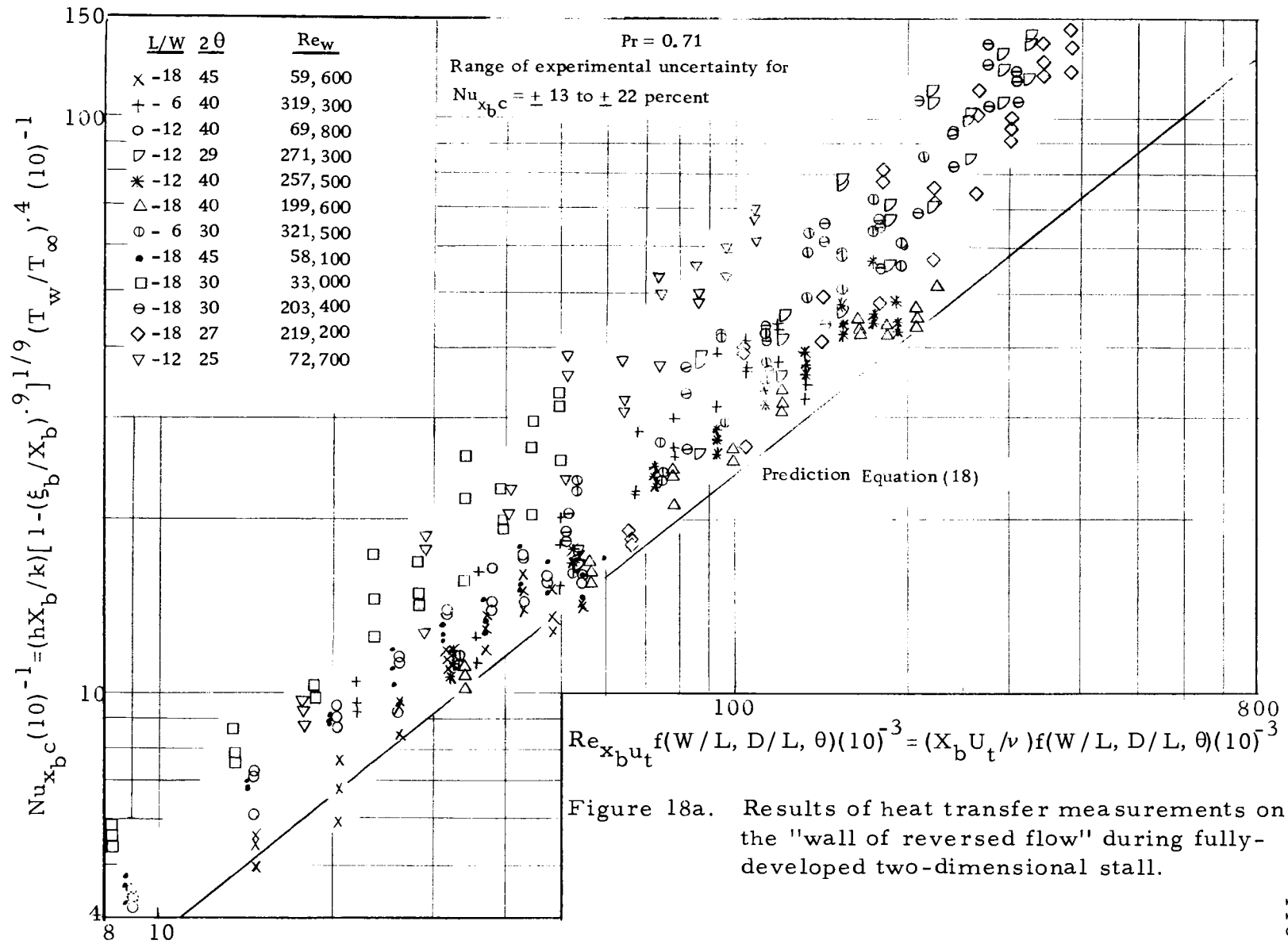
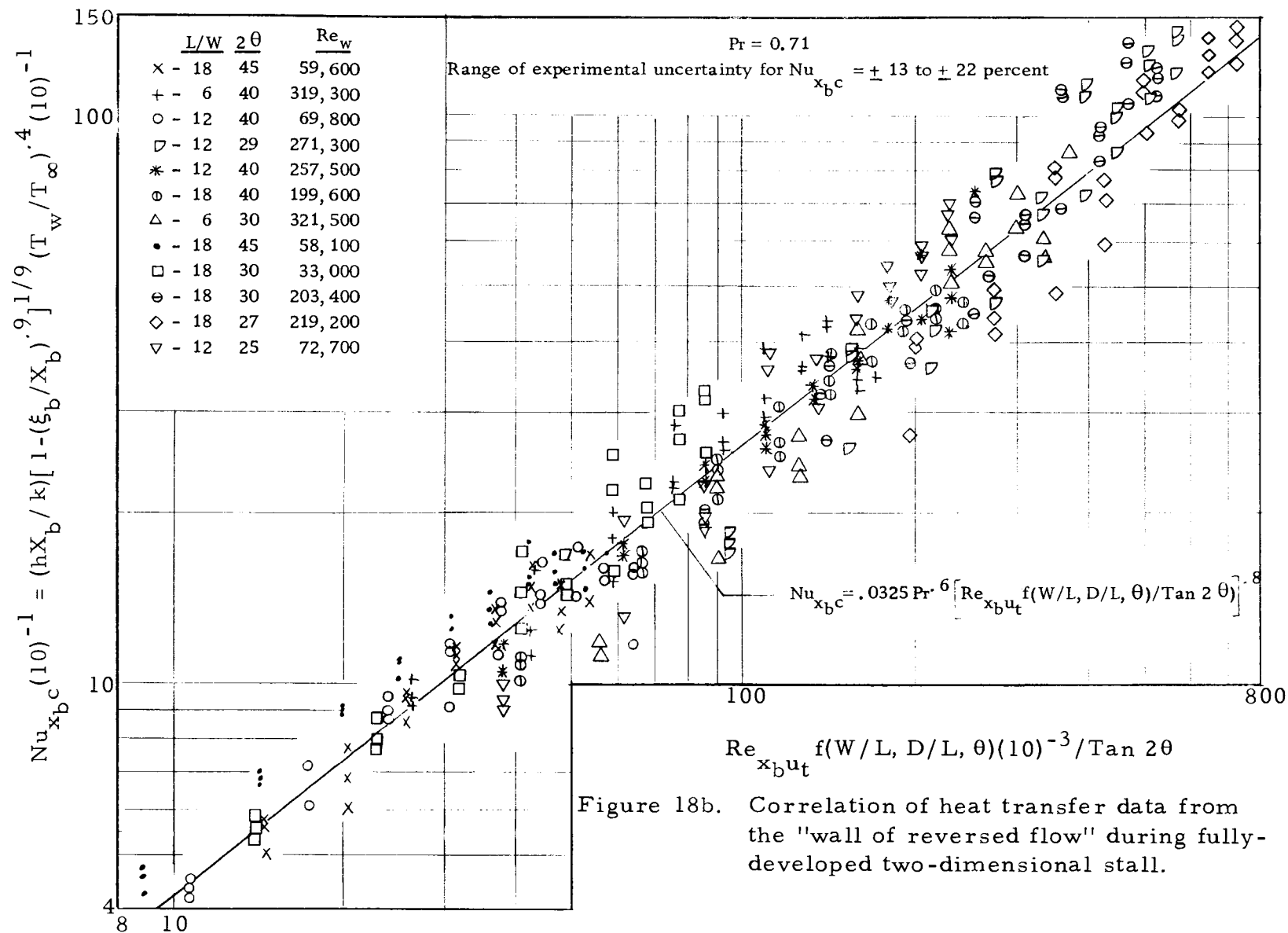


Figure 17b. Results of heat transfer measurements on the "wall of jet flow" during fully-developed two-dimensional stall [U'_m determined from a correlation of experimental measurements, Equation (20)].





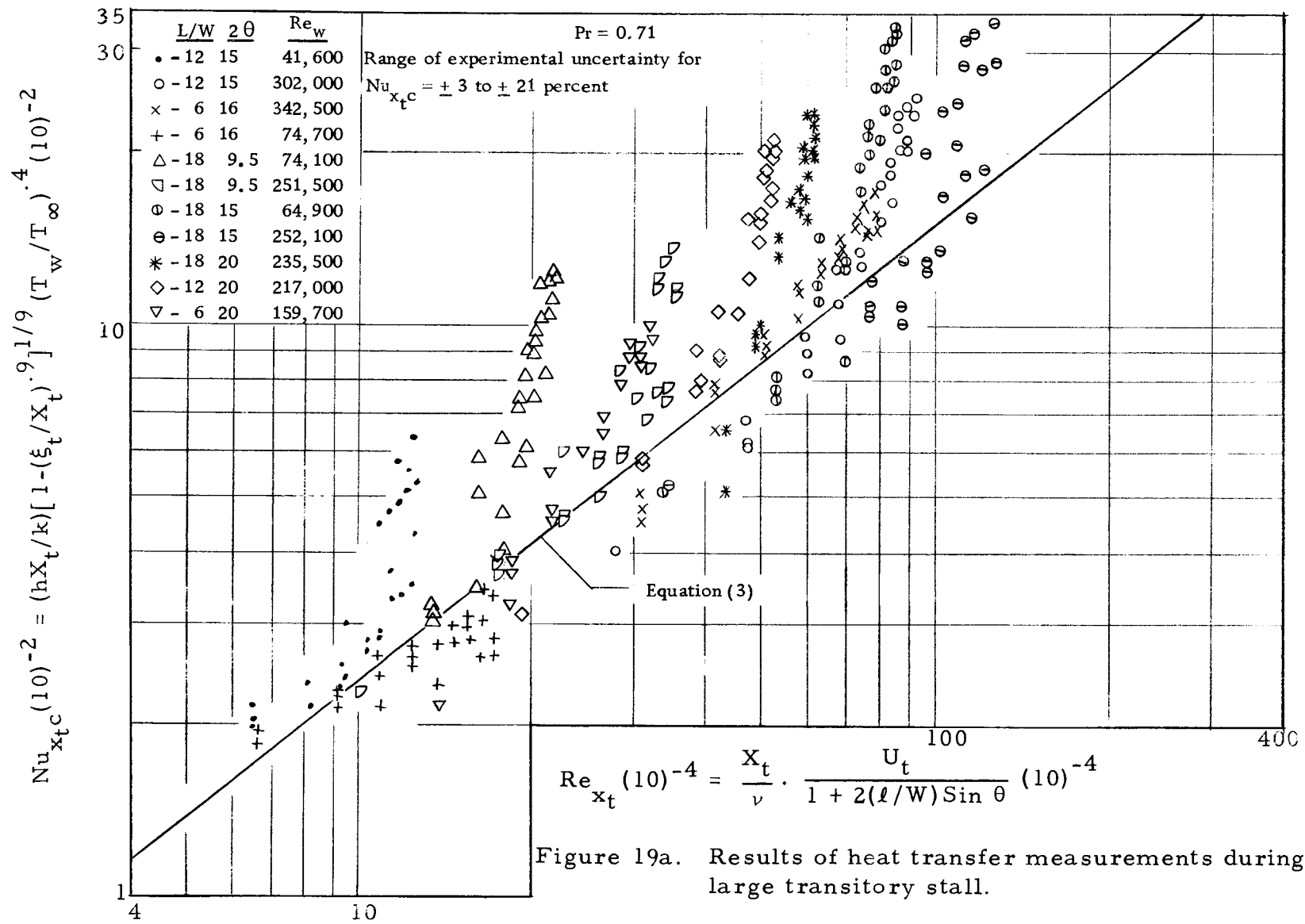
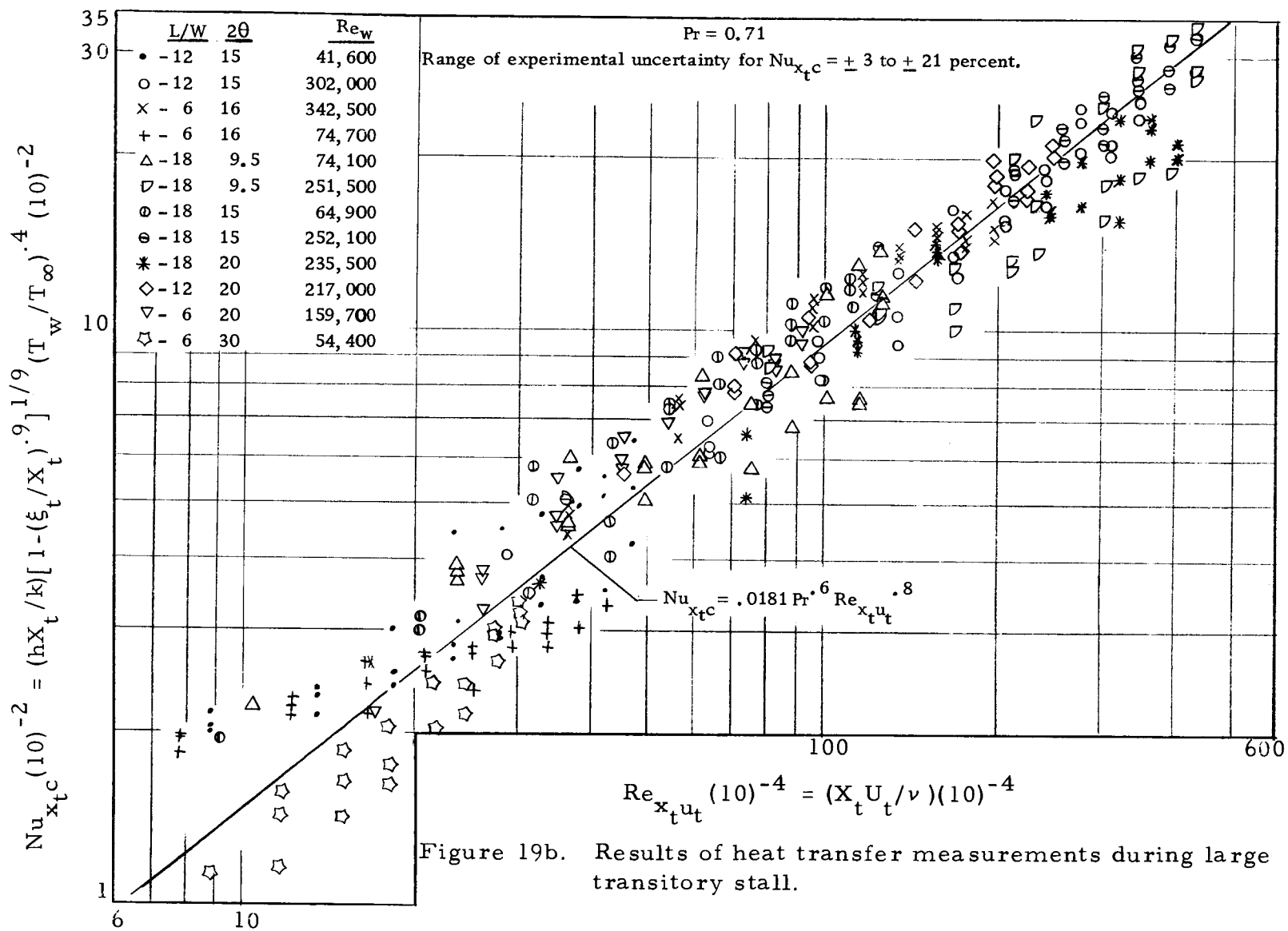


Figure 19a. Results of heat transfer measurements during large transitory stall.



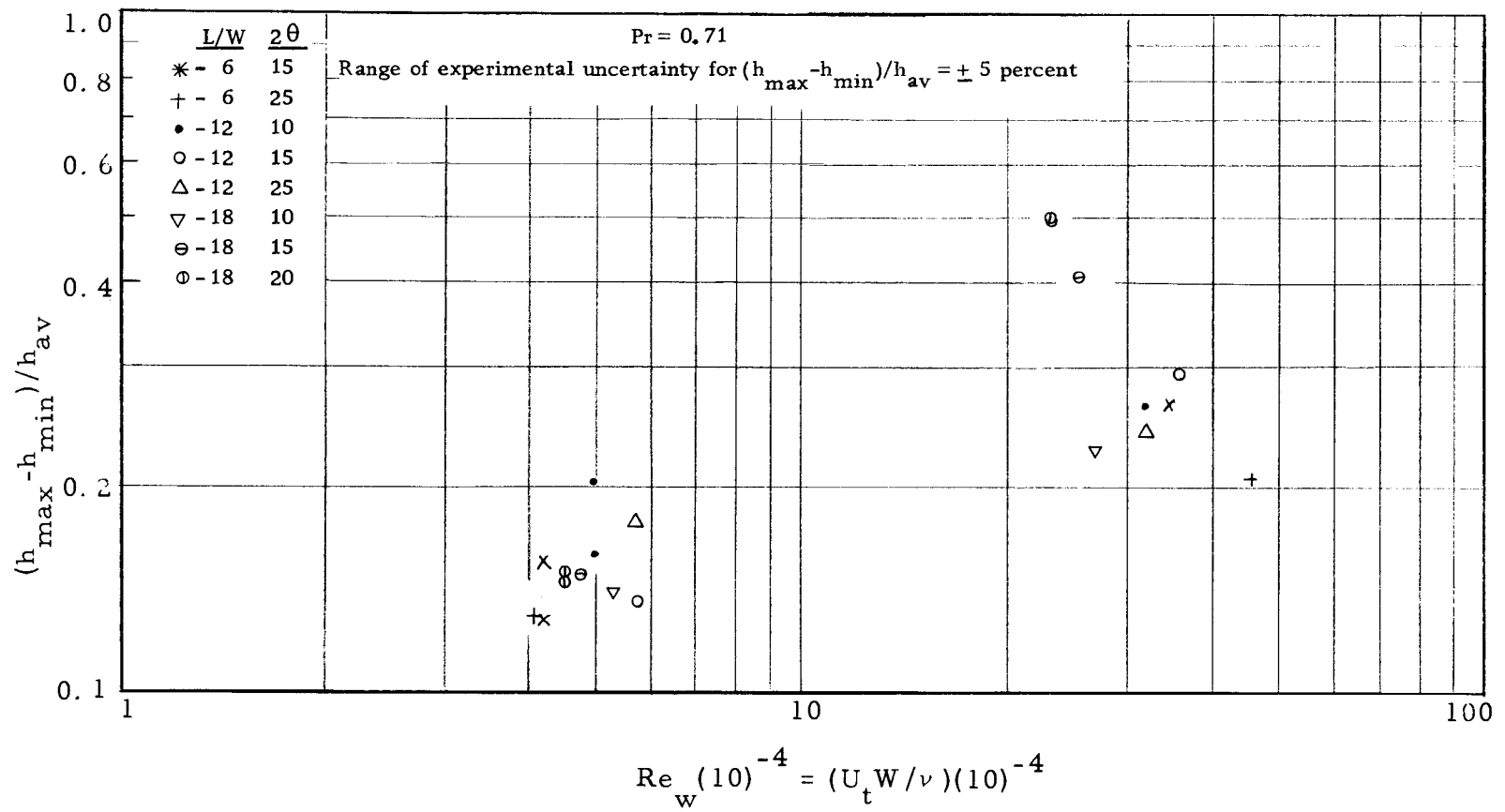


Figure 20a. Results of measurements taken with the transient heat meters during large transitory stall.

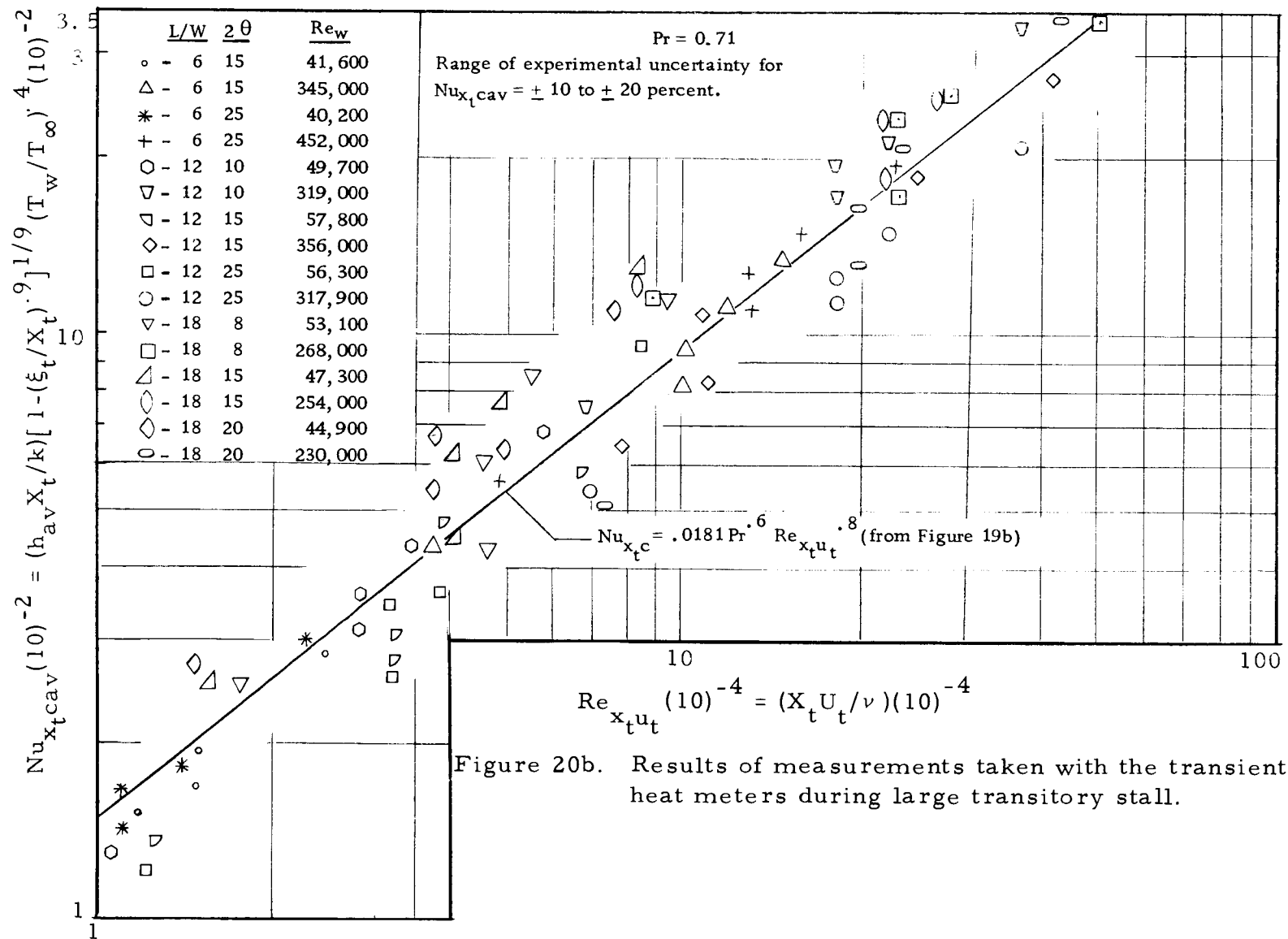


Figure 20b. Results of measurements taken with the transient heat meters during large transitory stall.

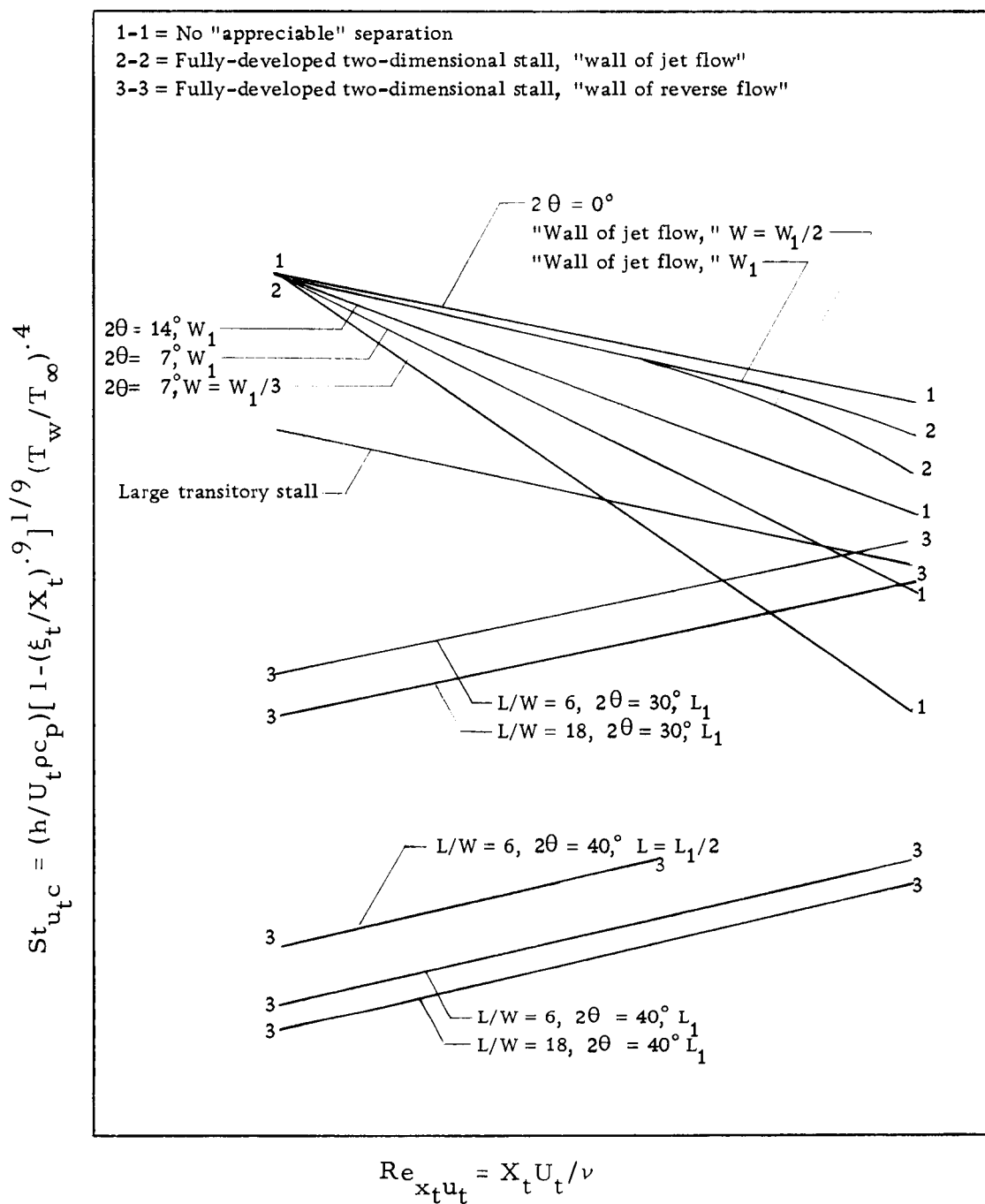


Figure 21. A comparison of heat transfer results from three regimes of diffuser flow.

APPENDIX G

TABLES

TABLE III

Results of Transient Heat Transfer Measurements

The values of the parameter $(h_{\max} - h_{\min})/h_{av}$ are for a single location. However, only the values associated with the location having the largest recorded magnitude of $(h_{\max} - h_{\min})h/av$ are presented.

L/W	θ deg.	$Re_w (10)^{-5}$	$\frac{(h_{\max} - h_{\min})}{h_{av}}$
6	15	0.416	.127
	15	3.450	.265
	25	0.402	.130
	25	4.520	.197
12	10	0.497	.204
	10	3.190	.265
	15	0.578	.136
	15	1.150	.175
	15	2.960	.253
	15	3.560	.296
	25	0.563	.179
	25	1.280	.136
	25	2.630	.202
	25	3.179	.242
18	10	0.531	.140
	10	1.210	.143
	10	2.620	.212
	10	2.680	.230
	15	0.473	.149
	15	1.070	.177
	15	2.530	.393
	15	2.540	.410
	20	0.449	.145
	20	1.150	.311
	20	1.810	.345
	20	2.300	.508

TABLE IV
Heat Transfer Data for the No "Appreciable" Separation Regime.
(h =Btu/Hr-Ft²-°F; Q_m =Btu/Hr; $T_b - T_a$ =°F)

Pos	L/W=6					L/W=6				
	Run 11153.30	W=6.00 in.	Flow=980 cfm			Run 2174.30	W=6.03 in.	Flow=1381 cfm		
	2θ=0.0 deg.	Re _w =50200	U _t =16.3 fps			2θ=4.0 deg.	Re _w =70500	U _t =22.9 fps		
	Nu _{x,c}	Re _{x,t}	T _b -T _a	Q _m	h	Nu _{x,c}	Re _{x,t}	T _b -T _a	Q _m	h
1	205	82500	21.2	.1189	3.8	249	106000	29.6	.2084	4.6
2	245	141100	20.9	.0796	2.6	327	168700	27.8	.1531	3.5
3	378	199700	21.4	.0930	2.8	419	223200	27.4	.1368	3.1
4	445	258300	21.7	.0858	2.6	498	271100	27.6	.1239	2.9
5	152	53200	21.7	.1756	4.4	201	71000	30.8	.3322	5.9
6	224	111800	21.2	.0921	3.0	294	138500	29.1	.1668	4.0
7	281	170400	21.2	.0602	2.5	365	196900	27.8	.1159	3.1
8	404	229000	22.2	.1017	2.6	453	247900	28.6	.1507	2.9
9	395	287600	22.1	.0626	2.0	515	293000	29.0	.1102	2.6
10	17	24000	21.3	.0901	1.3	42	33200	30.0	.2158	3.2
11	103	53200	21.3	.1002	3.0	194	71000	30.4	.2899	5.7
12	162	82500	21.1	.0895	3.0	242	106000	29.2	.2093	4.4
13	247	111800	21.1	.1078	3.3	289	138500	28.5	.1730	3.9
14	297	141100	21.3	.1004	3.6	338	168700	28.2	.1535	3.6
15	316	170400	21.3	.0862	2.8	396	196900	27.8	.1458	3.5
16	368	199700	21.5	.0869	2.7	437	223200	27.8	.1390	3.3
17	459	229000	22.2	.1062	3.0	503	247900	28.3	.1516	3.3
18	446	258300	21.9	.0756	2.6	496	271100	28.3	.1126	2.8
19	427	287600	22.2	.0814	2.2	506	293000	29.1	.1284	2.6
20	174	53200	20.8	.1641	5.1	120	71000	29.5	.1519	3.5
21	221	111800	20.5	.0810	3.0	323	138500	28.3	.1753	4.3
22	322	170400	21.6	.1152	2.8	388	196900	27.9	.1769	3.4
23	367	229000	22.0	.0831	2.4	461	247900	28.3	.1365	3.0
24	370	287600	22.0	.0667	1.9	489	293000	28.7	.1157	2.5
25	199	82500	20.1	.1382	3.7	248	106000	27.8	.2355	4.6
26	252	141100	20.0	.0683	2.7	353	168700	26.2	.1422	3.7
27	352	199700	21.0	.0840	2.6	464	223200	26.9	.1538	3.5
28	423	258300	21.7	.1064	2.4	530	271100	27.4	.1667	3.0

TABLE IV (cont'd)
Heat Transfer Data for the No "Appreciable" Separation Regime.
($h = \text{Btu}/\text{Hr} \cdot \text{Ft}^2 \cdot ^\circ\text{F}$; $Q_m = \text{Btu}/\text{Hr}$; $T_b - T_a = ^\circ\text{F}$)

Pos	L/W=6					L/W=9				
	Run 10263.10	W=6.00 in.	Flow=6056 cfm			Run 10263.20	W=4.00 in.	Flow=5038 cfm		
	$2\theta = 9.6 \text{ deg.}$	$Re_w = 311100$	$U_t = 100.9 \text{ fps}$			$2\theta = 9.7 \text{ deg.}$	$Re_w = 255300$	$U_t = 125.9 \text{ fps}$		
	$Nu_{x_{tc}}$	Re_{x_t}	$T_b - T_a$	Q_m	h	$Nu_{x_{tc}}$	Re_{x_t}	$T_b - T_a$	Q_m	h
1	753	421100	18.5	.4390	13.9	797	476400	17.8	.4531	14.8
2	981	619000	18.0	.3402	10.4	936	664900	17.3	.3138	10.0
3	1206	768200	18.1	.3175	9.0	1155	794900	17.4	.2942	8.7
4	1340	884600	17.5	.2319	7.7	1339	889900	16.6	.2208	7.8
5	539	295800	19.2	.5643	15.8	571	346200	18.7	.5855	16.8
6	840	527500	17.8	.3023	11.3	851	580200	17.3	.3002	11.5
7	1026	698500	18.2	.2744	9.0	1038	735300	17.4	.2683	9.2
8	1287	829800	19.1	.3400	8.4	1316	845800	18.7	.3439	8.6
9	1375	933800	17.8	.1952	7.1	1428	928500	16.5	.1891	7.4
10	280	146000	17.0	.6283	21.1	324	178300	16.3	.6934	24.5
11	535	295800	18.8	.5287	15.6	579	346200	18.1	.5575	17.0
12	760	421100	18.5	.4863	14.0	803	476400	17.7	.4985	14.9
13	861	527500	17.6	.3457	11.6	890	580200	17.0	.3489	12.1
14	980	619000	17.9	.3133	10.4	972	664900	17.4	.3037	10.4
15	1074	698500	17.8	.2814	9.4	1107	735300	17.3	.2841	9.8
16	1165	768200	17.8	.2715	8.7	1173	794900	17.3	.2684	8.8
17	1106	829800	18.5	.2502	7.2	1102	845800	17.8	.2417	7.2
18	1325	884600	17.8	.2321	7.6	1383	889900	17.0	.2346	8.0
19	1303	933800	17.8	.2129	6.7	1380	928500	16.9	.2152	7.2
20	535	295800	18.6	.4770	15.6	612	346200	17.6	.5218	18.0
21	890	527500	17.5	.3297	12.0	930	580200	16.8	.3352	12.6
22	1026	698500	18.1	.2925	9.0	1077	735300	17.3	.2955	9.5
23	1255	829800	18.3	.2501	8.1	1308	845800	17.6	.2521	8.6
24	1374	933800	17.8	.2054	7.0	1432	928500	17.1	.2072	7.4
25	718	421100	17.0	.4055	13.2	760	476400	16.1	.4097	14.1
26	1010	619000	16.8	.3103	10.7	1034	664900	16.1	.3066	11.1
27	1199	768200	17.3	.2905	8.9	1240	794900	16.7	.2932	9.3
28	1356	884600	17.5	.2610	7.8	1456	889900	16.7	.2693	8.4

TABLE IV (cont'd)
Heat Transfer Data for the No "Appreciable" Separation Regime.
($h=\text{Btu}/\text{Hr}\cdot\text{Ft}^2\cdot^\circ\text{F}$; $Q_m=\text{Btu}/\text{Hr}$; $T_b-T_a=^\circ\text{F}$)

Pos	L/W=9					L/W=12				
	Run 10263. 30 $2\theta=9.7$ deg.		$W=4.00$ in. $Re_w=89400$	Flow=1771 cfm $U_t=44.2$ fps		Run 2174. 20 $2\theta=6.5$ deg.		$W=3.02$ in. $Re_w=224500$	Flow=4399 cfm $U_t=145.6$ fps	
	$Nu_{x_t c}$	Re_{x_t}		Q_m	h	$Nu_{x_t c}$	Re_{x_t}		Q_m	h
1	361	166900	31.3	.3365	6.7	901	570800	17.5	.5034	16.7
2	516	232900	29.9	.2822	5.5	1076	810200	16.3	.3409	11.5
3	533	278500	30.2	.2057	4.0	1348	980100	16.3	.3241	10.1
4	620	311800	30.6	.1762	3.6	1594	1106800	16.0	.2561	9.2
5	288	121300	32.3	.5052	8.4	679	410200	18.8	.6961	20.0
6	390	203200	30.3	.2337	5.3	947	701600	17.0	.3282	12.8
7	478	257600	30.1	.1818	4.2	1167	901800	16.6	.2897	10.3
8	611	296300	31.7	.2412	4.0	1407	1047700	17.8	.3512	9.2
9	628	325300	30.7	.1459	3.2	1477	1158900	16.2	.1918	7.7
10	158	62500	29.6	.6394	12.0	365	208200	15.7	.7492	27.6
11	269	121300	31.8	.4331	7.9	683	410200	17.9	.6499	20.1
12	363	166900	30.5	.3550	6.7	910	570800	17.6	.5618	16.8
13	397	203200	30.1	.2604	5.4	1006	701600	16.6	.3860	13.6
14	436	232900	30.3	.2206	4.6	1140	810200	16.2	.3343	12.2
15	506	257600	30.3	.2112	4.4	1238	901800	15.2	.2988	10.9
16	495	278500	30.5	.1778	3.7	1363	980100	16.3	.2952	10.2
17	514	296300	31.8	.1758	3.3	1583	1047700	17.0	.3419	10.3
18	604	311800	31.1	.1607	3.5	1584	1106800	16.6	.2638	9.1
19	611	325300	31.3	.1699	3.1	1567	1158900	16.8	.2427	8.1
20	295	121300	30.9	.4298	8.6	685	410200	17.8	.5889	20.1
21	392	203200	34.0	.2630	5.3	1030	701600	16.2	.3585	13.9
22	514	257600	30.5	.2525	4.5	1149	901800	16.4	.2964	10.1
23	571	296300	31.5	.1912	3.7	1397	1047700	16.6	.2532	9.1
24	583	325300	31.0	.1501	3.0	1531	1158900	16.4	.2115	7.9
25	375	166900	28.9	.3666	6.9	851	570800	16.0	.4526	15.8
26	481	232900	28.3	.2261	5.1	1180	810200	15.3	.3344	12.6
27	568	278500	29.5	.2160	4.2	1405	980100	15.7	.3119	10.5
28	617	311800	30.6	.2161	3.5	1580	1106800	15.8	.2740	9.1

TABLE IV (cont'd)
Heat Transfer Data for the No "Appreciable" Separation Regime.
($h = \text{Btu}/\text{Hr} \cdot \text{Ft}^2 \cdot ^\circ\text{F}$; $Q_m = \text{Btu}/\text{Hr}$; $T_b - T_a = ^\circ\text{F}$)

Pos	L/W=18					L/W=18				
	Run 10193.10	W=2.00 in.	Flow=3252 cfm			Run 2174.10	W=2.02 in.	Flow=4190 cfm		
	$2\theta = 0.0 \text{ deg.}$	$Re_w = 166800$	$U_t = 162.6 \text{ fps}$			$2\theta = 6.0 \text{ deg.}$	$Re_w = 212400$	$U_t = 207.4 \text{ fps}$		
	$Nu_{x_t c}$	Re_{x_t}	$T_b - T_a$	Q_m	h	$Nu_{x_t c}$	Re_{x_t}	$T_b - T_a$	Q_m	h
1	1351	850500	12.6	.5399	23.6	1065	744800	15.3	.5257	19.8
2	1893	1434200	11.7	.4481	19.6	1276	1010300	14.4	.3620	13.7
3	2585	2017900	12.6	.5079	19.0	1713	1184800	14.5	.3767	12.9
4	3254	2601600	11.7	.3875	18.5	2195	1308200	13.4	.3006	12.7
5	1007	558700	13.8	.6680	26.7	490	552400	16.1	.4353	14.5
6	1692	1142400	12.3	.4194	24.6	1119	892800	15.2	.3499	15.2
7	3092	1726100	12.6	.4706	26.6	1398	1105700	15.1	.3239	12.4
8	3015	2309800	14.3	.6650	19.4	1700	1251400	16.1	.3913	11.1
9	3382	2893500	12.0	.3323	16.8	1946	1357400	14.2	.2250	10.1
10	535	266800	12.0	.6736	34.2	453	292200	13.5	.7986	34.4
11	966	558700	13.3	.6338	26.7	802	552400	16.0	.6907	23.7
12	1269	850500	13.5	.6232	22.1	738	744800	15.8	.4080	13.7
13	1601	1142400	12.2	.4591	20.8	1043	892800	16.2	.3933	14.2
14	1938	1434200	12.5	.4522	20.0	1397	1010300	14.7	.3772	15.0
15	2407	1726100	12.2	.4635	20.7	1386	1105700	14.4	.3019	12.3
16	2804	2017900	12.8	.4918	19.9	1472	1184800	14.8	.2928	11.1
17	2674	2309800	13.5	.4716	16.5	1753	1251400	15.3	.3471	11.5
18	3310	2601600	12.5	.4545	18.9	1773	1308200	15.0	.2713	10.3
19	3451	2893500	12.4	.4066	17.7	1832	1357400	15.0	.2553	9.5
20	1011	558700	13.4	.5936	26.8	843	552400	15.3	.6254	24.9
21	1715	1142400	12.5	.4564	22.3	1153	892800	14.3	.3589	15.7
22	2306	1726100	12.6	.4320	19.8	1362	1105700	14.8	.3180	12.0
23	2983	2309800	12.9	.4283	19.1	1721	1251400	14.9	.2806	11.3
24	3424	2893500	12.5	.3663	17.5	1897	1357800	14.6	.2355	9.9
25	1314	850500	11.8	.4944	22.9	987	744800	14.0	.4612	18.4
26	1954	1434200	11.5	.4281	20.2	1284	1010300	14.0	.3360	13.8
27	2561	2017900	12.2	.4653	18.8	1529	1184800	14.3	.3129	11.5
28	3344	2601600	12.3	.4510	19.1	1724	1308200	14.6	.2778	10.0

TABLE V
Heat Transfer Data from the Fully-Developed Two-Dimensional Stall Regime--on the "Wall of Jet Flow."
($h = \text{Btu}/\text{Hr} \cdot \text{Ft}^2 \cdot ^\circ\text{F}$; $Q_m = \text{Btu}/\text{Hr}$; $T_b - T_a = ^\circ\text{F}$)

Pos	L/W = 6						L/W = 6					
	Run 1084, 61		W = 6.00 in.		Flow = 6326 cfm		Run 11083, 21		W = 6.00 in.		Flow = 817 cfm	
	2 θ = 30.0 deg.		Re _w = 325000		U _t = 105.4 fps		2 θ = 40.0 deg.		Re _w = 41500		U _t = 13.6 fps	
	Nu _{x_tc}	Re _{x_tu_m}	Re _{x_tu_m'}	T _b -T _a	Q _m	h	Nu _{x_tc}	Re _{x_tu_m}	Re _{x_tu_m'}	T _b -T _a	Q _m	h
1	963	605000	552000	15.6	.4302	16.0	228	80000	73000	45.2	.2394	3.6
2	1368	984100	898000	14.4	.3610	13.6	276	128400	117200	43.1	.1688	2.7
3	1835	1363300	1243900	14.7	.3888	13.1	342	176800	161300	42.4	.1443	2.4
4	2081	1742400	1589800	14.0	.2835	11.6	459	225200	205500	42.4	.1623	2.5
5	691	415400	379100	16.0	.5128	17.2	223	55800	50900	46.3	.4415	5.2
6	1103	794600	725000	14.4	.2983	13.7	259	104200	95100	44.6	.1996	3.1
7	1522	1173700	1070900	14.5	.3198	12.7	297	152600	139300	42.8	.1157	2.4
8	2037	1552800	1416900	16.0	.4506	12.7	383	201000	183400	43.5	.1703	2.3
9	2163	1932000	1762800	14.3	.2425	10.8	409	249400	227600	42.4	.1173	2.0
10	430	225900	206100	13.9	.5622	23.2	36	31600	28800	44.7	.2226	1.8
11	679	415400	379100	15.6	.4748	16.9	199	55800	50900	45.6	.3509	4.7
12	1019	605000	552000	15.6	.4989	16.9	217	80000	73000	44.6	.2294	3.4
13	1162	794600	725000	14.3	.3552	14.5	266	104200	95100	44.5	.2162	3.2
14	1365	984100	898000	14.4	.3353	13.6	288	128400	117200	43.9	.1780	2.8
15	1582	1173700	1070900	14.3	.3212	13.2	327	152600	139300	44.0	.1674	2.6
16	1892	1363300	1243900	14.4	.3497	13.5	360	176800	161300	43.0	.1541	2.5
17	2114	1552800	1416900	15.3	.4022	13.2	401	201000	183400	43.5	.1603	2.4
18	2187	1742400	1589800	14.5	.3133	12.2	415	225200	205500	42.9	.1225	2.3
19	2319	1932000	1762800	14.5	.3000	11.6	429	249400	227600	43.1	.1498	2.1
20	701	415400	379100	15.2	.4345	17.4	215	55800	50900	44.4	.3460	5.0
21	1154	794600	725000	14.3	.3252	14.4	268	104200	95100	43.5	.1886	3.2
22	1414	1173700	1070900	14.4	.3025	11.8	315	152600	139300	43.8	.2116	2.5
23	1949	1552800	1416900	14.9	.3029	12.2	396	201000	183400	43.7	.1667	2.4
24	2297	1932000	1762800	14.3	.2677	11.5	363	249400	227600	42.4	.1190	1.8
25	936	605000	552000	13.7	.3823	15.5	230	80000	73000	43.0	.2931	3.6
26	1360	984100	898000	13.3	.3156	13.6	287	128400	117200	41.3	.1480	2.8
27	1749	1363300	1243900	14.0	.3309	12.5	356	176800	161300	41.8	.1538	2.5
28	2192	1742400	1589800	13.9	.3176	12.2	392	225200	205500	42.0	.1811	2.1

TABLE V (cont'd)
Heat Transfer Data from the Fully-Developed Two-Dimensional Stall Regime--on the "Wall of Jet Flow."
($h = \text{Btu}/\text{Hr}\cdot\text{Ft}^2\cdot^\circ\text{F}$; $Q_m = \text{Btu}/\text{Hr}$; $T_b - T_a = ^\circ\text{F}$)

Pcs	L/W=6						L/W=12					
	Run 11083.11		W=6.00 in.		Flow=6244 cfm		Run 1044.21		W=3.00 in.		Flow=1071 cfm	
	2 θ =40.0 deg.		$Re_w = 317000$		$U_t = 104.0 \text{ fps}$		2 θ =29.0 deg.		$Re_w = 54900$		$U_t = 35.7 \text{ fps}$	
	$Nu_{x_{tc}}$	$Re_{x_{tc}u_m}$	$Re_{x_{tc}u_m}'$	$T_b - T_a$	Q_m	h	$Nu_{x_{tc}}$	$Re_{x_{tc}u_m}$	$Re_{x_{tc}u_m}'$	$T_b - T_a$	Q_m	h
1	1008	611200	557700	16.7	.4678	16.3	372	204300	177900	30.4	.2968	6.1
2	1387	981000	895100	15.9	.3977	13.6	473	332300	289300	29.0	.2287	4.7
3	1847	1350800	1232600	16.6	.4366	13.1	662	443900	400800	29.1	.2422	4.7
4	2166	1720600	1570000	16.0	.3364	12.0	817	536600	483400	29.2	.2174	4.5
5	688	426300	389000	17.5	.5341	16.4	285	140300	122100	31.3	.4063	7.0
6	1120	796100	726400	16.2	.3339	13.7	405	268300	233600	29.9	.2187	5.0
7	1528	1165900	1063900	16.3	.3570	12.6	536	394000	345100	29.2	.1885	4.4
8	2096	1535700	1401300	17.9	.5133	13.0	728	491300	442700	30.3	.2676	4.5
9	2346	1905500	1738700	16.0	.2934	11.7	817	579800	522400	29.4	.1782	4.1
10	444	241400	220300	15.6	.6021	22.2	184	76300	66400	28.6	.5192	9.9
11	694	426300	389000	17.0	.5082	16.6	281	140300	122100	30.4	.3609	6.9
12	986	611200	557700	16.9	.5080	16.0	359	204300	177900	30.0	.3020	5.9
13	1183	796100	726400	16.0	.3944	14.4	424	268300	233600	29.6	.2503	5.2
14	1400	981000	895100	16.2	.3806	13.8	500	332300	289300	29.6	.2317	4.9
15	1596	1165900	1063900	16.0	.3603	13.1	578	394000	345100	29.3	.2216	4.8
16	1816	1350800	1232600	16.4	.3788	12.8	648	443900	400800	29.5	.2212	4.6
17	2180	1535700	1401300	17.3	.4685	13.5	766	491300	442700	30.1	.2541	4.7
18	2252	1720600	1570000	16.6	.3683	12.4	810	536600	483400	29.6	.2080	4.5
19	2305	1905500	1738700	16.2	.3313	11.5	853	579800	522400	29.9	.2215	4.2
20	705	426300	389000	16.6	.4594	16.8	288	140300	122100	29.6	.3356	7.1
21	1107	796100	726400	15.7	.3368	13.5	448	268300	233600	29.3	.2384	5.5
22	1524	1165900	1063900	16.2	.3614	12.5	541	394000	345100	29.7	.2442	4.5
23	2030	1535700	1401300	17.0	.3577	12.6	698	491300	442700	30.0	.2143	4.3
24	2347	1905500	1738700	16.1	.3068	11.6	820	579800	522400	29.6	.1947	4.1
25	965	611200	557700	15.2	.4263	15.6	338	204300	177900	28.3	.2900	5.5
26	1428	981000	895100	15.1	.3695	14.0	471	332300	289300	28.1	.2013	4.7
27	1904	1350800	1232600	15.7	.4021	13.5	606	443900	400800	28.3	.2101	4.3
28	2300	1720600	1570000	16.2	.3854	12.7	767	536600	483400	28.8	.2398	4.2

TABLE V (cont'd)
Heat Transfer Data from the Fully-Developed Two-Dimensional Stall Regime--on the "Wall of Jet Flow."
(h =Btu/Hr-Ft²-°F; Q_m =Btu/Hr; T_b-T_a =°F)

Pcs	L/W=12						L/W=12					
	Run 1044, 11		W=3.00 in.		Flow=5201 cfm		Run 1024, 21		W=3.00 in.		Flow=1390 cfm	
	2θ=29.0 deg.		Re _w =269100		U _t =173.3 fps		2θ=40.0 deg.		Re _w =69800		U _t =46.3 fps	
	Nu _{x_tc}	Re _{x_tu_m}	Re _{x_tu_m}	T _b -T _a	Q _m	h	Nu _{x_tc}	Re _{x_tc}	Re _{x_tu_m}	T _b -T _a	Q _m	h
1	1304	1001800	872100	16.2	.6076	21.5	465	269100	234300	28.3	.3466	7.5
2	1754	1629600	1418600	15.3	.4908	17.4	639	431900	376000	26.5	.2908	6.3
3	2402	2176600	1965200	16.2	.5648	17.1	772	571500	517800	25.3	.2518	5.5
4	2751	2630900	2370500	15.2	.4093	15.2	933	688700	620500	26.6	.2292	5.1
5	895	687900	598800	16.6	.6813	22.1	339	187700	163400	29.1	.4360	8.1
6	1533	1315700	1145400	15.2	.4394	19.0	498	350500	305100	28.1	.2518	6.1
7	2121	1931800	1691900	15.7	.4926	17.6	671	508400	446900	26.0	.2215	5.5
8	2768	2409100	2170700	17.8	.6916	17.2	873	631500	569000	27.2	.2957	5.4
9	2588	2843100	2561700	15.3	.3108	12.9	1014	743500	669900	27.3	.2090	5.0
10	559	374000	325600	14.3	.7400	30.0	226	106300	92500	26.6	.5460	11.3
11	897	687900	598800	16.3	.6590	22.2	351	187700	163400	28.3	.4109	8.4
12	1309	1001800	872100	16.2	.6703	21.6	467	269100	234300	27.8	.3705	7.5
13	1540	1315700	1145400	14.9	.4905	19.1	564	350500	305100	27.3	.3097	6.9
14	1870	1629600	1418600	15.3	.4905	18.6	642	431900	376000	27.0	.2755	6.3
15	2171	1931800	1691900	15.2	.4731	18.0	678	508400	446900	26.1	.2344	5.6
16	2534	2176600	1965200	15.8	.5186	18.0	755	571500	517800	25.3	.2254	5.3
17	2941	2409100	2170700	16.9	.6286	18.3	929	631500	569000	26.9	.2832	5.8
18	3129	2630900	2370500	15.9	.4988	17.3	986	688700	620500	27.2	.2419	5.4
19	3389	2843100	2561700	15.4	.4644	16.9	1000	743500	669900	27.5	.2408	5.0
20	923	687900	598800	15.8	.5954	22.8	360	187700	163400	27.7	.3840	8.6
21	1498	1315700	1145400	15.0	.4463	18.6	592	350500	305100	27.0	.2954	7.2
22	1969	1931800	1691900	15.8	.4557	16.3	695	508400	446900	26.1	.2719	5.7
23	2613	2409100	2170700	16.4	.4442	16.3	947	631500	569000	26.6	.2600	5.9
24	3107	2843100	2561700	15.3	.3844	15.5	1095	743500	669900	26.9	.2374	5.4
25	1205	1001800	872100	14.4	.5118	19.9	464	269100	234300	26.0	.3556	7.5
26	1784	1629600	1418600	14.4	.4488	17.7	657	431900	376000	24.9	.2619	6.4
27	2343	2176600	1965200	15.5	.4923	16.6	803	571500	517800	24.4	.2496	5.7
28	2971	2630900	2370500	15.2	.4642	16.4	1028	688700	620500	26.1	.2885	5.7

TABLE V (cont'd)
Heat Transfer Data from the Fully-Developed Two-Dimensional Stall Regime--on the "Wall of Jet Flow."
($h = \text{Btu}/\text{Hr}\cdot\text{Ft}^2\cdot^{\circ}\text{F}$; $Q_m = \text{Btu}/\text{Hr}$; $T_b - T_a = ^{\circ}\text{F}$)

Pcs	L/W=12						L/W=18					
	Run 1064.21		W=3.03 in.		Flow=5087 cfm		Run 1084.41		W=2.00 in.		Flow=4471 cfm	
	2 θ =40.0 deg.		$Re_w = 259600$		$U_t = 167.8 \text{ fps}$		2 θ =28.0 deg.		$Re_w = 226600$		$U_t = 223.5 \text{ fps}$	
	$Nu_{x_{\xi}c}$	$Re_{x_t u_m}$	$Re_{x_t u_m}'$	$T_b - T_a$	Q_m	h	$Nu_{x_{\xi}c}$	$Re_{x_t u_m}$	$Re_{x_t u_m}'$	$T_b - T_a$	Q_m	h
1	1223	991000	863400	14.3	.4917	19.7	1472	1265400	1067100	18.7	.8021	24.5
2	1694	1590700	1385800	13.1	.4020	16.6	2156	1950800	1702600	17.4	.6947	21.6
3	2297	2109300	1908200	13.7	.4553	16.2	2865	2497100	2179400	16.6	.7021	20.5
4	2706	2542500	2292600	13.0	.3432	14.9	3129	2981200	2601900	14.8	.4591	17.5
5	801	691300	602200	15.3	.5427	19.1	734	868900	732700	19.2	.6548	18.3
6	1336	1290900	1124600	13.6	.3359	16.3	1883	1647000	1401500	17.1	.6163	23.5
7	1933	1876100	1647000	13.2	.3728	15.9	2889	2233000	1948900	17.3	.7586	24.1
8	2541	2331000	2101800	14.7	.5205	15.8	3364	2745800	2396500	18.5	.8917	21.1
9	3013	2745000	2475100	13.3	.3177	15.0	3615	3205000	2797300	15.3	.4432	18.2
10	524	391500	341000	13.0	.5909	26.2	254	472400	398400	16.4	.4048	13.8
11	821	691300	602200	14.8	.5266	19.6	952	868900	732700	17.4	.7533	23.7
12	1200	991100	863400	14.4	.5325	19.4	1715	1265400	1067100	17.8	.9851	28.5
13	1408	1290900	1124600	13.4	.3979	17.2	2153	1647000	1401500	17.0	.7978	26.9
14	1687	1590700	1385800	13.3	.3786	16.6	2465	1950800	1702600	17.8	.7705	24.7
15	1920	1876100	1647000	12.7	.3460	15.8	2771	2233000	1948900	17.8	.7208	23.1
16	2208	2109300	1908200	13.2	.3737	15.6	2962	2497100	2179400	18.4	.7137	21.2
17	2630	2331000	2101900	13.9	.4590	16.3	3124	2745800	2396500	19.2	.7698	19.6
18	2705	2542500	2292600	13.1	.3525	14.9	3135	2981200	2601900	17.8	.5647	17.5
19	2909	2745000	2475100	13.5	.3483	14.5	3213	3205000	2797300	17.3	.4966	16.1
20	872	691300	602200	14.2	.4874	20.8	1172	868900	732700	16.1	.7741	29.2
21	1506	1290900	1124600	13.2	.3893	18.4	1885	1647000	1401500	17.4	.6654	23.5
22	1866	1876100	1647000	13.0	.3518	15.3	1816	2233000	1948900	19.2	.5141	15.2
23	2498	2331000	2101800	13.6	.3507	15.5	1948	2745800	2396500	19.7	.4031	12.2
24	3098	2745000	2475100	13.1	.3285	15.4	1965	3205000	2797300	18.3	.2934	9.9
25	1178	991100	863400	12.7	.4340	19.0	1163	1265400	1067100	17.0	.5900	19.3
26	1821	1590700	1385800	11.9	.3757	17.9	1128	1950800	1702600	20.6	.4014	11.3
27	2351	2109300	1908200	12.5	.3979	16.6	1158	2497100	2179400	21.8	.3377	8.3
28	2945	2542500	2292600	12.8	.3861	16.3	1394	2981200	2601900	21.0	.3123	7.8

TABLE V (cont'd)
Heat Transfer Data from the Fully-Developed Two-Dimensional Stall Regime--on the "Wall of Jet Flow."
($h = \text{Btu}/\text{Hr}-\text{Ft}^2-\text{°F}$; $Q_m = \text{Btu}/\text{Hr}$; $T_b - T_a = \text{°F}$)

Pos	L/W=18						L/W=18					
	Run 1084, 21		W=2.00 in.		Flow=4046 cfm		Run 12233, 11		W=2.00 in.		Flow=1154 cfm	
	2θ=40.0 deg.		Re _w =206400		U _t =202.3 fps		2θ=45.0 deg.		Re _w =58300		U _t =57.7 fps	
	Nu _{x_tc}	Re _{x_tu_m}	Re _{x_tu_m'}	T _b -T _a	Q _m	h	Nu _{x_tc}	Re _{x_tu_m}	Re _{x_tu_m'}	T _b -T _a	Q _m	h
1	1327	1194300	1007100	15.4	.5722	21.3	561	343000	289200	14.8	.2210	9.0
2	1874	1807700	1577800	13.6	.4605	18.4	765	514800	449300	13.9	.1850	7.5
3	2525	2301800	2009000	14.5	.5303	17.8	979	653900	570700	14.3	.1877	9.6
4	3103	2740200	2391500	14.1	.4280	17.1	1109	777400	678500	14.3	.1489	6.1
5	885	833000	702500	16.0	.6258	21.0	399	240900	203100	15.5	.2698	9.4
6	1516	1533400	1311800	14.4	.4044	18.4	674	437600	375300	14.3	.1739	8.2
7	2151	2062900	1800400	14.4	.4551	17.6	855	586600	512000	14.0	.1587	7.0
8	2942	2526900	2205500	16.5	.6796	18.2	1092	717300	626100	15.1	.2122	6.8
9	3313	2942900	2568500	14.6	.3821	16.4	1244	834600	728400	14.3	.1363	6.2
10	529	471700	397800	13.8	.6318	26.4	257	138800	117100	14.2	.3196	12.5
11	868	833000	702500	15.6	.5871	20.7	410	240900	203100	15.3	.2578	9.6
12	1283	1194300	1007100	15.6	.6192	20.6	544	343000	289200	14.6	.2299	8.7
13	1517	1533400	1311800	14.3	.4560	18.5	657	437600	375300	14.0	.1855	8.0
14	1829	1807700	1577800	14.0	.4322	17.9	759	514800	449300	14.0	.1708	7.4
15	2114	2062900	1800400	14.2	.4267	17.3	844	586600	512000	14.0	.1595	6.9
16	2446	2301800	2009000	14.6	.4593	17.2	959	653900	570700	14.3	.1663	6.8
17	2933	2526900	2205500	15.4	.5697	18.1	1121	717300	626100	14.8	.1928	6.9
18	3020	2740200	2391500	14.8	.4455	16.6	1206	777400	678500	14.4	.1613	6.7
19	3282	2942900	2568500	14.8	.4293	16.3	1260	834600	728400	14.4	.1608	6.3
20	979	833000	702500	14.7	.5657	23.3	411	240900	203100	14.7	.2309	9.6
21	1414	1533400	1311800	16.0	.4399	17.2	634	437600	375300	13.8	.1616	7.7
22	1871	2062900	1800400	15.9	.4316	15.3	820	586600	512000	14.2	.1734	6.7
23	2826	2526900	2205500	14.7	.4290	17.5	1166	717300	626100	14.6	.1769	7.2
24	3518	2942900	2568500	14.3	.4076	17.5	1438	834600	728400	14.4	.1676	7.2
25	1402	1194300	1007100	13.0	.5214	22.5	555	343000	289200	13.5	.2190	8.9
26	2186	1807700	1577800	12.5	.4727	21.4	809	514800	449300	13.0	.1716	7.9
27	2805	2301800	2009000	13.4	.5085	19.8	1108	653900	570700	13.5	.1967	7.8
28	3457	2740200	2391500	14.0	.4900	19.0	1329	777400	678500	14.0	.1973	7.3

TABLE VI
Heat Transfer Data from the Fully-Developed Two-Dimensional Stall Regime--on the "Wall of Reversed Flow."
($h = \text{Btu}/\text{Hr}\cdot\text{Ft}^2\cdot^\circ\text{F}$; $Q_m = \text{Btu}/\text{Hr}$; $T_b - T_a = ^\circ\text{F}$; $f_1(\text{Re}_x) = \text{Re}_{x_b} u_t f(W/L, D/L, \theta)$; $f_2(\text{Re}_x) = f_1(\text{Re}_x)/\tan 2\theta$)

Pos	L/W = 6						L/W = 6					
	Run 1084.52 2 θ = 30.0 deg.		W = 6.00 in. Re _w = 321500	Flow = 6257 cfm U _t = 104.2 fps			Run 11233.32 2 θ = 40.0 deg.		W = 6.00 in. Re _w = 319300	Flow = 6216 cfm U _t = 103.6 fps		
	Nu _{x_bc}	f ₁ (Re _x)	f ₂ (Re _x)	T _b -T _a	Q _m	h	Nu _{x_bc}	f ₁ (Re _x)	f ₂ (Re _x)	T _b -T _a	Q _m	h
1	730	173900	300600	24.0	.1544	4.3	438	118400	140800	19.0	.0648	2.6
2	641	133500	230700	22.2	.1840	4.9	316	90900	108000	18.3	.0631	2.4
3	422	93100	160800	21.7	.1784	4.7	223	63300	75300	18.3	.0654	2.5
4	235	52600	90900	22.0	.1670	4.6	124	35800	42600	18.3	.0683	2.4
5	556	194100	335600	24.5	.1248	2.9	328	132200	157100	18.8	.0525	1.7
6	584	153700	265700	24.0	.1341	3.9	365	104600	124400	18.8	.0648	2.4
7	427	113200	195700	22.9	.1232	3.8	265	77100	91700	18.6	.0502	2.4
8	276	72800	125800	23.5	.1740	3.9	180	49600	58900	19.1	.0842	2.5
9	108	32400	55900	23.5	.1202	3.5	95	22000	26200	19.5	.0872	3.1
10	871	214400	370500	23.5	.2049	4.1	346	145900	173500	18.2	.0859	1.6
11	615	194100	335600	24.3	.1224	3.2	342	132200	157100	18.6	.0457	1.8
12	555	173900	300600	24.1	.1141	3.2	378	118400	140800	18.6	.0500	2.2
13	509	153700	265700	24.0	.1239	3.4	366	104600	124400	18.6	.0662	2.4
14	395	133500	230700	23.5	.1046	3.0	295	90900	108000	18.6	.0588	2.3
15	356	113200	195700	23.5	.1124	3.2	257	77100	91700	18.6	.0605	2.3
16	295	93000	160800	23.5	.1165	3.2	222	63300	75300	18.6	.0651	2.4
17	232	72800	125800	23.9	.1282	3.3	152	49600	58900	18.9	.0584	2.1
18	162	52600	90900	23.5	.1084	3.2	112	35800	42600	18.9	.0525	2.2
19	115	32400	55900	24.0	.1544	3.8	92	22000	26200	19.6	.0997	3.0
20	555	194100	335600	23.6	.0966	2.9	375	132200	157100	18.3	.0447	2.0
21	583	153700	265700	23.6	.1268	3.9	416	104600	124400	18.3	.0656	2.8
22	378	113200	195700	23.6	.1495	3.4	300	77100	91700	18.8	.0962	2.7
23	235	72800	125800	23.7	.1274	3.3	203	49600	58900	19.0	.0876	2.9
24	111	32400	55900	23.7	.1370	3.6	103	22000	26200	19.5	.1043	3.3
25	641	173900	300600	22.6	.1582	3.7	433	118400	140800	17.8	.0854	2.5
26	591	133500	230700	21.4	.1467	4.5	391	90900	108000	17.6	.0703	3.0
27	426	93000	160800	21.7	.1786	4.7	285	63300	75300	18.0	.0911	3.1
28	225	52600	90900	22.2	.1924	4.4	161	35800	42600	18.6	.1174	3.2

TABLE VI (cont'd)
Heat Transfer Data from the Fully-Developed Two-Dimensional Stali Regime--on the "Wall of Reversed Flow."
(h =Btu/Hr-Ft²-°F; Q_m =Btu/Hr; $T_b - T_a$ =°F; $f_1(Re_x) = Re_{x_b} u_t f(W/L, D/L, \theta)$; $f_2(Re_x) = f_1(Re_x)/\tan 2\theta$)

Pos	L/W=12						L/W=12					
	Run 1034.12		W=3.00 in.		Flow=1448 cfm		Run 1044.32		W=3.00 in.		Flow=5281 cfm	
	2θ=25.0 deg.		Re _w =72700		U _t =48.2 fps		2θ=29.0 deg.		Re _w =271300		U _t =176.0 fps	
	Nu _{x_bc}	f ₁ (Re _x)	f ₂ (Re _x)	T _b -T _a	Q _m	h	Nu _{x_bc}	f ₁ (Re _x)	f ₂ (Re _x)	T _b -T _a	Q _m	h
1	597	96500	206600	27.6	.1409	3.5	1323	281400	506700	17.3	.2197	7.7
2	488	74100	158500	25.4	.1542	3.8	1096	216000	388800	15.6	.2349	8.4
3	388	51600	110500	25.6	.1918	4.3	798	150500	271000	16.0	.2738	8.8
4	196	29200	62400	26.3	.1659	3.9	390	85100	153200	15.9	.2089	7.6
5	682	107700	230600	28.3	.1822	3.6	1193	314100	565600	17.8	.2058	6.3
6	551	85300	182500	27.3	.1455	3.7	1001	248700	447800	17.0	.1664	6.6
7	380	62800	134500	26.9	.1250	3.4	718	183300	329900	16.5	.1708	6.5
8	228	40400	86500	28.2	.1678	3.2	453	117800	212100	17.5	.2311	6.4
9	98	18000	38400	27.5	.1288	3.2	177	52400	94300	17.0	.1485	5.7
10	1488	118900	254600	26.9	.3655	7.1	2588	346900	624500	16.2	.3598	12.3
11	704	107700	230600	28.0	.1662	3.7	1379	314200	565600	17.4	.2164	7.2
12	583	96500	206600	27.4	.1403	3.4	1087	281400	506700	17.3	.1903	6.4
13	501	85300	182500	27.5	.1411	3.3	858	248700	447800	17.0	.1576	5.7
14	379	74100	158500	27.3	.1169	2.9	712	216000	388800	17.0	.1477	5.4
15	311	62800	134500	27.1	.1120	2.8	560	183300	329900	17.0	.1370	5.1
16	238	51600	110500	27.2	.1043	2.6	470	150500	271000	17.1	.1475	5.2
17	190	40400	86500	28.0	.1183	2.7	361	117800	212100	17.6	.1609	5.1
18	128	29200	62400	27.8	.0946	2.5	262	85100	153200	17.3	.1443	5.1
19	87	18000	38400	28.1	.1359	2.8	186	52400	94300	17.5	.1859	6.0
20	613	107700	230600	27.6	.1288	3.2	1428	314100	565600	17.0	.2037	7.5
21	477	85300	182500	26.6	.1141	3.2	1026	248700	447800	16.6	.1700	6.8
22	321	62800	134500	27.4	.1501	2.9	680	183300	329900	16.9	.1887	6.1
23	204	40400	86500	28.2	.1312	2.9	419	117800	212100	17.4	.1717	5.9
24	93	18000	38400	27.9	.1357	3.0	170	52400	24300	17.3	.1535	5.5
25	532	96500	206600	26.6	.1570	3.1	1254	281400	506700	15.7	.2115	7.3
26	535	74100	158500	25.2	.1545	4.1	1158	216000	388800	14.8	.2222	8.9
27	361	51600	110500	26.1	.1779	4.0	789	150500	271000	15.4	.2505	8.7
28	178	29200	62400	26.6	.1863	3.5	385	85100	153200	16.1	.2338	7.6

TABLE VI (cont'd)

Heat Transfer Data from the Fully-Developed Two-Dimensional Stall Regime--on the "Wall of Reversed Flow."

 $(h=\text{Btu}/\text{Hz}-\text{Ft}^2-\text{F}; Q_m=\text{Btu}/\text{Hz}; T_b-T_a=^{\circ}\text{F}; f_1(\text{Re}_x)=\text{Re}_{x_b} u_t (W/L, D/L, \theta); f_2(\text{Re}_x)=f_1(\text{Re}_x)/\tan 2\theta)$

Pos	L/W=12						L/W=12					
	Run 1024.12		W=3.00 in.		Flow=1390 cfm		Run 1064.12		W=3.05 in.		Flow=5029 cfm	
	2 θ =40.0 deg.		Re _w =69800		U _t =46.3 fps		2 θ =40.0 deg.		Re _w =257500		U _t =164.9 fps	
	Nu _{x_bc}	f ₁ (Re _x)	f ₂ (Re _x)	T _b -T _a	Q _m	h	Nu _{x_bc}	f ₁ (Re _x)	f ₂ (Re _x)	T _b -T _a	Q _m	h
1	153	48400	57500	19.9	.0084	0.9	571	172900	205600	27.9	.1345	3.4
2	139	37100	44100	19.3	.0147	1.1	394	132700	157800	27.3	.1271	3.0
3	111	25900	30800	18.8	.0188	1.2	287	92500	110000	28.3	.1443	3.2
4	71	14600	17400	18.6	.0361	1.4	171	52300	62200	28.0	.1519	3.4
5	156	54000	64200	20.1	.0206	0.8	439	193000	229500	28.5	.1123	2.3
6	176	42800	50800	20.0	.0324	1.2	474	152800	181700	28.3	.1287	3.2
7	139	31500	37500	19.2	.0121	1.3	337	112600	133900	28.3	.1107	3.0
8	87	20300	24100	19.0	.0285	1.2	236	72400	86100	29.2	.1804	3.3
9	42	9000	10700	19.0	.0335	1.4	105	32200	38200	28.2	.1413	3.4
10	140	59600	70900	19.6	.0620	0.7	746	213100	253400	28.1	.2192	3.6
11	118	54000	64200	20.0	.0068	0.6	483	193000	229500	28.6	.1087	2.5
12	153	48400	57500	19.7	.0011	0.9	442	172900	205600	28.3	.0977	2.6
13	174	42800	50800	19.9	.0275	1.2	430	152800	181700	28.4	.1225	2.9
14	165	37100	44100	19.6	.0289	1.3	372	132700	157800	28.6	.1196	2.9
15	114	31500	37500	19.2	.0195	1.0	317	112600	133900	28.6	.1202	2.9
16	92	25900	30800	18.9	.0155	1.0	276	92500	110000	28.6	.1323	3.1
17	90	20300	24100	18.9	.0256	1.3	243	72400	86100	29.1	.1665	3.4
18	72	14600	17400	18.7	.0245	1.4	172	52300	62200	28.5	.1428	3.4
19	45	9000	10700	19.0	.0444	1.5	117	32200	38200	28.8	.1898	3.8
20	160	54000	64200	19.5	.0091	0.9	422	193000	229500	27.9	.0810	2.2
21	143	42800	50800	19.3	.0127	1.0	426	152800	181700	28.2	.1048	2.8
22	138	31500	37500	19.5	.0496	1.3	332	112600	133900	28.7	.1622	3.0
23	95	20300	24100	19.3	.0379	1.4	229	72400	86100	29.2	.1537	3.2
24	43	9000	10700	19.2	.0424	1.4	112	32200	38200	28.3	.1658	3.6
25	159	48400	57500	19.0	.0354	0.9	440	172900	205600	27.8	.1359	2.6
26	144	37100	44100	18.6	.0072	1.1	359	132700	157800	27.4	.0974	2.8
27	111	25900	30800	18.6	.0204	1.2	261	92500	110000	27.9	.1267	2.9
28	61	14600	17400	18.3	.0458	1.2	175	52300	62200	27.9	.1909	3.4

TABLE VI (cont'd)

Heat Transfer Data from the Fully-Developed Two-Dimensional Stall Regime--on the "Wall of Reversed Flow."

 $(h = \text{Btu}/\text{Hr}\cdot\text{Ft}^2\cdot^\circ\text{F}; Q_m = \text{Btu}/\text{Hr}; T_b - T_a = ^\circ\text{F}; f_1(\text{Re}_x) = \text{Re}_{x_b} u_t f(W/L, D/L, \theta); f_2(\text{Re}_x) = f_1(\text{Re}_x)/\tan 2\theta)$

Pcs	L/W=18						L/W=18					
	Run 1084.32 2 θ =27.5 deg.		W=2.00 in. Re _w =219200		Flow=4326 cfm U _t =216.3 fps		Run 2114.42 2 θ =30.0 deg.		W=2.03 in. Re _w =33000		Flow=647 cfm U _t =31.8 fps	
	Nu _{x_bc}	f ₁ (Re _x)	f ₂ (Re _x)	T _b -T _a	Q _m	h	Nu _{x_bc}	f ₁ (Re _x)	f ₂ (Re _x)	T _b -T _a	Q _m	h
1	1374	340700	653200	17.6	.2353	8.1	307	44200	76500	34.0	.0682	1.8
2	1103	261500	501300	16.0	.2436	8.5	255	33900	58700	32.6	.0813	1.9
3	782	182200	349400	16.2	.2732	8.7	173	23700	40900	32.7	.0777	1.9
4	390	103000	197500	16.6	.2205	7.7	86	13400	23100	33.1	.0794	1.7
5	1230	380300	729200	18.6	.2236	6.5	338	49400	85400	34.3	.0984	1.8
6	979	301100	577300	18.6	.1800	6.5	226	39100	67600	34.7	.0716	1.5
7	773	221900	425400	17.1	.1939	7.0	167	28800	49800	33.5	.0350	1.5
8	490	142600	273400	18.4	.2670	7.0	102	18500	32000	34.3	.0674	1.4
9	182	63400	121500	18.0	.1628	5.9	56	8200	14200	34.1	.0842	1.8
10	2425	419900	805100	17.2	.3611	11.6	806	54500	94200	33.1	.2712	3.8
11	1454	380300	729200	18.2	.2416	7.7	320	49400	85400	34.3	.0760	1.7
12	1201	340700	653200	17.8	.2214	7.1	207	44200	76500	34.3	.0224	1.2
13	935	301100	577300	17.4	.1781	6.2	201	39100	67600	34.8	.0571	1.3
14	753	261500	501300	17.4	.1626	5.8	155	33900	58700	34.7	.0455	1.2
15	575	221900	425400	17.4	.1458	5.2	141	28800	49800	34.6	.0480	1.3
16	485	182200	349400	17.7	.1593	5.4	124	23700	40900	34.6	.0501	1.4
17	412	142600	273400	17.9	.1921	5.9	99	18500	32000	34.9	.0536	1.4
18	269	103000	197500	17.8	.1537	5.3	76	13400	23100	34.4	.0482	1.5
19	185	63400	121500	18.2	.1932	6.0	58	8200	14200	34.8	.1057	1.9
20	1364	380300	729200	17.7	.2042	7.2	252	49400	85400	33.7	.0434	1.3
21	1015	301100	577300	17.3	.1767	6.8	190	39100	67600	34.3	.0388	1.3
22	703	221900	425400	17.3	.2013	6.4	147	28800	49800	35.1	.0927	1.3
23	439	142600	273400	17.8	.1847	6.2	103	18500	32000	35.3	.0743	1.4
24	186	63400	121500	17.9	.1750	6.0	54	8200	14200	34.5	.0941	1.7
25	1280	340700	653200	16.8	.2323	7.6	268	44200	76500	33.1	.0995	1.6
26	1145	261500	501300	15.5	.2315	8.8	219	33900	58700	32.7	.0478	1.7
27	816	182200	349400	15.5	.2635	9.0	145	23700	40900	34.0	.0619	1.6
28	406	103000	197500	16.4	.2522	8.0	79	13400	23100	34.0	.1075	1.5

TABLE VI (cont'd)

Heat Transfer Data from the Fully-Developed Two-Dimensional Stall Regime--on the "Wall of Reversed Flow."

 $(h = \text{Btu/Hr-Ft}^2\text{-}^\circ\text{F}; Q_m = \text{Btu/Hr}; T_b - T_a = ^\circ\text{F}; f_1(\text{Re}_x) = \text{Re}_{x_b} u_t f(W/L, D/L, \theta); f_2(\text{Re}_x) = f_1(\text{Re}_x)/\tan 2\theta)$

Pos	L/W=18						L/W=18					
	Run 2114.52 29=30.0 deg.		W=2.03 in. $\text{Re}_w = 203400$		Flow=3987 cfm $U_t = 196.4 \text{ fps}$		Run 1084.12 29=40.0 deg.		W=2.00 in. $\text{Re}_w = 199600$		Flow=3911 cfm $U_t = 195.5 \text{ fps}$	
	$\text{Nu}_{x_b c}$	$f_1(\text{Re}_x)$	$f_2(\text{Re}_x)$	$T_b - T_a$	Q_m	h	$\text{Nu}_{x_b c}$	$f_1(\text{Re}_x)$	$f_2(\text{Re}_x)$	$T_b - T_a$	Q_m	h
1	1367	273200	472300	18.8	.2484	8.0	493	185300	220300	28.4	.1127	2.9
2	1080	209700	362400	17.3	.2576	8.3	369	142200	169000	28.5	.1199	2.8
3	660	146100	252600	18.0	.2491	7.3	269	99100	117800	28.8	.1329	2.9
4	328	82600	142800	18.8	.2059	6.4	163	56000	66600	28.7	.1457	3.2
5	1075	305000	527200	19.3	.2010	5.7	469	206800	245900	28.9	.1218	2.4
6	934	241400	417300	18.6	.1705	6.2	432	163700	194600	29.0	.1185	2.8
7	673	177900	307500	18.1	.1741	6.1	342	120600	143400	28.9	.1142	3.1
8	429	114400	197700	19.7	.2445	6.1	239	77500	92200	29.9	.1259	3.4
9	190	50800	87900	20.3	.1913	6.1	110	34500	41000	29.2	.1517	3.5
10	2288	336800	582100	18.3	.3635	10.9	520	228300	271500	28.2	.1697	2.5
11	1226	305000	527200	18.8	.2067	6.4	454	206800	245900	28.7	.1004	2.4
12	1049	273200	472300	19.2	.2037	6.2	427	185300	220300	28.5	.0921	2.5
13	827	241400	417300	18.6	.1661	5.5	433	163700	194600	29.0	.1246	2.9
14	683	209700	362400	18.7	.1564	5.2	382	142200	169000	29.2	.1246	2.9
15	560	177900	307500	18.7	.1518	5.1	309	120600	143400	29.9	.1209	2.8
16	442	146100	252600	19.0	.1527	4.9	253	99100	117800	29.3	.0000	2.6
17	362	114400	197700	19.8	.1823	5.1	242	77500	92200	29.8	.1683	3.4
18	267	82600	142800	20.2	.1719	5.2	170	56000	66600	29.5	.1439	3.3
19	201	50800	87900	20.7	.2397	6.5	108	34500	41000	29.8	.1790	3.5
20	1179	305000	527200	18.6	.1819	6.2	433	206800	245900	27.8	.0824	2.3
21	949	241400	417300	18.1	.1711	6.3	454	163700	194600	28.3	.1129	3.0
22	645	177900	307500	18.6	.1978	5.8	323	120600	143400	29.5	.1613	2.9
23	420	114400	197700	19.5	.1927	5.9	212	77500	92200	29.9	.1440	3.0
24	188	50800	87900	20.2	.1991	6.1	100	34500	41000	29.6	.1537	3.2
25	1269	273200	472300	17.2	.2347	7.5	447	185300	220300	27.9	.1374	2.6
26	1117	209700	362400	16.3	.2348	8.6	372	142200	169000	27.9	.1032	2.8
27	715	146100	252600	17.1	.2507	7.9	254	99100	117800	28.6	.1241	2.8
28	375	82600	142800	18.8	.2664	7.4	155	56000	66600	28.7	.1743	3.0

TABLE VI (cont'd)
Heat Transfer Data from the Fully-Developed Two-Dimensional Stall Regime--on the "Wall of Reversed Flow."
($h = \text{Btu}/\text{Hr}\cdot\text{Ft}^2\cdot^\circ\text{F}$; $Q_m = \text{Btu}/\text{Hr}$; $T_b - T_a = ^\circ\text{F}$; $f_1(\text{Re}_x) = \text{Re}_{x_b} u_t f(W/L, D/L, \theta)$; $f_2(\text{Re}_x) = f_1(\text{Re}_x)/\tan 2\theta$)

Pos	L/W=18						L/W=18					
	Run 1 2213.12		W=2.00 in.		Flow=1168 cfm		Run 1 2263.12		W=2.00 in.		Flow=1153 cfm	
	2 θ =45.0 deg.		$\text{Re}_w=59600$		$U_t=58.4$ fps		2 θ =45.0 deg.		$\text{Re}_w=58100$		$U_t=57.6$ fps	
	$\text{Nu}_{x_b c}$	$f_1(\text{Re}_x)$	$f_2(\text{Re}_x)$	$T_b - T_a$	Q_m	h	$\text{Nu}_{x_b c}$	$f_1(\text{Re}_x)$	$f_2(\text{Re}_x)$	$T_b - T_a$	Q_m	h
1	135	48200	48100	20.4	.0047	0.8	157	47500	47400	25.1	.0116	0.9
2	117	37000	36900	20.0	.0081	0.9	145	36500	36400	24.4	.0205	1.1
3	85	25800	25700	19.6	.0073	0.9	102	25400	25400	24.5	.0189	1.1
4	55	14600	14500	19.9	.0268	1.1	70	14400	14300	24.9	.0467	1.4
5	169	53800	53700	20.5	.0236	0.9	171	53100	52900	25.6	.0298	0.9
6	149	42600	42500	20.6	.0279	1.0	179	42000	41900	25.3	.0413	1.2
7	113	31400	31300	20.0	.0029	1.0	126	31000	30900	24.7	.0094	1.1
8	60	20200	20100	20.0	.0131	0.9	89	19900	19800	25.3	.0397	1.3
9	35	9000	8900	20.1	.0286	1.2	47	8800	8800	25.4	.0520	1.5
10	123	59400	59300	20.5	.0620	0.6	171	58600	58400	25.3	.0856	0.8
11	139	53800	53700	20.8	.0110	0.7	160	53100	52900	25.3	.0185	0.8
12	152	48200	48100	20.3	.0008	0.9	150	47500	47400	25.0	.0000	0.9
13	163	42600	42500	20.7	.0256	1.0	154	42000	41900	25.3	.0287	1.0
14	136	37000	36900	20.4	.0220	1.0	128	36500	36400	25.3	.0248	1.0
15	117	31400	31300	20.3	.0210	1.1	124	31000	30900	25.1	.0288	1.1
16	95	25800	25700	20.3	.0177	1.1	110	25400	25400	25.3	.0300	1.2
17	68	20200	20100	20.3	.0139	1.0	92	19900	19800	25.7	.0355	1.3
18	50	14600	14500	20.3	.0093	1.0	68	14400	14300	25.5	.0292	1.3
19	35	9000	8900	20.3	.0340	1.1	46	8800	8800	25.9	.0611	1.5
20	140	53800	53700	20.2	.0046	0.7	145	53100	52900	24.7	.0078	0.8
21	137	42600	42500	20.2	.0117	0.9	151	42000	41900	25.0	.0184	1.0
22	109	31400	31300	20.4	.0418	1.0	132	31000	30900	25.5	.0622	1.2
23	77	20200	20100	20.4	.0306	1.1	90	19900	19800	25.7	.0469	1.3
24	37	9000	8900	20.3	.0379	1.2	42	8800	8800	25.6	.0550	1.4
25	126	48200	48100	19.9	.0296	0.7	171	47500	47400	24.6	.0489	1.0
26	129	37000	36900	19.4	.0027	1.0	134	36500	36400	24.0	.0054	1.0
27	97	25800	25700	19.7	.0146	1.0	111	25400	25400	24.6	.0269	1.2
28	57	14600	14500	19.9	.0467	1.1	67	14400	14300	24.9	.0685	1.3

TABLE VII
Heat Transfer Data from the Large Transitory Stall Regime
($h = \text{Btu}/\text{Hr}-\text{Ft}^2-\text{°F}$; $Q_m = \text{Btu}/\text{Hr}$; $T_b - T_a = \text{°F}$)

Pos	L/W=6						L/W=6					
	Run 12273.23		W=6.00 in.		Flow=1469 cfm		Run 12273.13		W=6.00 in.		Flow=6690 cfm	
	2 θ =16.0 deg.		$Re_w = 74700$		$U_t = 24.4 \text{ fps}$		2 θ =16.0 deg.		$Re_w = 342500$		$U_t = 111.5 \text{ fps}$	
	$Nu_{x_t c}$	Re_{x_t}	$Re_{x_t u_t}$	$T_b - T_a$	Q_m	h	$Nu_{x_t c}$	Re_{x_t}	$Re_{x_t u_t}$	$T_b - T_a$	Q_m	h
1	229	90900	122800	29.1	.1860	4.2	748	416700	562900	16.1	.3821	13.8
2	271	125300	210000	27.6	.1202	2.9	1140	574500	962500	15.1	.3357	12.1
3	301	148600	297200	27.5	.0856	2.2	1400	681000	1362100	15.3	.3185	10.5
4	347	165300	384300	27.5	.0809	2.0	1453	757800	1761700	14.4	.2089	8.4
5	194	66700	79200	30.3	.3151	5.7	447	305500	363100	16.5	.4042	13.1
6	216	110000	166400	28.3	.1182	2.9	916	504100	762700	15.2	.2831	12.4
7	238	138000	253600	27.8	.0591	2.1	1233	632400	1162300	15.3	.2844	10.8
8	283	157600	340800	28.3	.0801	1.8	1483	722300	1561900	16.4	.3426	9.7
9	284	172000	427900	28.1	.0539	1.5	1518	788600	1961500	15.0	.1829	7.9
10	114	34700	35600	28.3	.4548	8.6	264	159100	163300	14.0	.4904	20.0
11	183	66700	79200	29.8	.2672	5.4	477	305500	363100	15.9	.3978	14.0
12	213	90900	122800	28.6	.1753	3.9	761	416700	562900	15.9	.4203	14.1
13	242	110000	166400	28.3	.1409	3.3	961	504100	762700	14.9	.3305	13.0
14	255	125300	210000	28.1	.1107	2.7	1146	574500	962500	15.1	.3136	12.2
15	272	138000	253600	28.0	.0937	2.4	1271	632400	1162300	14.9	.2823	11.2
16	281	148600	297200	28.0	.0801	2.1	1336	681000	1362100	15.1	.2681	10.0
17	311	157600	340800	28.3	.0798	2.0	1503	722300	1561900	15.7	.2997	9.8
18	306	165300	384300	27.9	.0538	1.8	1430	757800	1761700	15.1	.2147	8.3
19	332	172000	427900	28.4	.0783	1.7	1445	788600	1961500	15.0	.2004	7.5
20	194	66700	79200	28.9	.2573	5.7	499	305500	363100	15.3	.3669	14.6
21	265	110000	166400	27.7	.1366	3.6	892	504100	762700	14.9	.2825	12.1
22	273	138000	253600	28.2	.1284	2.4	1182	632400	1162300	15.2	.2821	10.4
23	297	157600	340800	28.3	.0840	1.9	1487	722300	1561900	15.5	.2518	9.7
24	264	172000	427900	28.1	.0597	1.4	1694	788600	1961500	14.9	.2123	8.8
25	224	90900	122800	27.2	.2089	4.1	649	416700	562900	14.5	.3152	12.0
26	265	125300	210000	26.4	.0970	2.8	1026	574500	962500	14.2	.2677	10.9
27	299	148600	297200	27.0	.0861	2.2	1328	681000	1362100	14.8	.2768	9.9
28	258	165300	384300	27.3	.0831	1.5	1602	757800	1761700	14.1	.2478	9.2

TABLE VII (cont'd)
Heat Transfer Data from the Large Transitory Stall Regime
($h = \text{Btu}/\text{Hr}\cdot\text{Ft}^2\cdot^{\circ}\text{F}$; $Q_m = \text{Btu}/\text{Hr}$; $T_b - T_a = ^{\circ}\text{F}$)

Pos	L/W = 6						L/W = 6					
	Run 3204.33		W = 6.00 in.		Flow = 3193 cfm		Run 2114.33		W = 6.03 in.		Flow = 1066 cfm	
	2 θ = 20.0 deg.		$Re_w = 159700$		$U_t = 53.2 \text{ fps}$		2 θ = 30.0 deg.		$Re_w = 54400$		$U_t = 17.6 \text{ fps}$	
	$Nu_{x_t c}$	Re_{x_t}	$Re_{x_t u_t}$	$T_b - T_a$	Q_m	h	$Nu_{x_t c}$	Re_{x_t}	$Re_{x_t u_t}$	$T_b - T_a$	Q_m	h
1	386	182500	262400	32.3	.3773	7.2	113	54900	272000	32.5	.0824	2.1
2							186	68200	208900	31.7	.0812	2.0
3	789	282500	635000	30.6	.3356	5.9	256	76100	145800	32.6	.0786	2.0
4	894	309600	821300	29.1	.2513	5.2	296	81000	82600	33.5	.0809	1.7
5	179	137100	169300	32.1	.3104	5.3	72	43700	303600	33.2	.1170	2.1
6	456	216800	355600	30.8	.2801	6.2	154	62600	240500	32.8	.0963	2.1
7	654	264900	541900	30.3	.2717	5.8	203	72900	177300	32.7	.0511	1.8
8	892	297100	728200	31.6	.3747	5.8	240	79100	114200	34.2	.0750	1.6
9	953	320200	914500	30.0	.2242	4.9	332	82900	51100	34.0	.0793	1.7
10	101	73700	76100	29.9	.4326	7.6	19	26100	335200	32.7	.1427	1.4
11							59	43700	303600	33.0	.0768	1.7
12	323	182500	262400	30.3	.3112	6.0	84	54900	272000	32.4	.0430	1.5
13	474	216800	355600	30.0	.3159	6.4	140	62600	240500	33.0	.0848	1.9
14	590	243500	448700	30.5	.3112	6.3	139	68200	208900	33.1	.0602	1.5
15							174	72900	177300	33.5	.0620	1.5
16	789	282500	635000	30.3	.3031	5.9	197	76100	145800	34.0	.0561	1.5
17	918	297100	728200	31.3	.3458	6.0	215	79100	114200	34.6	.0541	1.4
18	867	309600	821300	29.9	.3416	5.0	261	81000	82600	34.3	.0489	1.5
19							308	82900	51100	34.5	.0873	1.6
20	212	137100	169300	30.2	.2977	6.2	146	43700	303600	34.0	.1198	4.3
21	554	216800	355600	29.5	.3358	7.5	114	62600	240500	32.3	.0513	1.5
22	690	264900	541900	30.4	.3361	6.1	159	72900	177300	33.7	.0938	1.4
23	906	297100	728200	31.0	.3047	5.9	473	79100	114200	34.6	.0708	3.1
24	1000	320200	914500	30.2	.2534	5.2	318	82900	51100	34.3	.0882	1.6
25	368	182500	262400	28.2	.3533	6.8	96	54900	272000	31.3	.1070	1.8
26							161	68200	208900	31.1	.0480	1.7
27	785	282500	635000	29.6	.3160	5.9	241	76100	145800	32.4	.0735	1.8
28	900	309600	821300	29.0	.2951	5.2	299	81000	82600	33.3	.1171	1.7

TABLE VII (cont'd)
Heat Transfer Data from the Large Transitory Stall Regime
($h = \text{Btu}/\text{Hr}\cdot\text{Ft}^2\cdot^\circ\text{F}$; $Q_m = \text{Btu}/\text{Hr}$; $T_b - T_a = ^\circ\text{F}$)

Pos	L/W=1.2						L/W=1.2					
	Run 1074.13		W=3.00 in.	Flow=819 cfm			Run 1074.23		W=3.00 in.	Flow=5959 cfm		
	2 θ =15.00 deg.		Re _w =41600	U _t =27.3 fps			2 θ =15.0 deg.		Re _w =302000	U _t =198.6 fps		
	Nu _{x_tc}	Re _{x_t}	Re _{x_tu_t}	T _b - T _a	Q _m	h	Nu _{x_tc}	Re _{x_t}	Re _{x_tu_t}	T _b - T _a	Q _m	h
1	237	82400	136600	28.5	.1896	4.4	829	598700	992600	18.6	.4917	15.4
2	284	103100	233600	27.9	.1287	3.0	1258	748700	1697300	17.4	.4311	13.5
3	336	115000	330700	28.5	.1050	2.5	1650	835200	2402000	18.2	.4529	12.4
4	353	122700	427700	28.6	.0863	2.0	2026	891400	3106700	17.8	.3650	11.7
5	205	65100	88100	29.3	.3239	6.0	618	473100	640300	19.7	.6662	18.2
6	256	94300	185100	28.3	.1409	3.4	947	685400	1345000	19.5	.3770	12.8
7	292	109700	282200	27.8	.0835	2.6	1538	797100	2049600	17.7	.4205	13.6
8	333	119200	379200	28.6	.1017	2.2	2056	866000	2754300	19.8	.5903	13.4
9	431	125600	476200	28.3	.0885	2.2	2350	912700	3459000	17.9	.3446	12.2
10	88	37800	39600	28.0	.3611	6.7	404	274500	287900	16.6	.8812	30.7
11	201	65100	88100	29.1	.2893	5.9	626	473100	640300	19.1	.6360	18.4
12	213	82400	136600	27.9	.1711	3.9	903	598700	992600	18.2	.5799	16.8
13	242	94300	185100	27.7	.1388	3.3	1089	685400	1345000	17.0	.4301	14.8
14	269	103100	233600	27.7	.1163	2.9	1360	748700	1697300	17.2	.4285	14.5
15	290	109700	282200	27.5	.1000	2.5	1558	797100	2049600	17.2	.4058	13.7
16	377	115000	330700	27.4	.1147	2.8	1920	835200	2402000	17.4	.4536	14.4
17	498	119200	379200	28.1	.1496	3.2	2325	866000	2754300	18.8	.5760	15.2
18	518	122700	427700	27.4	.1160	3.0	2414	891400	3106700	18.3	.4602	14.0
19	538	125600	476200	27.8	.1318	2.8	2510	912700	3459000	17.9	.4166	13.0
20	218	65100	88100	28.2	.2845	6.4	697	473100	640300	18.5	.6245	20.5
21	306	94300	185100	27.3	.1587	4.1	1278	685400	1345000	16.7	.4651	17.3
22	453	109700	282200	27.4	.2018	4.0	1779	797100	2049600	17.1	.4750	15.7
23	579	119200	379200	27.6	.1699	3.8	2242	866000	2754300	18.1	.4434	14.7
24	647	125600	476200	27.3	.1468	3.3	2505	912700	3459000	17.6	.3727	13.0
25	239	82400	136600	26.4	.2164	4.4	960	598700	992600	16.0	.5130	17.8
26	447	103100	233600	25.1	.1839	4.7	1648	748700	1697300	15.2	.4723	17.6
27	478	115000	330700	26.0	.1547	3.6	1847	835200	2402000	16.9	.4468	13.9
28	558	122700	427700	26.3	.1683	3.2	2109	891400	3106700	17.8	.4078	12.2

TABLE VII (cont'd)
Heat Transfer Data from the Large Transitory Stall Regime
($h = \text{Btu}/\text{Hr}\cdot\text{Ft}^2\cdot^\circ\text{F}$; $Q_m = \text{Btu}/\text{Hr}$; $T_b - T_a = ^\circ\text{F}$)

Pos	L/W=12						L/W=18					
	Run 3204.23		W=3.02 in.		Flow=4310 cfm		Run 12313.13		W=2.00 in.		Flow=1474 cfm	
	2 θ =20.0 deg.		$Re_w = 217000$		$U_t = 142.7 \text{ fps}$		2 θ =9.5 deg.		$Re_w = 74100$		$U_t = 73.7 \text{ fps}$	
	$Nu_{x_t c}$	Re_{x_t}	$Re_{x_t u_t}$	$T_b - T_a$	Q_m	h	$Nu_{x_t c}$	Re_{x_t}	$Re_{x_t u_t}$	$T_b - T_a$	Q_m	h
1	806	378900	708400	18.3	.4728	15.0	606	224700	365400	29.2	.5518	11.2
2							842	283300	624800	27.5	.4440	9.0
3	1394	492700	1714100	20.2	.4198	10.5	848	317500	884200	29.0	.3434	6.3
4	1674	517500	2217000	19.2	.3242	9.7	746	339900	1143600	30.0	.2122	4.3
5	585	311500	456900	17.9	.5753	17.3	376	176400	235700	31.8	.6526	11.0
6	887	422500	959800	19.0	.3456	12.1	580	258400	495100	29.0	.3375	7.8
7	1214	475400	1462700	19.6	.3594	10.7	924	302300	754500	28.5	.3821	8.1
8	1829	506300	1965600	21.7	.5708	12.0	1177	329700	1013900	30.6	.4947	7.7
9	2036	526700	2468500	19.5	.3237	10.6	1171	348400	1273300	29.7	.2756	6.1
10	307	193000	205500	15.1	.6129	23.3	226	101300	106000	28.6	.8620	17.1
11							368	176400	235700	31.1	.5914	10.8
12	777	378900	708400	18.7	.5084	14.4	460	224700	365400	30.2	.4621	8.5
13	886	422500	959800	18.3	.3754	12.0	501	258400	495100	29.8	.3321	6.8
14	1054	452900	1211200	19.1	.3639	11.3	596	283300	624800	30.0	.3084	6.4
15							756	302300	754500	29.7	.3231	6.6
16	1586	492700	1714100	18.6	.3972	11.9	962	317500	884200	29.7	.3683	7.2
17	2015	506300	1965600	20.1	.5285	13.2	1216	329700	1013900	30.9	.4658	7.9
18	1976	517500	2217000	19.0	.3868	11.5	1299	339900	1143600	30.0	.3830	7.5
19							1374	348400	1273300	30.2	.3817	7.1
20	568	311500	456900	17.3	.4762	16.8	396	176400	235700	30.5	.5779	11.6
21	1075	422500	959800	17.8	.4133	14.6	583	258400	495100	29.2	.3516	7.9
22	1524	475400	1462700	18.5	.4416	13.5	577	302300	754500	30.6	.2845	5.1
23	1836	506300	1965600	19.4	.3908	12.0	772	329700	1013900	31.3	.2605	5.0
24	2117	526700	2468500	19.1	.3421	11.0	1136	348400	1273300	30.5	.2906	5.9
25	916	378900	708400	16.4	.5031	17.0	464	224700	365400	28.3	.4436	8.6
26							593	283300	624800	28.4	.2913	6.3
27	1520	492700	1714100	18.2	.3947	11.4	681	317500	884200	30.3	.2754	5.1
28	1718	517500	2217000	18.4	.3482	10.0	778	339900	1143600	30.9	.2728	4.5

TABLE VII (cont'd)
Heat Transfer Data from the Large Transitory Stall Regime
($h = \text{Btu}/\text{Hr}\cdot\text{Ft}^2\cdot^{\circ}\text{F}$; $Q_m = \text{Btu}/\text{Hr}$; $T_b - T_a = ^{\circ}\text{F}$)

Pcs	L/W=18						L/W=18					
	Run 12313. 23		W= 2.00 in.		Flow=5012 cfm		Run 12303. 13		W= 2.00 in.		Flow=1276 cfm	
	2 θ =9.5		$Re_w = 251500$		$U_t = 250.6 \text{ fps}$		2 θ =15.0 deg.		$Re_w = 64900$		$U_t = 63.8 \text{ fps}$	
	$Nu_{x_t c}$	Re_{x_t}	$Re_{x_t u_t}$	$T_b - T_a$	Q_m	h	$Nu_{x_t c}$	Re_{x_t}	$Re_{x_t u_t}$	$T_b - T_a$	Q_m	h
1	1206	762400	1239700	14.8	.5832	22.5	585	161000	319900	20.1	.3671	10.8
2	2009	961100	2119900	13.3	.5347	21.6	741	188600	547000	19.6	.2775	7.9
3	1816	1077100	3000000	15.5	.4307	13.7	747	203000	774100	21.3	.2182	5.6
4	1543	1153100	3880200	16.4	.2552	9.0	824	211800	1001200	21.3	.1679	4.7
5	868	598500	799700	16.8	.8012	25.7	300	134900	206300	22.1	.3614	8.8
6	1001	876800	1679800	16.4	.3384	13.7	644	177400	433500	20.4	.2645	8.7
7	2345	1025800	2560000	14.3	.5385	20.8	903	196800	660600	20.5	.2683	7.9
8	2839	1118700	3440100	17.2	.7268	18.7	1035	207800	887700	21.9	.3070	6.7
9	2810	1182100	4320300	14.7	.3433	14.7	1106	215000	1114800	21.0	.1838	5.7
10	521	343700	359600	13.5	.9213	39.8	195	86500	92800	19.6	.5148	14.7
11	832	598500	799700	16.1	.7264	24.7	304	134900	206300	21.6	.3365	8.9
12	1083	762400	1239700	15.7	.6101	20.2	350	161000	319900	21.0	.2361	6.5
13	1093	876800	1679800	14.7	.3771	14.9	403	177400	433500	20.7	.1824	5.4
14	1266	961100	2119900	15.1	.3519	13.6	580	188600	547000	20.8	.2082	6.2
15	1670	1025800	2560000	15.1	.3851	14.8	808	196800	660600	20.8	.2437	7.1
16	2483	1077100	3000000	15.3	.5223	18.8	933	203000	774100	20.8	.2503	7.0
17	3103	1118700	3440100	16.4	.6877	20.4	1118	207800	887700	21.3	.2933	7.3
18	3252	1153100	3880200	14.9	.5135	18.9	1193	211800	1001200	20.6	.2395	6.9
19	3401	1182100	4320300	14.3	.4531	17.8	1199	215000	1114800	21.0	.2316	6.2
20	930	598500	799700	15.6	.7085	27.6	319	134900	206300	20.7	.3143	9.4
21	1299	876800	1679800	14.3	.4072	17.7	468	177400	433500	20.5	.1943	6.3
22	1349	1025800	2560000	15.7	.3348	12.0	603	196800	660600	21.2	.2058	5.3
23	1848	1118700	3440100	16.2	.3289	12.2	972	207800	887700	21.5	.2267	6.3
24	2873	1182100	4320300	14.3	.3496	15.0	1242	215000	1114800	20.9	.2182	6.4
25	1052	762400	1239700	14.0	.4917	19.7	505	161000	319900	19.3	.3288	9.3
26	1304	961100	2119900	14.2	.3475	14.0	723	188600	547000	19.6	.2537	7.7
27	1585	1077100	3000000	15.9	.3618	12.0	886	203000	774100	20.7	.2521	6.6
28	1890	1153100	3880200	16.0	.3336	11.0	1037	211800	1001200	20.7	.2409	6.0

TABLE VII (cont'd)
Heat Transfer Data from the Large Transitory Stall Regime
($h = \text{Btu/Hr} - \text{Ft}^2 - ^\circ\text{F}$; $Q_m = \text{Btu/Hr}$; $T_b - T_a = ^\circ\text{F}$)

Pos	L/W=18						L/W=18					
	Run 12303.23		W=2.00 in.		Flow=4958 cfm		Run 3204.13		W=2.02 in.		Flow=4679 cfm	
	29=15.0 deg.		$Re_w = 252100$		$U_t = 247.9 \text{ fps}$		26=20.0 deg.		$Re_w = 235500$		$U_t = 231.6 \text{ fps}$	
	$Nu_{x_t c}$	Re_{x_t}	$Re_{x_t u_t}$	$T_b - T_a$	Q_m	h	$Nu_{x_t c}$	Re_{x_t}	$Re_{x_t u_t}$	$T_b - T_a$	Q_m	h
1	1188	625600	1242900	15.7	.6055	22.1	930	499900	1149700	17.3	.5193	17.3
2	1921	732700	2125200	15.0	.5703	20.5						
3	2279	788500	3007600	16.1	.5652	17.1	1985	591100	2782200	17.7	.5376	15.0
4	2656	822800	3890000	15.3	.4147	15.4	2265	608900	3598500	16.5	.3820	13.2
5	742	524000	801700	16.6	.6725	21.9	511	436800	741600	18.3	.5156	15.1
6	1251	689200	1684100	15.1	.3893	17.0	1343	536900	1557900	17.4	.4851	18.3
7	1988	764400	2566400	15.7	.4934	17.5	1737	578300	2374100	18.0	.4906	15.4
8	2782	807500	3448800	17.8	.7316	18.2	1523	601000	3190400	19.2	.4143	10.0
9	3303	835400	4331100	15.0	.4098	17.2	2113	615300	4006600	16.5	.2850	11.0
10	511	336000	360500	14.0	.9299	38.7	361	304200	333500	15.3	.7262	27.5
11	778	524000	801700	16.3	.6796	22.9						
12	1094	625600	1242900	15.9	.6197	20.3	961	499900	1149741	17.3	.5885	17.9
13	1273	689200	1684100	14.4	.4298	17.3	1345	536900	1557900	16.2	.5126	18.3
14	1691	732700	2125200	14.0	.4392	18.1	1637	561200	1966000	17.0	.5154	17.6
15	2165	764400	2566400	14.4	.4792	19.1						
16	2575	788500	3007600	15.0	.5279	19.3	2058	591100	2782200	17.3	.4856	15.5
17	3023	807500	3448800	16.5	.6662	19.8	2324	601000	3190400	18.5	.5672	15.2
18	3119	822800	3890000	15.8	.5183	18.1	2317	608900	3598500	17.4	.4202	13.5
19	3226	835400	4331100	15.6	.4648	16.8						
20	817	524000	801700	15.8	.6271	24.1	659	436800	741600	16.6	.5327	19.5
21							1432	536900	1557900	16.8	.5280	19.5
22	2231	764400	2566400	15.0	.5177	19.7	1593	578300	2374100	18.1	.4531	14.1
23	2633	807500	3448800	16.4	.4702	17.2	1834	601000	3190400	18.7	.3770	12.0
24	2842	835400	4331100	16.1	.3875	14.8	1984	615300	4006600	17.3	.2919	10.3
25	1412	625600	1242900	13.1	.6108	26.2	1000	499900	1149700	15.8	.5287	18.6
26	1915	732700	2125200	13.4	.4851	20.5						
27	2118	788500	3007600	15.3	.4638	15.9	1650	591100	2782200	17.9	.4218	12.4
28	2388	822800	3890000	16.6	.4280	13.8	1992	608900	3598500	17.4	.3798	11.6